Sandy beaches in low-energy, non-tidal environments

Unraveling and predicting morphodynamics

Ton, A.M.

DOI
10.4233/uuid:5978034d-f9e5-4094-99dc-dd8591828125

Publication date
2023

Document Version
Final published version

Citation (APA)
Ton, A. M. (2023). *Sandy beaches in low-energy, non-tidal environments: Unraveling and predicting morphodynamics*. [Dissertation (TU Delft), Delft University of Technology].
https://doi.org/10.4233/uuid:5978034d-f9e5-4094-99dc-dd8591828125

Important note
To cite this publication, please use the final published version (if applicable).
Please check the document version above.

Sandy beaches in low-energy, non-tidal environments

Unraveling and predicting morphodynamics

Sandy beaches in low-energy, non-tidal environments

Unraveling and predicting morphodynamics

Proefschrift

ter verkrijging van de graad van doctor
aan de Technische Universiteit Delft,
op gezag van de Rector Magnificus prof. dr. ir. T.H.J.J. van der Hagen,
voorzitter van het College voor Promoties,
in het openbaar te verdedigen op woensdag 28 juni 2023 om 15.00 uur

door

Anne Marije TON

Master of Science in Civiele Techniek,
Technische Universiteit Delft, Nederland,
geboren te Middelburg, Nederland.

Dit proefschrift is goedgekeurd door de promotoren.

Samenstelling promotiecommissie:

Rector Magnificus,	voorzitter
Prof. dr. ir. S.G.J. Aarninkhof,	Technische Universiteit Delft, promotor
Dr. ir. V. Vuik,	Technische Universiteit Delft, copromotor
Onafhankelijke leden:	
Prof. dr. ir. A.J.H.M. Reniers,	Technische Universiteit Delft
Prof. dr. ir. A. Kroon,	University of Copenhagen, Denmark
Prof. dr. A. Vila-Concejo,	University of Sydney, Australia
Dr. ir. T.D. Price,	Universiteit Utrecht
Dr. ir. J.M. van Loon-Steensma,	Wageningen University & Research, Van Hall Larenstein, University of Applied Sciences
Prof. dr. ir. W.S.J. Uijttewaal,	Technische Universiteit Delft, reservelid

TU Delft Delft University of Technology

Rijkswaterstaat
Ministerie van Infrastructuur en Waterstaat

Keywords: Sandy beaches, morphodynamics, low-energy, LakeSIDE

Printed by: ProefschriftMaken

Front & Back: Simone Golob

ISBN 978-94-6469-414-7

An electronic version of this dissertation is available at
https://repository.tudelft.nl/.

Contents

Summary

Sandy foreshores, beaches and dunes play an eminent role in flood risk reduction in coastal areas, reducing the impact of wind waves and storm surges on the hinterland. In some areas, sandy protection is naturally present. In other coastal areas, engineering solutions are needed to provide safety. “Soft” sediment-based solutions often serve multiple objectives, including flood safety, but also provide other ecosystem services. Knowledge of morphodynamics of these “soft” solutions (i.e. beaches) is crucial for protecting and managing coastal areas prone to flood risk.

Most research on coastal morphodynamics concerns high-energy or open coasts. Beaches in lakes, estuaries and bays are generally placed in the category of low-energy beaches, and have received less attention. The physical relation between hydrodynamics and morphology for low-energy beaches has only been described in general terms and morphological evolution over time has received even less attention. Therefore, morphological development of these areas is difficult to predict quantitatively, despite the importance of low-energy beaches.

The aim of this thesis is to understand and quantify how hydrodynamic processes drive morphological development of low-energy, non-tidal, sandy beaches. The beaches in the IJsselmeer region, the Netherlands, are used to reach this aim, with a focus on the Houtribdijk and Marker Wadden beaches. The Houtribdijk is a dam in between two lakes, that was reinforced between 2018 and 2020. The reinforcement was partially constructed with sandy foreshores, creating gradual transitions and with the goal to improve biodiversity and water quality in the lake. Most importantly, the sandy foreshores protect the dam from wave impact. The Marker Wadden archipelago consists of shallow marsh islands in lake Markermeer, protected by two stretches of sandy beaches and dunes on the northwest and southwest side and a rubble mound breakwater in the west. These islands are meant to improve biodiversity and water quality in the lake. They were constructed between 2016 and 2018 and expansion works are still ongoing. The beaches on both locations can be categorized as low-energy, non-tidal beaches. On all locations, both hydrodynamics and morphology were monitored for almost two years during the LakeSIDE campaign.

The general features of low-energy, non-tidal, sandy beaches usually include a narrow, steep beach face, connecting to a low-gradient subaqueous platform. They would commonly fall under the “reflective beach state” as defined by Wright *et al.* (1984). However, the single reflective beach state cannot adequately describe the wide range of profiles and concavities observed. Through studying several morphotype models for low-energy beaches, we concluded that the least exposed sites generally have the steepest and narrowest beach face and the

most distinct transition between swash zone and platform.

The Houtribdijk and Marker Wadden beaches were constructed with initially plane slopes and showed rapid profile adjustments towards the described, more natural profile shape. For in-depth analysis of the morphological development, three vertical sections were defined in the cross-shore profile: the beach face section, the platform section and the offshore section. The beach face section is mostly affected by cross-shore erosion, which is strongly linked to wave height in relatively energetic events (95% value). The platform elevation reaches a dynamic equilibrium after the initial profile adjustment. Based on the measurements of wave heights and water levels at our study sites, the depth of closure was calculated with the theoretical formulation by Hallermeier (1980), defined as the depth at which wave action has negligible effect on sediment transport. The platform elevation is near the calculated depth of closure, deepening a little during more energetic events and heightening during calmer periods, as sediment is brought in from the beach face.

Based on flow measurements and bathymetric surveys, a relationship was determined between longshore sediment transport capacity and sediment volume flux in the longshore direction at the platform and offshore section. The longshore flow is induced by wave-driven flow and flow that originates from large-scale lake circulations. These large-scale, horizontal circulations are caused by bathymetry-induced differences in water level set-up throughout the lake. The circulation-driven nearshore flow is dominant over the wave-driven flow for most wind directions at our study sites. Local geometric features, such as groynes, also affect the flow, inducing smaller-scale nearshore circulation cells under distinct conditions. The gradients in longshore transport determine whether the platform extends offshore.

As more insight is gained into the hydrodynamic processes steering the morphological development, these can be quantified and used for prediction methods. Yearly cross-shore beach face erosion is linked to the yearly 95^{th} percentile wave height, implying the importance of higher energy conditions. Longshore sediment transport can be quantified through an adjusted version of the Van Rijn (2014) bulk equation. In the Van Rijn (2014) formula, longshore flow is derived from incoming wave direction combined with ambient flow. Based on an hindcast of longshore transports at our study sites, it appeared that the original Van Rijn (2014) formula overestimates the effect of wave-driven currents in comparison to the ambient flow. Therefore, the longshore flow is replaced by the total measured or modelled longshore flow for application at our study sites. The adjusted formula is recalibrated with measurements from one of the Houtribdijk monitoring sites. When obtaining yearly longshore transports with this new method, two uncertainties have to be taken into account. The first is the uncertainty of the calibration and the second the uncertainty of the yearly wind climate. Both give a relatively high uncertainty, but on the timescale of one year, the uncertainty from the calibration is more than 2.5 times larger than the wind climate variability.

By combining cross-shore beach face erosion, platform depth and longshore

sediment distribution at the platform and offshore, beach development can be predicted. Given the nature of the prediction method, we were only able to assess beach face erosion due to high-energy waves on a yearly basis. However, the sedimentation lower in the profile due to longshore transport can be predicted per event. Based on these new prediction methods, the robustness and required maintenance of low-energy, non-tidal, sandy beaches can be assessed more reliably.

Samenvatting

Zandige vooroevers, stranden en duinen spelen een belangrijke rol bij het verlagen van overstromingsrisico's in kustgebieden, door het verkleinen van de impact van windgolven en stormvloeden op het achterland. In sommige gebieden is van nature zandige bescherming aanwezig. In andere kustgebieden zijn technische oplossingen nodig om veiligheid te bieden. "Zachte" oplossingen met sediment dienen vaak meerdere doelen, waaronder overstromingsoverstromingsrisicoreductie, maar ook het leveren van ecosysteemdiensten. Kennis van de morfodynamiek van deze "zachte" oplossingen (d.w.z. stranden) is cruciaal voor de bescherming en het beheer van kustgebieden die kwetsbaar zijn voor overstromingen.

Het meeste onderzoek naar de morfodynamica van kusten betreft hoogenergetische of open kusten. Stranden in meren, estuaria en baaien vallen over het algemeen in de categorie laagenergetische stranden, en kregen tot dusver minder aandacht. De fysische relatie tussen hydrodynamica en morfologie voor laagenergetische stranden is alleen in algemene termen beschreven en de morfologische temporele ontwikkeling heeft nog minder aandacht gekregen. Daarom is de morfologische ontwikkeling van deze gebieden moeilijk kwantitatief te voorspellen.

Het doel van dit proefschrift is om te begrijpen en te kwantificeren hoe hydrodynamische processen sturend zijn in de morfologische ontwikkeling van laagenergetische, getijloze zandstranden. De stranden in het IJsselmeergebied worden hiervoor bestudeerd, met een focus op de stranden langs de Houtribdijk en Marker Wadden. De Houtribdijk is een dam tussen het IJsselmeer en het Markermeer, die tussen 2018 en 2020 is versterkt, voor de helft met gepenetreerd breuksteen en voor de andere helft met zandige vooroevers. Door de zandige vooroever ontstaan geleidelijke overgangen tussen land en water en met als doel om de biodiversiteit en de waterkwaliteit in het meer te verbeteren. Nog belangrijker is dat de zandige voorlanden de dam beschermen tegen golfslag. De Marker Waddenarchipel bestaat uit ondiepe moeraseilanden in het Markermeer, beschermd door twee zandstranden met duinen aan de noordwest- en zuidwestkant en een stenen golfbreker in het westen. Deze eilanden zijn bedoeld om de biodiversiteit en de waterkwaliteit in het meer te verbeteren. Ze zijn gebouwd tussen 2016 en 2018 en de uitbreidingswerkzaamheden zijn nog gaande. Op beide locaties kunnen de stranden worden gecategoriseerd als laagenergetische stranden zonder getij. Zowel de hydrodynamica als de morfologie zijn gemonitord op alle locaties gedurende twee jaar tijdens de LakeSIDE campagne.

Over het algmeen kenmerken laagenergetische zandstranden met microgetij zich door een smal, steil gebied rond de waterlijn dat aansluit op een flauw on-

derwaterplateau. Deze stranden vallen gewoonlijk onder de “reflective beach state” zoals gedefinieerd door Wright *e.a.* (1984). Deze “reflective beach state” kan echter het brede scala aan waargenomen profielen en concaviteiten niet adequaat beschrijven. Door verschillende morfotypemodellen voor laagenergetische stranden bestuderen, concluderen we dat de minst blootgestelde locaties over het algemeen het steilste en smalste zone rond de waterlijn hebben en de meest karakteristieke overgang tussen swash-zone en plateau.

De stranden langs de Houtribdijk en Marker Wadden zijn aangelegd met een aanvankelijk vlakke helling en transformeerden al snel richting de beschreven, meer natuurlijke profielvorm. Voor een grondige analyse van de morfologische ontwikkeling zijn drie verticale secties gedefinieerd voor het dwarsprofiel: de waterlijnsectie, de plateausectie en de offshore sectie. De waterlijnsectie wordt voornamelijk beïnvloed door erosie in dwarsrichting, die sterk verband houdt met de golfhoogte tijdens relatief energetische periodes (95% waarde). De plateauhoogte bereikt een dynamisch evenwicht na de initiële profielaanpassing. Op basis van golfhoogte- en waterstandsmetingen op de onderzoekslocaties is de sluitdiepte berekend met de theoretische formulering van Hallermeier (1980), gedefinieerd als de diepte waarop golfslag een verwaarloosbaar effect heeft op het sedimenttransport. De hoogte van het plateau ligt dichtbij de berekende sluitdiepte en verdiept tijdens meer energieke periodes en verhoogt tijdens rustigere periodes, omdat er sediment wordt aangevoerd vanaf de waterlijn.

Op basis van gemeten stroming en bathymetrie is een relatie bepaald tussen de transportcapaciteit van sediment in langsrichting en de sedimentflux in de langsrichting op het plateau en het offshore gedeelte. De langsstroming wordt veroorzaakt door golfgedreven stroming en stroming die afkomstig is van grootschalige meercirculaties. Deze grootschalige, horizontale circulaties worden veroorzaakt door verschillen in windopzet binnen het meer, veroorzaakt door verschillen in waterdiepte. Bij de meeste windrichtingen hebben deze grootschalige circulaties meer invloed op de stroming nabij de oevers van het meer dan golfgedreven stroming. Lokale constructies, zoals opsluitdammen, hebben ook invloed op de stroming, en veroorzaken onder verschillende omstandigheden kleinschalige circulatiecellen dichtbij de kust. De gradiënten in langstransport bepalen of het platform zich meerwaarts uitbouwt.

Naarmate er meer inzicht wordt verkregen in de hydrodynamische processen die de morfologische ontwikkeling sturen, kunnen deze worden gekwantificeerd en gebruikt voor voorspellingsmethoden. De jaarlijkse erosie rond de waterlijn dwars op de kust is het best te beschrijven op basis van het jaarlijkse 95^{e} percentiel van de golfhoogte, wat het belang van energetische condities impliceert. Langstransport van sediment kan worden gekwantificeerd met een aangepaste versie van de Van Rijn (2014) bulkvergelijking. In de Van Rijn (2014) formule wordt langsstroming gebaseerd op inkomende golfrichting in combinatie met omgevingsstroming. Gebaseerd op een hindcast van langstransporten op onze onderzoekslocaties, bleek dat de originele Van Rijn (2014) formule het effect van golfgedreven stromingen overschat in vergelijking met de omgevingsstroming. Daarom is de langsstroming vervangen door de totale gemeten of gemodelleerde

langsstroming voor toepassing op onze studielocaties. Deze aangepaste formule is herijkt met metingen van één van de meetpunten bij de Houtribdijk. Bij het berekenen van jaarlijkse langstransporten met deze nieuwe methode moet rekening worden gehouden met twee onzekerheden. De eerste is de onzekerheid van de kalibratie en de tweede de onzekerheid van het jaarlijkse windklimaat. Beide geven een relatief hoge variabiliteit, maar op jaarbasis is de onzekerheid door de kalibratie meer dan 2,5 keer zo hoog als de windklimaatvariabiliteit.

Door het combineren van waterlijnerosie, platformhoogte en de distributie van sediment in de langsrichting op het plateau en in de offshore sectie, kan de morfologische ontwikkeling van het strand worden voorspeld. Stranderosie door hoogenergetische golven kan met de ontwikkelde voorspellingsmethode alleen op jaarlijkse basis worden beoordeeld. Echter, de sedimentatie lager in het profiel door langstransport kan voor elke periode worden voorspeld. Op basis van deze nieuwe voorspellingsmethoden kan de robuustheid en het benodigde onderhoud van laagenergetische, getijloze zandstranden betrouwbaarder worden beoordeeld.

1

Introduction

1

1.1. Motivation

Regions near open coasts, estuaries and lakes are some of the most densely populated areas of the world (Neumann *et al.*, 2015). Sandy foreshores, beaches and dunes play an eminent role in flood risk reduction in these areas, reducing the impact of wind waves and storm surges on the hinterland. In some areas, sandy protection is naturally present. In other coastal areas, engineering solutions are needed to provide safety. Traditionally, these engineering solutions include "hard" structures, such as dikes and dams. Classic hard structures have the disadvantage that they are not adaptive to a changing climate and they can induce disturbance of the ecosystem (Van Wesenbeeck *et al.*, 2014). Nowadays, a shift towards more sustainable and multi-functional solutions is made, following the Building with Nature principle (de Vriend *et al.*, 2015). This means that solutions are being developed that serve multiple objectives, starting from thorough understanding of the natural system and using nature's ecosystem services if and when possible. Though not applicable in every situation (for instance due to space limitations), this approach often results in "soft", sediment-based solutions.

Knowledge of morphodynamics of these "soft" solutions (i.e. beaches) is crucial for protecting and managing coastal areas prone to flood risk. Most coastal research on morphodynamics concerns high-energy or open coasts. Beaches in lakes, estuaries and bays are generally placed in the category of low-energy beaches (Jackson *et al.*, 2002; Nordstrom *et al.*, 2012), and have received less attention (Eliot *et al.*, 2006; Fellowes *et al.*, 2021; Lorang, Stanford, *et al.*, 1993; Lowe *et al.*, 2016; Nordstrom *et al.*, 2012). However, knowledge in this field has been growing over the last years. Studies have focused on wave signatures (Rahbani *et al.*, 2022), the interaction between hydrodynamics and morphology (Eelsalu *et al.*, 2022; Fellowes *et al.*, 2021; Gallop *et al.*, 2020; Mujal-Colilles *et al.*, 2019; Steetzel *et al.*, 2017), modelling (Tran *et al.*, 2021) and providing a review (Vila-Concejo *et al.*, 2020).

Low-energy beaches are commonly characterised by a small prevailing wave height and limited storm wave height. Lakes, estuaries and bays do differ from each other in presence of non-locally generated waves, such as swell and infragravity, tide and fresh-water river influx. As daily conditions in low-energy environments are minimal, morphodynamics are considered storm-driven (Vila-Concejo *et al.*, 2020).

Morphodynamics of low-energy or sheltered beaches cannot easily be categorised as a beach state, as developed for high-energy beaches (Hegge *et al.*, 1996), as for instance done by Wright *et al.* (1985). Moreover, the physical relation between hydrodynamics and morphology for low-energy beaches has only been described in general terms and morphological evolution over time has received even less attention (Jackson *et al.*, 2002; Vila-Concejo *et al.*, 2020). Therefore, morphological development of these areas is difficult to quantitatively predict, despite the importance of low-energy beaches for coastal protection, recreation, and ecology. This holds for natural coasts as well as artificial, nourished beaches.

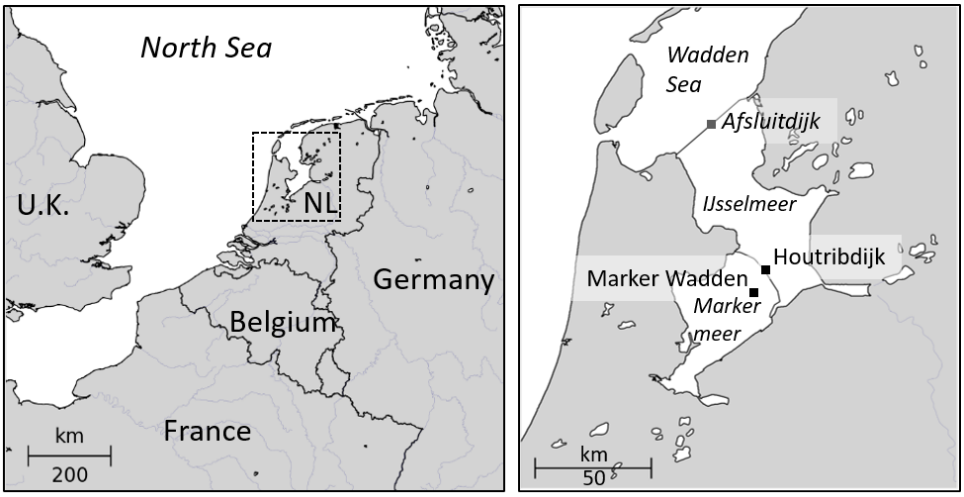

Figure 1.1: Map of IJsselmeer region

An example of an ecosystem that was altered by a traditional engineering intervention and turned into a low-energy lake environment, is the IJsselmeer region in the Netherlands (fig. 1.1). The main tidal estuary of the river IJssel was converted into a freshwater lake, lake IJsselmeer, by constructing a 32-km long dam called the Afsluitdijk between 1927 and 1933. This dam was built for improving the flood safety of the former Zuiderzee region. Between 1942 and 1968 three large land reclamations were completed: the Noordoostpolder, Oostelijk Flevoland and Zuidelijk Flevoland. In 1976 a second dam was completed, the 27-km long Houtribdijk, dividing the IJsselmeer into two lakes: the new lake Markermeer with limited riverine input and lake IJsselmeer, still fed by river IJssel. Lake Markermeer was originally also meant to become a land reclamation but in 2003, the Dutch government officially terminated these plans. Therefore, the Houtribdijk needed to be reinforced, to act as dam, with water on both sides instead of one.

The traditional engineering structures did not introduce elements commonly observed in well-functioning, natural, lowland freshwater lakes, such as gradual land–water transitions, heterogeneity in water depths or water-level fluctuations (Schindler *et al.*, 2002). Therefore, the reinforcement of the Houtribdijk, between 2018 and 2020, was partially constructed with sandy foreshores, creating gradual transitions, with the goal to improve biodiversity and water quality in the lake (fig. 1.2). Most importantly, the sandy foreshores protect the dike from wave impact. With that a low-energy, non-tidal beach developed on both sides of the dam.

To enhance the ecological integrity of lake Markermeer further, an archipelago of shallow marsh islands was constructed between 2016 and 2018 to add the structure and dynamics that are more typical for a natural freshwater lake, while maintaining the lake's current ecosystem services (Van Leeuwen *et al.*, 2021).

This archipelago is called the Marker Wadden and is protected by two stretches of sandy beaches and dunes on the northwest and southwest side and a rubble mound breakwater in the west (fig. 1.1 and 1.2).

In both the dike reinforcement project and the design of the Marker Wadden, the lack of morphodynamic knowledge became especially apparent. A pilot study generated useful insights regarding expected hydrodynamic conditions, profile shape and sand losses (Steetzel *et al.*, 2017). However, it remained uncertain which hydrodynamic and morphological processes are dominant in shaping the foreshore. This leads to uncertainties in sedimentation and erosion predictions. Since extra safety needs to be built in, to compensate for the uncertainties, a very robust design was chosen. Moreover, no regulated safety assessment and maintenance methods are in place for this type of dike reinforcement, at least in the Netherlands.

Figure 1.2: Drone images of the Houtribdijk with the FL67 measurement stations (A, March 2020, by Bureau Start the Future commissioned by Rijkswaterstaat) and the southwestern side and spit of the Marker Wadden (B, April 2022, by Niels van Kouwen and Anne Ton)

1.2. Aim of this dissertation

The aim of this dissertation is to understand and quantify how hydrodynamic processes drive the morphological evolution of low-energy, non-tidal, sandy beaches and to develop methods to predict these morphodynamics. The beaches in the IJsselmeer region are used to reach this aim, with a focus on the Houtribdijk and Marker Wadden beaches.

The main question is:

How can the robustness and required maintenance of low-energy, non-tidal, sandy beaches be assessed?

Robustness is defined as the resistance against extreme events and future developments. The main research question is answered through four key questions:

RQ1. What are the general features of low-energy, non-tidal, sandy beaches?

RQ2. How do hydrodynamic processes affect the morphological development of low-energy, non-tidal, sandy beaches in the cross-shore direction?

RQ3. How do (large-scale) hydrodynamic processes affect the morphological development of low-energy, non-tidal, sandy beaches in the longshore direction?

RQ4. How can morphological development be predicted for low-energy, non-tidal, sandy beaches?

1.3. Approach and outline

The general features of low-energy, microtidal, sandy beaches are researched through a literature review. Besides describing and analysing low-energy sites, several scholars have aimed to develop conceptual models describing the morphotype of these beaches. These descriptions range from beach states applicable to all energy levels (Wright *et al.*, 1984) to morphotypes for the low-energy beach face only (Makaske *et al.*, 1998). This review can be found in Ch. 2 (RQ1).

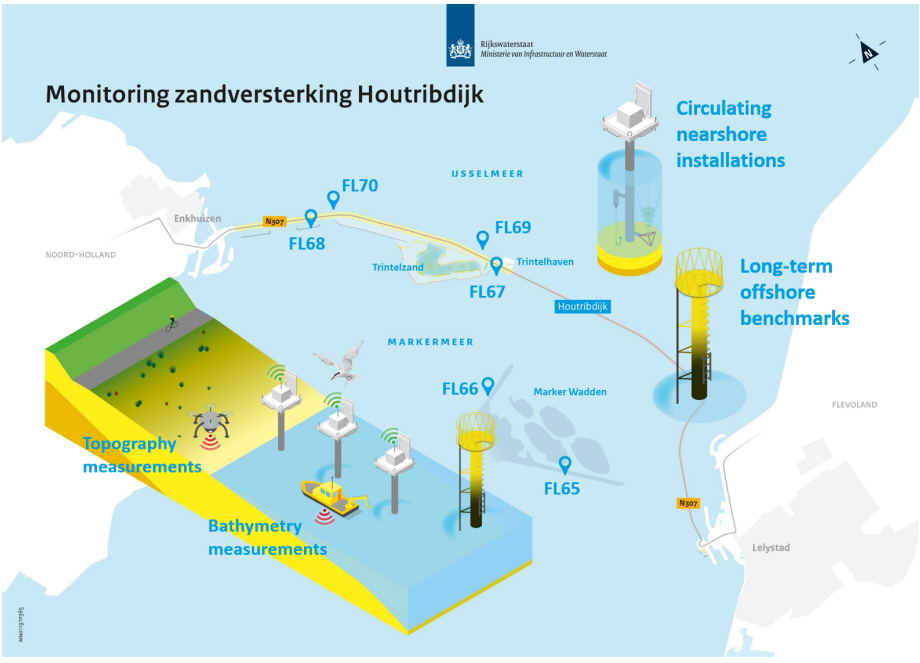

Figure 1.3: Overview monitoring campaign

For researching cross-shore morphodynamic processes, field measurements from the Houtribdijk pilot study (Steetzel *et al.*, 2017) and the Marker Wadden were analysed (fig. 1.3). From wave measurements the depth of closure, as proposed by Hallermeier (1979), was calculated and related to the profile shape of all locations. Results can also be found in Ch. 2 (RQ2).

Longshore morphodynamic processes were analysed from a large field measurement campaign, called LakeSIDE, with monitoring stations at 6 locations, of which 4 around the Houtribdijk and 2 at the Marker Wadden (fig. 1.3). Comparison of field measurements and model predictions of waves, currents and water levels, yields new insights into the relation between large-scale lake currents and nearshore longshore transport (Ch. 3, RQ3).

Both cross-shore and longshore transport can be predicted, by adjusting and re-calibrating a bulk longshore sediment transport formula and finding an empirical relation between wave height and cross-shore sediment transport for our system. Through finding where cross-shore and longshore sediment transport work separately and where they interact, a method is developed for designing and maintaining sandy beaches in low-energy, non-tidal environments (Ch. 4, RQ4) (fig. 1.4).

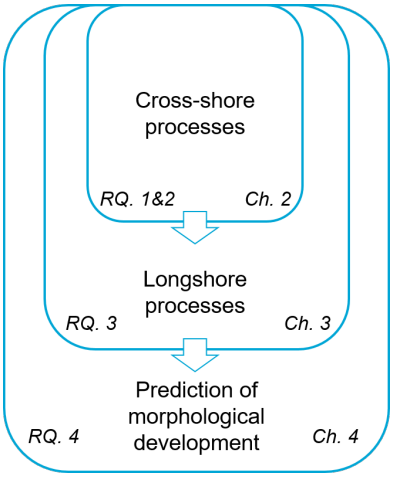

Figure 1.4: Overview of thesis subjects and chapters

2

Linking morphological development to hydrodynamic forcing

Highlights:

- Low-energy beaches generally have a narrow, steep beach face, connecting to a low gradient, subaqueous platform.
- The Houtribdijk and Marker Wadden beaches show rapid initial profile adjustment after construction towards the natural profile shape.
- The elevation of the platform is in dynamic equilibrium around the Hallermeier (1979) depth of closure
- Erosion of the beach face is caused primarily by wave-driven cross-shore transport, after which the sediment is most likely diffused in both cross-shore and longshore direction over the platform and offshore section.

This chapter has been published as: **Ton, A.M.**, Vuik, V., Aarninkhof, S.G.J. (2021). Sandy beaches in low-energy, non-tidal environments: Linking morphological development to hydrodynamic forcing. Geomorphology, 374, 107522.

2.1. Abstract

The morphodynamic behaviour of low-energy beaches is poorly understood, compared to that of exposed coasts. This study analyses the morphological development of sandy, low-energy beaches and the steering hydrodynamic processes. Four densely-monitored study sites in the non-tidal lake Markermeer in the Netherlands offered a unique opportunity to examine the relation between their hydraulic boundary conditions and morphodynamics. Regular bathymetric surveys were executed at all locations. Furthermore, the wave climate was monitored at one of these four sites. All four sites exhibit a commonly found low-energy beach morphology, with a narrow beach face and a low-gradient, subaqueous platform. This platform reaches an equilibrium depth quickly and then stays relatively stable. The stable elevation of the platform is located near Hallermeier's depth of closure. A sediment budget analysis over time demonstrates that the beach faces at all study sites have eroded during more energetic periods, and sediment accumulated offshore. During the monitoring periods of 2 to 4 years, the elevation of the platforms reached an equilibrium, but other morphological dimensions are still developing. The new insights gained from this study enable the prediction of platform elevations along sandy beaches in low-energy, non-tidal environments, and have contributed to our insight in the underlying processes driving the morphological evolution.

2.2. Introduction

Coastal regions near open coasts, estuaries and lakes are some of the most densely populated regions of the world. Knowledge on morphodynamics is crucial for protecting and managing these areas. Most coastal research concerns high-energy or open coasts. Low-energy or sheltered beaches are expected to have similar, but less pronounced, morphodynamics compared to high-energy beaches. Therefore, only few studies have focussed on low-energy coasts (Eliot *et al.*, 2006; Lorang, Stanford, *et al.*, 1993; Nordstrom *et al.*, 2012; Vila-Concejo *et al.*, 2020) , implying that the knowledge on physical processes and morphodynamics in this field lags behind that of exposed beaches. Despite the importance of low-energy beaches for coastal protection, recreation, and ecology, morphodynamics remain poorly understood.

The terms low-energy, fetch-limited and sheltered are often used alternately to describe similar environments, such as the beaches of estuaries-, lakes, and reservoirs (Jackson et al., 2002; Nordstrom Jackson, 2012). The exact characteristics are poorly defined in the literature (Goodfellow *et al.*, 2005; Nordstrom *et al.*, 2012). According to Jackson *et al.* (2002) , definitions of low-energy vary from very small prevailing significant wave height, Hs<0.10 m (Nordstrom *et al.*, 1996) , to limited storm wave height, Hb<1.0 m (Hegge *et al.*, 1996) . The influence of tides is not explicitly considered in the definitions. In all definitions, it is agreed that morphological changes are storm-driven, as prevailing wave conditions have limited reshaping capacity (Jackson *et al.*, 2002; Nordstrom *et al.*, 2012).

Jackson *et al.* (2002) found that low-energy tidal sandy beaches often have a narrow, steep foreshore, with seaward a low gradient, subaqueous terrace. This terrace is often referred to as a "low tide terrace", "sub-tidal terrace" or "platform" and may be vegetated (Travers *et al.*, 2010). Several sites with such low-energy conditions and morphology are described in the literature (Eliot *et al.*, 2006; Goodfellow *et al.*, 2005; Lorang, Stanford, *et al.*, 1993; Lowe *et al.*, 2016; Mujal-Colilles *et al.*, 2019; Nordstrom *et al.*, 1996; Vila-Concejo *et al.*, 2010) .

Besides describing and analysing low-energy sites, several scholars have aimed to develop conceptual models describing the morphotype of these beaches. These descriptions range from beach states applicable to all energy levels (Wright *et al.*, 1984) to morphotypes for the low-energy beach face only (Makaske *et al.*, 1998). Although all these models roughly point in the same direction, described in section 2, the morphotypes are based on varying indicators. Some are based on wave energy and sediment characteristics, others just on one of both, or even just on the location of the beach (for a review, see Vila-Concejo *et al.* (2020)). Therefore, the morphodynamics of low-energy beaches as well as their most important drivers are largely unknown. Four study sites in lake Markermeer, the Netherlands, provide a unique opportunity to study the morphology of low-energy, non-tidal, sandy beaches. These beaches are subject to low-energy waves and have the commonly found steep foreshore and low-gradient platform.

The general profile shape of low-energy beaches is similar to profiles found in laboratory experiments with constant waves on an initially plane slope of sediment (Hallermeier, 1979). From these laboratory results, Hallermeier (1979) concluded that under controlled wave conditions, commonly an equilibrium profile is reached with a platform, which he called the submarine cut or wave cut with water depth dc (fig. 2.1). According to Hallermeier (1979), the equilibrium depth of this platform is at the depth where the surface waves reach the limit of their erosive action.

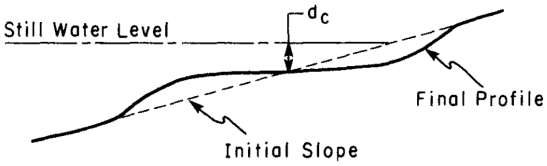

Figure 2.1: Equilibrium profile with sub-marine cut or wave cut as found from laboratory experiments with constant waves on an initially plane slope (reused from Hallermeier (1979)

Hallermeier (1980) developed a theoretical formulation to estimate the depth of closure, the depth at which wave action has negligible effect on sediment transport (d_s). It is calculated as follows:

$$d_s = 2.28H_s - 68.5\frac{H_{s,12h}^2}{gT_{p,12h}^2} \tag{2.1}$$

where $H_{s,12h}$ (m) and $T_{p,12h}$ (s) are the nearshore significant wave height that is exceeded for 12 hours per year and its associated wave period, and g is the gravitational acceleration (m/s^2). Hallermeier (1980) validated this formula with measured values for dc from laboratory tests. The laboratory experiments are representative for the hydrodynamic conditions and morphological platform development at our study sites, as is confirmed in section 4.1.

This study aims to analyse the morphological development of sandy, low-energy beaches and its relation to hydrodynamic forcing. Our central hypothesis is that the platform elevation at the study sites is governed by the depth of closure according to Hallermeier (1980). The next section describes conceptual models regarding morphotypes of low-energy beaches. Section 2.4 describes the field sites and methods. Section 2.5 shows the bathymetric features of the study sites, a quantification of hydrodynamic forcing and its relation to the cross-shore profile. In section 2.6 these results are discussed and lastly, section 2.7 gives the conclusions.

2.3. Low-energy beaches - morphotypes and classifications

Several researchers have pursued to classify the low-energy beach and describe its shape in different morphotypes. Wright *et al.* (1984) describe the beach state based on the dimensionless fall velocity, given by $\Omega = H_b/(w_s * T_p)$, where H_b is significant breaking wave height (m), w_s is fall velocity (m/s) and T_p is peak wave period (s). Beach states ranging from reflective ($\Omega < 2$) to intermediate ($2 < \Omega < 6$) to dissipative ($\Omega > 6$) are described and linked to wave steepness and sediment characteristics. A reflective morphology is expected for low-energy beaches. Features of a reflective beach according to Wright *et al.* (1984) are a steep, usually linear, beach face, with on the offshore side a pronounced step, after which the bed slope decreases considerably. Although beach states for a wide range of Ω (1 to >6) are described, the method is derived from high-energy beaches. Therefore doubts exist on whether low-energy beaches fall within the scope of this approach. Jackson *et al.* (2002) state that low-energy beaches can be classified as either reflective or dissipative if the nomenclature by Wright *et al.* (1984) is followed, since rips and other 3D bed forms are not observed at low-energy beaches. Hegge *et al.* (1996) consider low-energy beaches to be described by the reflective beach state. However, the single reflective beach state cannot adequately describe the wide range of profile slopes and concavities observed on low-energy beaches. Therefore they identified four classifications from 52 low-energy beach profiles, categorized by dimensions, slope curvature and grain size. The morphotypes for low-energy shores, ordered from less to more exposure are: (1) concave, (2) moderately concave, (3) moderately steep,

and (4) stepped, with the latter as exception since this type does not fit in this order (figure 2). The beaches were ordered from fully protected to fully exposed based on hydrographic charts, leaving hydraulic conditions unquantified.

Similar to the analysis by Hegge *et al.* (1996), Travers (2007) identified four low-energy beach types. She quantified the exposure with the exposure factor $E_f = log(Fl/Ms)$, where Fl is the direct fetch length and Ms is the marginal shoal width. The most protected sites have the lowest exposure factor. From least to most exposed, the beach types are: (1) exponential, (2) segmented, (3) concave-curvilinear and (4) convex-curvilinear (figure 2.2).

Although the shapes by Travers (2007) are different from Hegge *et al.* (1996), the general outline is quite similar. More sheltered beaches show a more pronounced terrace, while more exposed shores have a more or less plane slope.

Besides these state classifications, some conceptual models for the beach face of low-energy beaches have been developed. Based on field sites in estuaries in the U.S.A., Jackson *et al.* (1992) give a qualitative description of the morphodynamics. They found that sediment exchange is limited to a zone between the upper limit of swash at high water and the break in slope separating the foreshore from the low-tide terrace, since there is insufficient energy to mobilize sediment on the low-tide terrace. During a typical storm, the upper foreshore would erode and the sediment would be deposited on the lower foreshore. Parallel slope retreat of the foreshore can occur as a result of high-energy events or prolonged periods of unidirectional longshore currents.

A second low-energy beach face model is developed by Makaske *et al.* (1998). They described the morphological changes of the micro-tidal, low-wave beach face of the Rhone Delta in France, to extend the study by Wright *et al.* (1984). Cross-shore profiles were measured during one spring-neap tide cycle, excluding storm conditions from the results. Three types of "base profiles" were defined, ordered from lower to higher wave energy: the straight profile (daily $H_b < 0.25m$), the concave profile and the convex-concave profile (daily $H_b > 0.35m$).

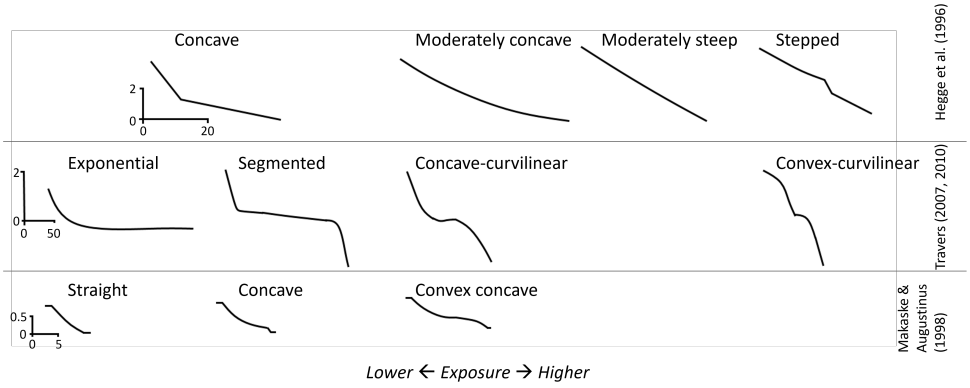

Figure 2.2: Low-energy cross-shore beach morphotypes by and adjusted from Hegge *et al.* (1996), Makaske *et al.* (1998), and Travers (2007)

The different morphotype models coincide more than seems. Figure 2.2 shows the conceptual models ordered from less (left) to more (right) exposure. Similar profile shapes from different sources are aligned vertically. For instance, the straight beach face coincides with the exponential/concave profile and a convex concave beach face is similar to the concave-curvilinear and moderately concave profile.

In summary, the least exposed sites generally have the steepest and narrowest beach face and the strongest breaks between the swash zone and the terrace. The different models all point towards wave energy and sediment characteristics as drivers for different morphotypes, but quantification is different per study or even absent. The physical relation between hydrodynamics and morphology has at most been described in general terms and morphological evolution over time has received even less attention.

2.4. Study Sites & Methods

2.4.1. Study sites

As mentioned above, the four study sites are artificial beaches located in lake Markermeer. Lake Markermeer is a shallow (~4 m deep) inland fresh-water lake without tide in the Netherlands (fig. 2.3). The lake has regulated summer and winter water levels, respectively NAP-0.2 m and -0.4 m, where NAP is the vertical reference datum in the Netherlands, close to mean sea level. Since waves are fully determined by local wind in this area, on average coming from the south-west, there is a strong positive correlation between wave height and wind set-up (Steetzel *et al.*, 2017). Since the lake is shallow, waves are depth-limited. The significant wave height does not exceed 1.5 m and the peak wave period is typically between 2.5 and 3.5 s during storms. Average and 95-percentile values of the significant wave height do not differ much between the study sites (table 2.1). Lake Markermeer is separated from Lake Ijsselmeer by a dam, the Houtribdijk, which is the location of the first study site, the Pilot Houtribdijk (fig. 2.3). This was a pilot study into dike reinforcement by sandy foreshores (Penning *et al.*, 2015). The 300 m long beach, closed off by a sheet pile wall at the northwest side, was constructed and monitored from 2014 until it merged into the sandy dike reinforcement in 2018. The other three study sites are located at the Marker Wadden, constructed in 2016 (fig. 2.3). This artificial archipelago consists of shallow marsh islands, protected by three stretches of sandy beaches and dunes and is meant to improve water quality and ecological habitats in this area. Pilot Houtribdijk was constructed of sand with a D50 of 270 μm and the Marker Wadden beaches of sand with a D50 of 350 μm.

2.4.2. Monitoring

At all sites, bathymetric data was collected using a singlebeam (Pilot Houtibdijk) or multibeam (Marker Wadden) echosounder, while shallow bathymetric data were measured by a moving RTK-GNSS-carrier (Rijkswaterstaat *et al.*, 2018). The

	Mean H_{m0} [m]	95-percentile H_{m0} [m]	Period
Pilot Houtribdijk	0.20	0.54	Oct 2014 – Mar 2018
Noorderstrand	0.26	0.53	Apr 2019 – Sep 2019
Zuiderstrand/ Recreatiestrand	0.27	0.63	Apr 2019 – Sep 2019

Table 2.1: Significant wave height characteristics study sites

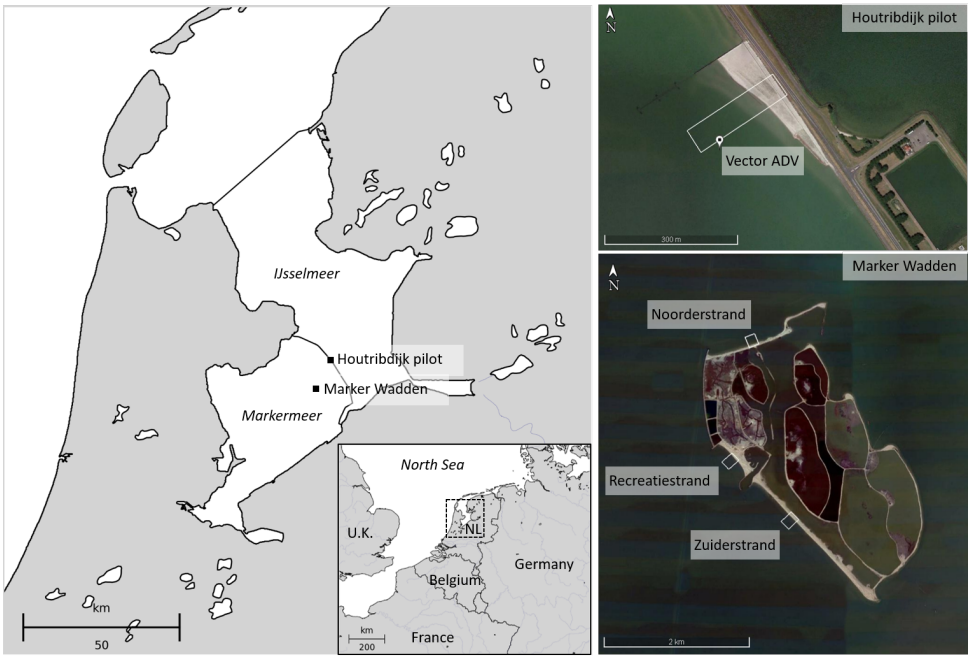

Figure 2.3: Overview location of the study sites, Pilot Houtribdijk and Marker Wadden beaches, in the Netherlands (NL), with considered transects within the white boxes. Right images from Google Earth, Landsat/Copernicus.

GNSS carrier was also used to monitor topography at Pilot Houtribdijk, while at the Marker Wadden, topographic data was collected by aerial mapping with a drone (structure-from-motion) (Natuurmonumenten, 2019). The singlebeam and multibeam have a typical vertical accuracy of respectively ±0.1 and ±0.2 m, while the RTK-GNSS and aerial mapping respectively have a typical vertical accuracy of ±0.03 m and ±0.05m.

At Pilot Houtribdijk, 43 transects with a spacing of 15 m were monitored from September 2014 to March 2018 at 23 occasions, with intervals ranging from 1 to 6 months (table 2.2, fig. 2.4). The measurements from January 2018 onwards are not taken into account, since the Pilot was excavated for other research purposes

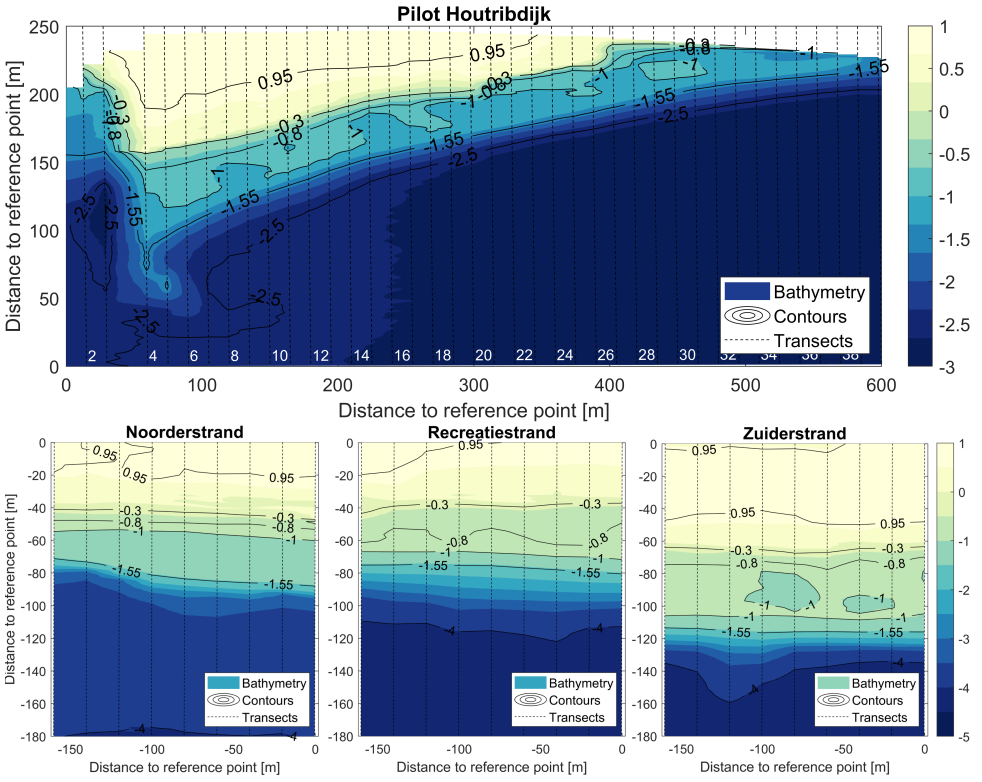

Figure 2.4: Bathymetry of the four study sites, the white numbers in the Houtribdijk plot represent the numbers of the transects. Pilot Houtribdijk was surveyed in April 2015, and the Marker Wadden sites in July 2018.

at that time. Longshore transport was evident at this location, proven by the rotation of the beach face due to varying wave angles. The platform elevation is similar over all transects (fig. 2.4), so to limit the effect of the rotation in the analysis, only the transects in the centre of the area (transect 10-14) are considered in this study. Morphological development of this 60 m wide area is studied by averaging these 5 profiles. At all three study sites on the Marker Wadden, 9 profiles with a spacing of 20 m were monitored every 3 months, from July 2018 to September 2019, and the same averaging method is followed (fig. 2.4).

Incoming waves and flow velocities were recorded from October 2014 to March 2018 by an underwater frame with a Nortek Vector ADV (8 Hz, velocity measurement point NAP-1.64 m, pressure gauge NAP-1.44 m), 100 m offshore of Pilot Houtribdijk (Steetzel *et al.*, 2017). The measurements were done in bursts of 8

19-9-2014	27-5-2016
25-10-2014	23-8-2016
19-11-2014	23-11-2016
28-12-2014	6-3-2017
23-1-2015	17-5-2017
15-2-2015	1-9-2017
18-3-2015	19-10-2017
6-4-2015	1-12-2017
21-8-2015	22-12-2017
25-1-2016	6-1-2018
28-2-2016	20-2-2018
	20-3-2018

Table 2.2: Monitoring occasions Pilot Houtribdijk

minutes per hour and corrected for atmospheric pressure and pressure attenuation.

2.4.3. Depth of Closure

To confirm that the morphological evolution of lake Markermeer beaches aligns with the conditions considered by Hallermeier (1980), we predict the depth of closure for Pilot Houtribdijk with equation 2.1. We use the classic definition of the depth of closure, where wave induced sediment transport is negligible, which should therefore be a proxy for the platform elevation. To make an accurate approximation and analyse the development over time, we predict the depth of closure for each storm event. This classic approach is different from the method often used nowadays, where the depth of closure is used to find the deepest limit where sediment transport is negligible for (multi-year) time series of coastal profile evolution, as for instance done by Hinton *et al.* (1998). Nicholls *et al.* (1998) demonstrated that the Hallermeier (1980) approach defines robust estimates for the depth of closure, particularly for individual erosional events.

The predicted depth of closure is compared to the level of the corresponding platform from the bathymetry (see section 3.5). The depth of closure relative to datum (z_{DoC}) is found by subtracting d_s from a representative water level applicable during said storm event (fig. 2.6).

2.4.4. Hydrodynamic analysis

To predict the depth of closure per storm event, information on wave height, period and water level is needed. We executed a storm analysis on the wave data from the offshore Vector ADV at Pilot Houtribdijk. Storm events are determined through a peak analysis on the spectral significant wave height, H_{m0}, derived from the ADV data. For each peak, the height, prominence and duration are calculated. The peak prominence measures how much the peak stands out from

the surrounding baseline of the signal and is defined as the vertical distance between the peak and its lowest contour line. A peak in H_{m0} is selected if it fulfils the following three conditions (fig. 2.5):

1. The peak height is higher than the threshold significant wave height of 0.5 m;
2. The peak prominence is at least 0.3 m;
3. The peak duration at 45% (from the top) of the peak prominence is at least 5 hours

After selecting the peaks, the 12-hour exceeded wave height $H_{m0,12h}$ is calculated with a rolling window of 12 hours, listing the minimum H_{m0}. Subsequently, the maximum value of $H_{m0,12h}$ for the period from 6 hours before to 6 hours after each peak moment is selected as the $H_{m0,12h}$ for that storm. The 12-hour average peak wave period at the storm peak is used for $T_{p,12h}$.

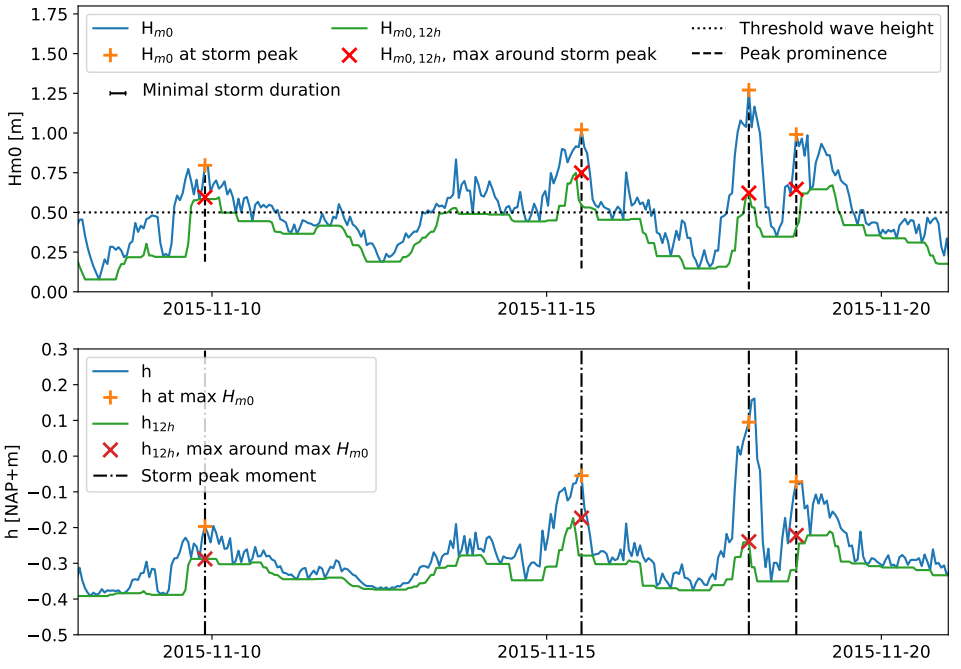

Figure 2.5: Example from storm peak analysis of H_{m0}, Pilot Houtribdijk. The wave heigh (H_{m0}), with the identified storm peaks, and the corresponding 12-hour exceeded wave height ($H_{m0,12h}$), with its storm peak height. The water level (h) at the storm peak moment and the corresponding 12-hour exceeded water level (h_{12h}), with its storm peak height.

For the representative water level needed to calculate z_{DoC}, Nicholls *et al.* (1998) suggest to use the Low Water Level or Mean Low Water. But since the

Lake Markermeer is non-tidal, we introduce another definition. We define the 12-hour exceeded water level during the storm, h_{12h}, as the vertical reference level to estimate the depth of closure (fig. 2.5). The 12-hour exceeded water level is calculated with a rolling window of 12 hours, listing the minimum water level. The maximum value of h_{12h} for the period from 6 hours before to 6 hours after each peak moment, as determined from H_{m0}, is the 12-hour exceeded water level for that storm. This calculation is identical to the method for $H_{m0,12h}$, but with the storm peak moments already determined from H_{m0}. The relative depth of closure is calculated as follows:

$$z_{DoC} = h_{12h} - d_s \tag{2.2}$$

To analyse the relation between hydrodynamics and morphological development, the storm analysis is extended to two-weekly characteristics, including cumulative wave energy. The wave energy is calculated, assuming a Rayleigh distribution, as $E = 1/16 \rho g H_{m0}^2$. The cumulative wave energy is equal to the sum of the wave energy at the peaks of all selected storms within the two weeks.

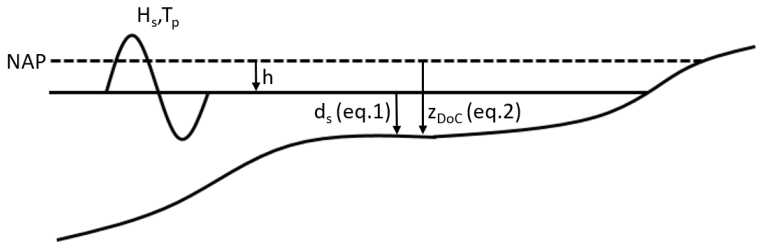

Figure 2.6: Visualisation definitions depth of closure (d_s), depth of closure relative to datum (z_{DoC})

2.4.5. Morphological quantification

We divided the cross-shore profile in three vertical sections to include the following morphological regions (fig. 2.7):

1. the beach face above the yearly average water level (beach face section),
2. the zone that includes the platform (platform section), and
3. the deeper part of the profile (offshore section).

These sections are separated by four vertical levels:

1. above the beach face (NAP+0.95 m),
2. at the annual average lake level (NAP-0.3 m),
3. at the submerged slope, just below the platform (NAP-1.55 m),

4. just below the lake bottom (Pilot Houtribdijk: NAP-2.8 m, Marker Wadden: NAP-4.2 m).

The vertical limits of these sections are chosen starting from the yearly average water level (NAP-0.3 m). From that level a distance is found that upward includes the beach face and downward the platform for all four locations, 1.25 m. The lowest limit is just below the flat lake bottom, offshore from the submerged slope below the platform. For Pilot Houtribdijk all sections are of equal height, and for the Marker Wadden locations the section height ratio for I:II:III is approximately 1:1:2. The upper vertical limit at NAP+0.95 m is translated into a horizontal limit for the first measurement in time per transect, to create a fixed onshore boundary and more clearly demonstrate beach face erosion. The offshore boundary for Pilot Houtribdijk is at 250 m, after which no bathymetric data is available. For the Marker Wadden sites, this boundary lies at 150 m, since data availability is variable offshore from that point. This method of following volume change in vertical sections over time is similar to that of Steetzel *et al.* (2017), but with a slightly adjusted volume definition, for a longer time span and for more study sites.

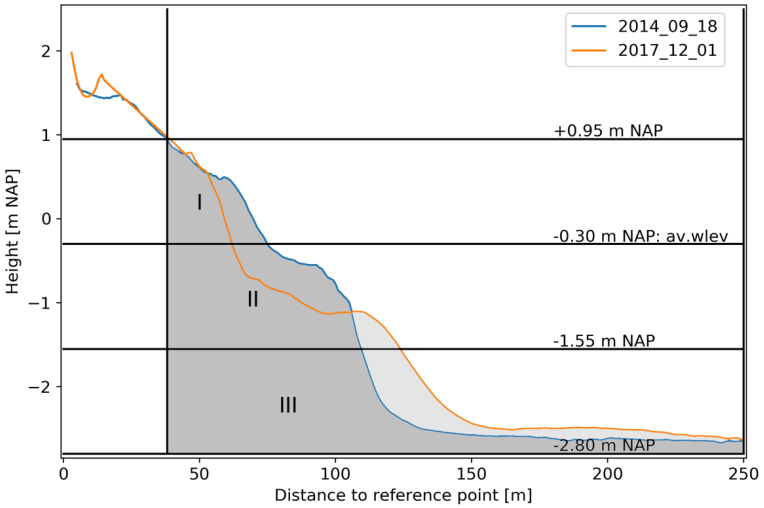

Figure 2.7: Method of volume calculation at Pilot Houtribdijk, showing section I: beach face section, section II: platform section and section III: offshore section. In dark grey the volume corresponding to the profile at September 18, 2014.

The average platform height is the average height of the profile in the platform section. The slopes of the beach face and the slope in the offshore section are determined at respectively the yearly average water level (NAP-0.3 m) and the transition between the platform section and the offshore section (NAP-1.55 m). The local slope in each of these two points is estimated from a 2 meter profile section centered around these two locations of interest.

2.5. Results

2.5.1. Bathymetric features

All four study sites in lake Markermeer display a similar profile shape and a similar development over time (fig. 2.8). At the Pilot Houtribdijk site, where morphological development has been monitored from construction onwards, a subaqueous platform evolved within the first months at NAP-1.0 m, on average at 0.7 m below water level (fig. 2.8). The same is visible for the sites at the Marker Wadden. The beaches at Noorderstrand and Recreatiestrand were constructed in late 2016, and reconstructed a few times between then and March 2018. The beach at Zuiderstrand was constructed and reconstructed between late 2017 and March 2018. Because of the number of human interventions, it is not possible to give an as-built situation, but below NAP+1 m the initial plane slope was approximately 1:20 for all the Marker Wadden beaches. At these sites, a platform is also visible at NAP-1.0 m, but the initial development took place before the first measurement (fig. 2.8). The platforms vary in width from 30 to almost 60 m, depending on the location and the time. The profiles connect to the original lake bottom at NAP-2.8 m (Pilot Houtribdijk) and -4.2 m (Marker Wadden) with a steeper slope.

All locations have a steep beach face, although at Noorderstrand it has a slightly lower gradient (table 2.3). Moreover, the Noorderstrand beach face slope varies substantially over time. The beach face slopes of the other three locations are very comparable. The average offshore slope is similar for all four locations.

	Slope (1:x)		Platform elevation (m NAP)
	Beach face ($\mu \pm \sigma$)	Offshore ($\mu \pm \sigma$)	
Pilot Houtribdijk	9 ± 1	14 ± 2	-0.93
Noorderstrand	20 ± 7	14 ± 4	-1.11
Recreatiestrand	11 ± 3	13 ± 2	-0.89
Zuiderstrand	11 ± 2	14 ± 3	-1.00

Table 2.3: Bathymetric features, averaged over time and transects

The bathymetric data show a retreat around the water line at all sites. Because of erosion on the beach face, the platform widens over time, growing in both onshore and offshore direction for all sites, except for Recreatiestrand. There the slope below NAP-1.55 m is more or less stable.

2.5.2. Depth of Closure

The characteristic storm wave height $H_{m0,12h}$, wave period $T_{p,12h}$ and base water level h_b are derived from the hydraulic data (fig. 2.9). The 12-hour exceeded H_{m0} varies around 0.5 m, while the maximum storm peak H_{m0} is around 1.3 m (fig. 2.9). The maximum storm wave height is relatively stable, since the wave height is depth-limited in lake Markermeer.

Per period of two weeks, the average, minimum and maximum values of $H_{m0,12h}$

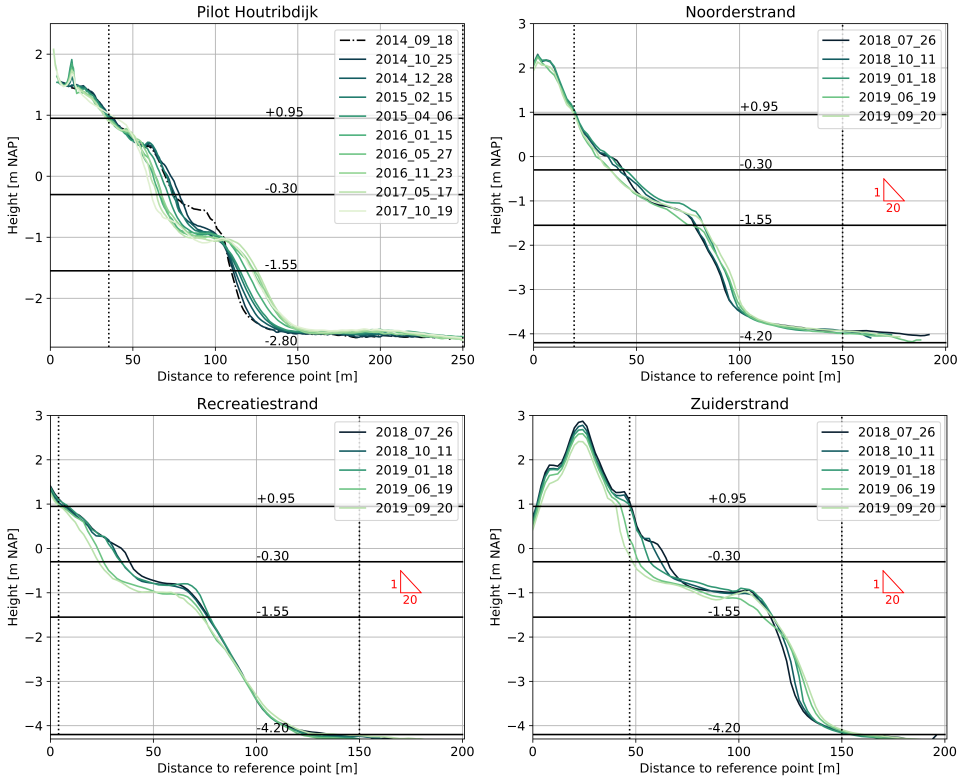

Figure 2.8: Development of the average cross-shore profile at the four study sites, with the as built profile at Pilot Houtribdijk (dashed line) and the as built angle at the Marker Wadden locations (1:20) and the vertical section division for the morphological quantification.

and $T_{p,12h}$ are used to calculate the average, minimum, and maximum depth of closure. At times with more than two different storms per two weeks, the minimum and maximum depth of closure can differ up to almost a meter. The instantaneous z_{DoC} per storm fluctuates between $z_{DoC,min}$ and $z_{DoC,max}$. Averaged over the whole period, $z_{DoC,av}$, $z_{DoC,min}$ and $z_{DoC,max}$ differ -0.07 m, 0.03 m and -0.18 m respectively from the average platform height. For individual storms, z_{DoC},max can be up to 0.42 m lower than the average platform height. However, the average z_{DoC} (av. h_b –av. d_s) stays relatively stable over time, and varies around NAP-1.0 m (standard deviation over all transects: 0.23m). This accurately corresponds to the actual average platform height at the Pilot Houtribdijk. At the study sites at the Marker Wadden the platform height is also situated around NAP-1.0 m (fig. 2.8). Unfortunately no long time series of hydrodynamic data is available for these sites. Analysis of short time series shows that the wave climate at the Marker Wadden is similar to that of Pilot Houtribdijk (table 2.1),

as are the sediment characteristics. Therefore, we can assume that the depth of closure for the Marker Wadden sites is in the same order of magnitude. The platform at these locations is also situated around NAP-1.0 m (fig. 2.8), which confirms the results at Pilot Houtribdijk.

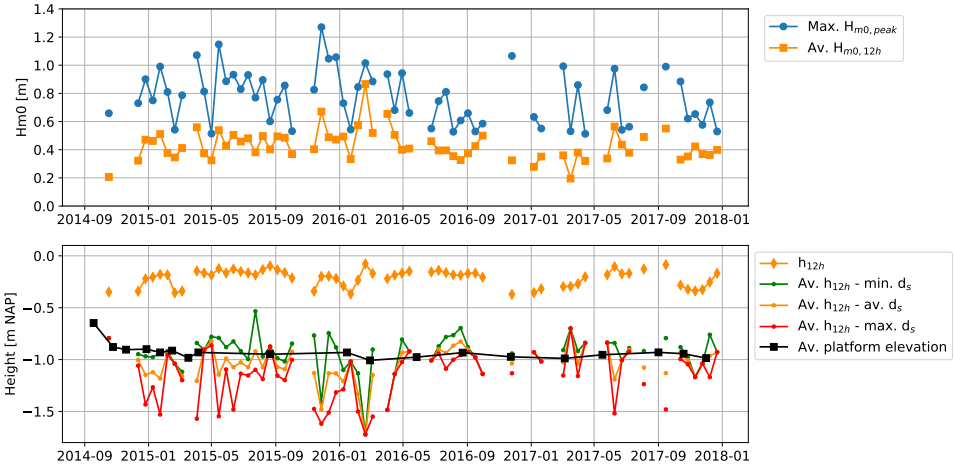

Figure 2.9: Top frame: Maximum peak storm wave height per 14 days (Max. $H_{m0,peak}$) and average peak storm wave height per 14 days (Av. $H_{m0,12h}$). Bottom frame: 12-hour exceeded water level (h_{12h}), subtracted by minimum (min.), average and maximum depth of closure (d_s), compared to the average platform elevation.

2.5.3. Volume changes in time

To quantify morphological developments in time, cross-shore volume changes are calculated for different sections (fig. 2.7). This analysis reveals that the volume of the beach face decreases over time for all four study sites (fig. 2.10, fig. 2.13). The volume around the platform steadily decreases at Pilot Houtribdijk, while for the sites at the Marker Wadden, the decrease in volume only occurs after a period of 6 months with stable or even increasing volumes. At Pilot Houtribdijk, Noorderstrand and Zuiderstrand, the beach face and platform per location develop at a comparable pace, while the offshore volume is gradually increasing. At Recreatiestrand, the offshore volume change fluctuates around zero, and increases and decreases mostly simultaneously with the platform volume, thus all sections develop in the same manner. The total volume at the selected transects of Pilot Houtribdijk and Noorderstrand increased over time, while at Recreatiestrand and Zuiderstrand, a nett decrease took place.

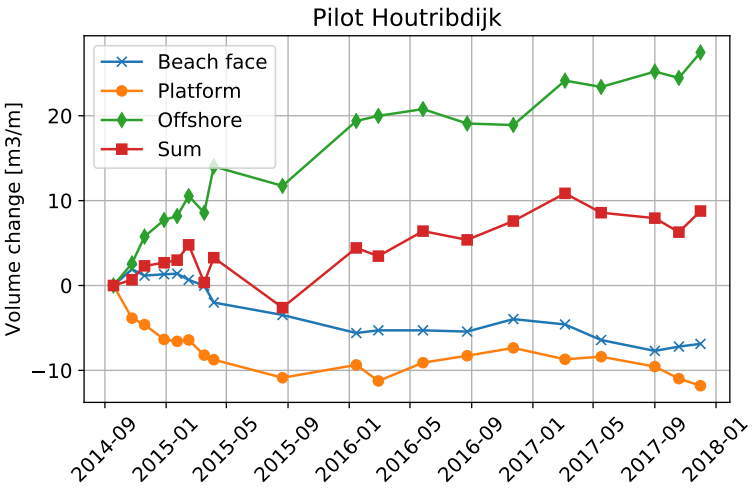

Figure 2.10: Volume change per section since September 2014, at Pilot Houtribdijk.

2.5.4. Relation between volume changes and wave conditions

The wave climate in 2015 is quite energetic year-round, whereas and especially 2016 and 2017 are relatively more calm, as is visible in the cumulative wave energy (fig. 2.12). In general, no seasonality in the wave climate is visible for these years, and both average wave height (0.6 to 0.9 m) and maximum peak storm wave height (0.8 to 1.2 m) are fairly constant throughout the year (fig. 2.12).

The erosion or sedimentation rate varies over the period of observation, with slightly higher rates at the beginning of the monitoring period (grey highlight) and a distinct deviation in April 2015 (fig. 2.12). The rapid changes in the first months after construction concern the initial profile development. The sedimentation peak of the offshore section in April 2015 does not coincide with a peak in wave energy event, the cause is unknown. Note that the rate of volume change (in $m^3/m/day$) in the lower panel is influenced by the interval between bathymetric surveys, with more frequent surveys, and therefore a more volatile rate of change in the first months after construction. The energetic periods between May 2015 and February 2016 and between February 2017 and September 2017 (red highlight) coincide with erosion of the beach face. Volume changes of the platform section do not strictly correspond with energetic periods, although erosion is slightly more common in periods with high wave energy. The offshore volume is growing in energetic periods, but not exclusively in these periods. During the energetic period between September and December 2017 (yellow highlight) the beach face volume is increasing, contradictory to the earlier trends. In this period, sedimentation on the top of the beach face is observed (fig. 2.8).

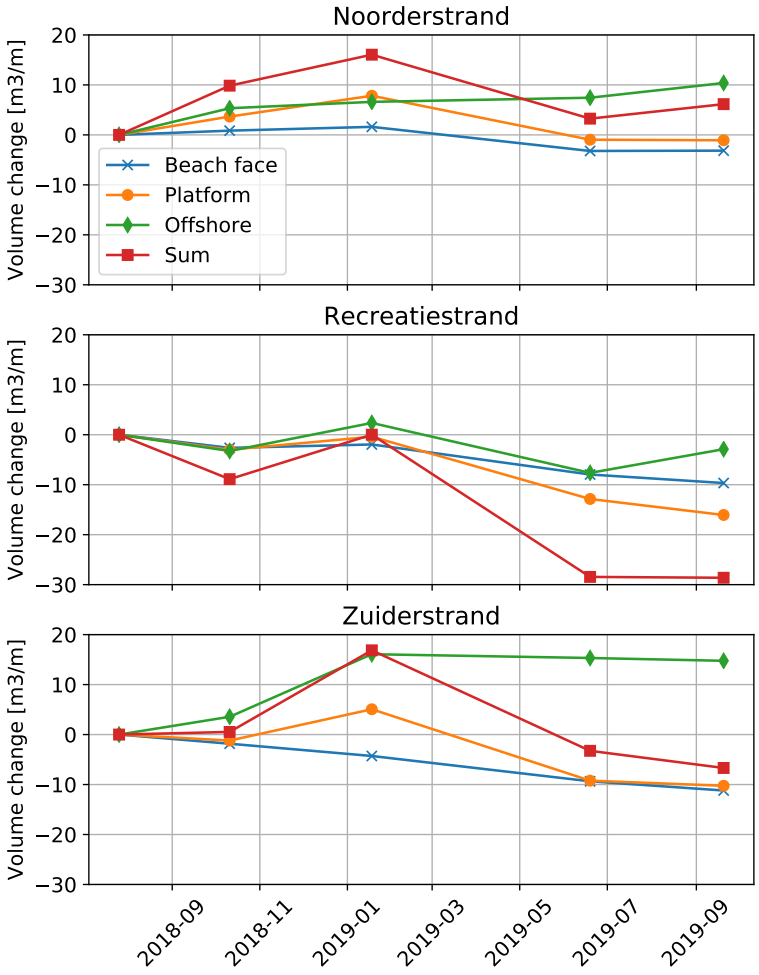

Figure 2.11: Volume change per section since July 2018, at Marker Wadden.

2.6. Discussion

The shape of low-energy beach profiles in lake Markermeer corresponds to the general description by Jackson *et al.* (2002), with a steep beach face and low-gradient platform. From the four considered sites, only the relatively sheltered site Noorderstrand has a less steep beach face and shows a less distinct break between the swash zone and the platform. The elevation of the characteristic platforms, at approximately NAP-1.0 m, might be explained by applying the depth of closure formula by Hallermeier (1980) (equation 2.1). The laboratory conditions to which his formula was validated, constant waves at a constant water level onto an initially plane slope, correspond well to the conditions at the study sites.

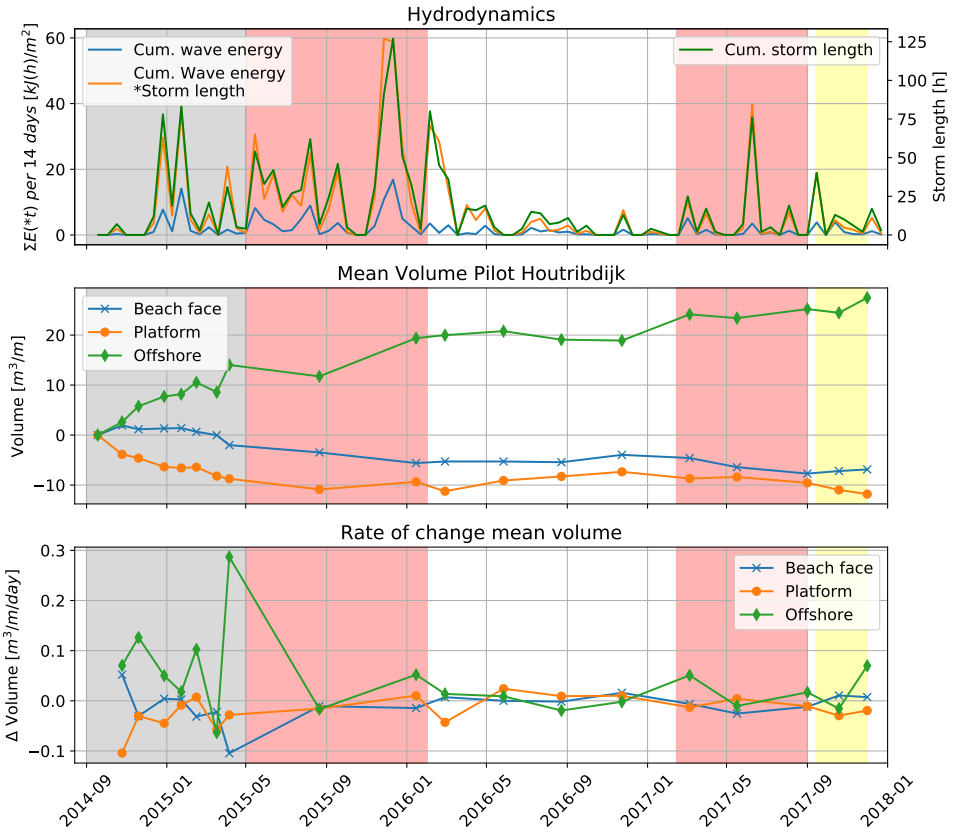

Figure 2.12: Hydro- and morphodynamics Pilot Houtribdijk. Top frame: Cumulative wave energy and average and maximum H_{m0} per 14 days. Middle frame: Volume change per section normalised to the first measurement. Bottom frame: Change to rate of volume change. Grey area: initial profile development after construction. Red areas: periods with energetic wave climate. White area: periods with calm wave climate. Yellow area: period with energetic wave climate but aberrant morphological change.

Despite these similarities, some assumptions in the calculation method are debatable. For non-stationary conditions, a time scale should be chosen for events that determine the equilibrium limit or potential depth of closure. In the analysis by Nicholls *et al.* (1998) for high-energy coasts, the 12-hour exceeded H_{m0} gave the best results for the event dependent depth of closure compared to 6 hours and 18 hours. This duration has also been applied in the current study for low-energy beaches in lake systems. However, the response of water levels and waves in a lake like Markermeer is much quicker than in oceans and seas. As this

choice influences z_{DoC} to a certain extent, a sensitivity analysis is added here.

Since water levels and waves in lake Markermeer respond quicker to wind variations than on open coasts, the 12-hour exceeded H_{m0} covers a large part of the storm, while on high-energy beaches, it only covers the peak. The use of for instance the 6-hour exceeded H_{m0}, would imply that the relative depth of closure, z_{DoC}, would be calculated relative to the 6-hour exceeded water level. From the hydrodynamic data of Pilot Houtribdijk, it follows that averaged over the full period, $H_{m0,6h}$ is higher than $H_{m0,12h}$, h_{6h} is higher than h_{12h} and $z_{DoC,6h}$ is deeper than $z_{DoC,12h}$, but the differences are small (table 2.4). However, for individual storms z_{DoC},6h can be up to 0.49 m deeper than $z_{DoC,12h}$. Although the method is sensitive for individual storms, it is robust when averaged over a longer period, independently of the exceedance period. The observed platform elevation is on average NAP-0.93 m and at the minimum NAP-1.01 m, therefore with the current information the exceedance period of 12 hours gives the best result.

	12h	6h	difference
$H_{m0,xh}$ [m]	0.42	0.53	0.11
h_{xh} [NAP+m]	-0.21	-0.16	0.05
z_{DoC} [NAP+m]	-1.03	-1.17	-0.14

Table 2.4: Sensitivity analysis of 12 hour compared to 6 hour exceedance values of significant wave height (H_{m0}), water level (h) and resulting depth of closure (z_{DoC}).

Although the time-averaged $z_{DoC,12h}$ fits very well with the observed platform elevation, it varies considerably over time. For a high-energy event with z_{DoC} significantly deeper that the platform elevation before the event, it is not expected that the platform will lower with for instance 0.42 m within 12 hours or a similar period. However, a series of events with a z_{DoC} lower than the platform elevation could cause a lowering. With more frequent monitoring of the bathymetry compared to fig. 2.9, the timescale of these morphological developments could be studied.

More elaborate monitoring on the depth of closure could also shed more light on the optimal reference water level for non-tidal environment. Nicholls *et al.* (1998) stated that the best reference is Low Water Level or Mean Low Water in tidal systems. The here used 12-hour exceeded water level is a somewhat conservative choice, since it basically represents the water level before and after the storm, while there is a set-up during the storm. However, the results presented in this chapter clearly demonstrate that the platform elevation is controlled by the depth of closure.

Development over time is described for our four study sites, but are they underway to equilibrium? According to Jackson *et al.* (2002), low-energy beaches do not reach an equilibrium state, but represent a storm artefact or state. But, since morphotypes are based on hydrodynamic conditions in more recent studies (Travers, 2007), we would expect that for relatively constant hydrodynamic conditions, a dynamic morphological equilibrium should be possible. After the short

adaptation time, the elevation of the platform of our four study sites reached an equilibrium. Since lake level fluctuations are minimal in the non-tidal lake Markermeer and wave height and surge are always positively correlated, this was expected and we can attribute the equilibrium elevation of the platform primarily to wave action. In other situations, most likely both wave action and continued water level variations are responsible for the platform elevation. The frequency and duration of these fluctuations may influence the elevation of the platform (Eliot *et al.*, 2006), and may lead to variations over time.

Yet, the analysis of the morphology revealed that at none of the four study sites the other morphological dimensions have reached equilibrium yet. For Pilot Houtribdijk, the rate of change slowed down over time, but it did not fully stop after four years. At the Marker Wadden, the morphology is still in full development after little over two years of transformation. Physically, we would expect this process to find an equilibrium once the platform is wide enough to bring the wave height down so wave-induced sediment transport is negligible near the shoreline. Since the platform has a very low gradient, a very wide platform might be needed to meet this condition.

Longshore transport processes are not explicitly addressed in this chapter. As natural morphologies of low-energy beaches look similar to laboratory results with only normally incident waves (Hallermeier, 1979), it is a fair assumption that the steering processes are alike and that this typical shape develops due to cross-shore sediment transport. This is also confirmed in field studies such as the study by Lorang, Komar, *et al.* (1993) at Flathead Lake in the United States, where morphology is said to develop through cross-shore transport. However, when inspecting the cross-shore development over time, the offshore-directed growth does not seem to balance out the onshore erosion (fig. 2.8). Moreover, the total volume at the selected transects of Pilot Houtribdijk and Noorderstrand increased over time, while at Recreatiestrand and Zuiderstrand, a net decrease took place. This is inevitably linked to longshore transport processes. At Pilot Houtribdijk, the total sediment budget, over all transects, was kept in dynamic equilibrium due to the presence of a sheet pile wall (Steetzel *et al.*, 2017). The increase at the middle transects was countered by a decrease at the off-centre transects. Noorderstrand, oriented under an angle compared to the common wave incidence (SW), must be influenced by longshore transport. Since Recreatiestrand and Zuiderstrand are constructed in such way that they are oriented normally to the average angle of wave incidence, negligible nett longshore transport was expected. The sediment budget was negative in September 2019, but perhaps the measurement period was too short to conclude nett erosion.

To summarize the above, we have attempted to introduce a conceptual model of the morphodynamic processes on the low-energy, non-tidal beach. The overall beach face erosion combined with simultaneous accretion lower in the profile suggests that sediment transport in this area is primarily in cross-shore direction. This sediment reaches the platform and most likely travels further in both cross-shore and longshore direction, to meet the equilibrium depth. During calm conditions the depth of closure is limited, causing sediment that has previously been

eroded from the beach face to accumulate on the platform. Since the depth of closure is deeper during more energetic periods, erosion over the total platform occurs primarily in these periods. Sediment that is transported "over the edge" of the platform will settle and be deposited on the slope below the platform. In accordance with the Hallermeier (1980) definition, no wave-driven transport can occur in the region below the depth of closure. Therefore, these sediments will not return shoreward causing profile changes in the region below depth of closure. Model simulations can be used to further our insight in the sensitivity and variability of these morphological processes.

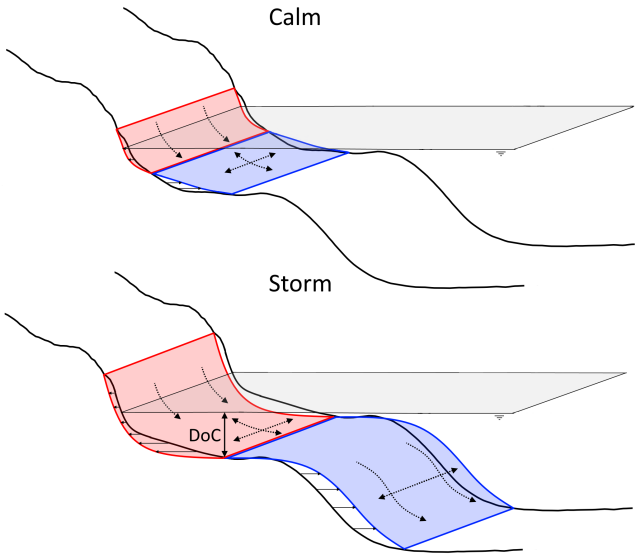

Figure 2.13: Visual summary of conceptual model of morphodynamics on a low-energy, non-tidal sandy beach during calm and stormy periods. Red: general erosion; blue: only sedimentation; dotted arrows: possible sediment transport directions; grey: yearly averaged water level.

2.7. Conclusions

The goal of this research was to understand the morphological development and hydrodynamic forcing of low-energy, sandy beaches. Through a literature analysis into morphotype classifications of these environments, the general morphology in these environments was characterized. Bathymetric developments were monitored at four low-energy, non-tidal study sites in the shallow lake Markermeer in the Netherlands. Here the typical low-energy morphology with a narrow beach face and low-gradient platform, as described by Jackson *et al.* (2002), was observed.

The sandy beaches at the study sites were all constructed in recent years, showing a rapid initial profile adjustment during the first years after implementation. Based on measurements of waves and water levels, the depth of closure (Hallermeier, 1980) was calculated and compared to the elevation of the platform. We conclude that the elevation of the platform is indeed located near this depth of closure, and that after reaching this depth, the platform elevation stays relatively stable.

The morphological development was quantified through calculating the volumes of three vertical zones in the cross-shore profile: beach face, platform, and offshore. Both longshore and cross-shore transport are responsible for the development of platform. Results suggest that erosion of the beach face is primarily by storm-driven cross-shore transport, after which the sediment is most likely diffused both cross-shore and longshore over the platform and offshore sections. Although the depth of the platform is stable, the platform width did not reach an equilibrium for the oldest study site (4 years) and the widening is still in full development at the younger sites (2 years).

The typical low gradient platform of the low-energy, non-tidal sandy beach develops at the depth of closure. This insight is an important step towards the prediction of morphology in low-energy environments and contributes to the future prospect of implementing sandy beaches in environments such as lakes, reservoirs and micro tidal seas for purposes such as shoreline protection, wave energy dissipation for flood risk reduction or recreation.

Acknowledgements

This research is part of the LakeSIDE project, which is funded by Rijkswaterstaat.

The partnership for the project pilot Houtribdijk consists of Rijkswaterstaat and an EcoShape consortium involving the research institutes Deltares and Wageningen Environmental Research, contractors Boskalis and Van Oord and engineering companies Arcadis Nederland BV, RoyalHaskoningDHV and HKV Consultants. Shore Monitoring is acknowledged for carrying out the morphological surveys for this project.

The research at the Marker Wadden was supported by the Marker Wadden Knowledge and Innovation Programme (KIMA), initiated by Rijkswaterstaat, Deltares, EcoShape and Natuurmonumenten. See https://kennismarkerwadden.nl/english/.

3

Longshore sediment transport by large-scale lake circulations: A field and model study

Highlights:

- In shallow, wind-dominated lakes, gradients in water level set-up can induce large-scale, horizontal circulations.
- These large-scale circulations influence the nearshore longshore currents and are dominant over wave-driven longshore currents for most wind conditions.
- The large-scale lake circulations influence longshore sediment transport on lake beaches and have a significant impact on design and maintenance.

This chapter has been published as: **Ton, A.M.**, Vuik, V., Aarninkhof, S.G.J. (2023). Longshore sediment transport by large-scale lake circulations at low-energy, non-tidal beaches: A field and model study. Coastal Engineering, 180.

3.1. Abstract

Low-energy, non-tidal lake beaches are known to be subject to longshore morphodynamics, but the impact of large-scale currents compared to wave-driven currents and the origin of these circulations is not known. Lake Markermeer is a shallow (~4 m deep), wind dominated lake, with even shallower areas in the northwestern part. A gradient in wind-induced water level set-up at the leeward shore induces a flow from shallow to deep, causing large-scale circulations. Flow measurements and results from a numerical Delft3D model of the lake show that these circulations are horizontal and impact the nearshore currents greatly, even more than wave-driven longshore currents for most wind conditions. From nearshore measurements at the first study site in lake Markermeer combined with bathymetrical data, we found a clear relation between longshore sediment transport capacity, based on flow, and volume flux. The model can predict flow direction and magnitude for several wind conditions. Using wind statistics, the net transport capacity for a short period or a long term mean can be predicted. This is validated with a second study site, which shows a distinct net transport capacity that would not be expected from wave-driven longshore flow alone. Concluding, large-scale lake circulations are of vital importance for the morphological development of low-energy, non-tidal beaches in shallow, wind-driven water bodies. Knowledge of these circulations and their dependence on wind characteristics can help better understand and predict longshore transport.

3.2. Introduction

Hydrodynamic and morphological processes at low-energy or sheltered beaches can be significantly different compared to open, high-energy coasts, contrary to what was thought in the past (Eliot *et al.*, 2006; Lorang, Stanford, *et al.*, 1993; Nordstrom *et al.*, 2012; Vila-Concejo *et al.*, 2020). Low-energy beaches, commonly characterised by a small prevailing wave height and limited storm wave height, are in all definitions considered to have storm-driven morphodynamics.

Ton *et al.*, 2021 have set up a conceptual model for morphological development of low-energy, sandy coasts during calm and storm conditions in the cross-shore direction, based on data from newly-constructed lake beaches. However, longshore morphological development is also deemed important. When low-energy environments are (partially) sheltered, large alongshore variations in wave energy can be found. Moreover, if waves are fetch-limited and therefore have a short period, they are less affected by refraction and increase the potential for strong wave-driven longshore currents. Dominance of cross-shore or longshore processes is dependent on shoreline orientation to the dominant winds and fetch, and the presence of (shore-normal) obstacles, such as groynes, that act as sediment traps (Jackson *et al.*, 2002).

Nutz *et al.*, 2018 describe that relatively shallow lake environments with a large fetch for the dominant wind direction, are influenced mostly by a wind-induced lake-scale water circulation and aforementioned wave-related processes. They concluded that water bodies, for which the ratio between the dominant fetch

[km] and mean depth [m] (I_{WWB}) is over 3, can be categorised as wind-driven water bodies. These water bodies are characterised by wind-induced surface currents, which go down at the downwind side of the lake, from where they generate a return flow in the lower part of the water column towards the upwind side of the lake. However, usually these lakes are narrow and have a dominant wind direction in longitudinal direction. A lake with irregularly shaped subbasins and an overall complex geometry, like Taihu lake, China, can show an intricate pattern of circulations (Liu *et al.*, 2018). For this very shallow lake (< 3 m), wind shear is thought to be an important driver of these circulations and vertical variations are bound to relatively deeper parts of the lake. The morphology of wind-driven water bodies commonly shows shoreface-connected ridges (e.g. longshore, flying or cuspate spits), wave-cut platforms and various cross-shore structures (e.g. surf bars, beach cusps and berms) (Ashton *et al.*, 2009; Schuster *et al.*, 2005).

Two study sites in lake Markermeer, the Netherlands, provide a unique opportunity to study longshore transport along low-energy, non-tidal beaches. With an I_{WWB} of approximately 10, lake Markermeer classifies as a wind-driven water body. Moreover, some of the sedimentary characteristics are also recognised in lake Markermeer, such as wave-cut platforms (Ton *et al.*, 2021), spits and cusps. These wind-driven hydrodynamics are confirmed by Van Ledden *et al.*, 2006 and Vijverberg, 2008, who report that the Markermeer circulation currents are induced by pressure gradients due to wind-driven water level set-up. Besides the vertical circulation, they also describe horizontal components for the Markermeer. The horizontal circulation direction is thought to be related to shallower areas in the lake and other bathymetrical features. This is not specified in the literature, but we hypothesize that in the shallow areas in the north and west of the lake, water level set-up due to wind will be higher than in deeper areas, inducing a flow from shallow to deep. Vertical circulation velocity was estimated to be up to 0.35 m/s during 8 Beaufort wind and horizontal circulation was estimated between 0.1 and 0.2 m/s.

Although both cross-shore and longshore processes have been appointed as drivers for morphological development on low-energy beaches, the importance of either one is not clear. Moreover, the influence of wind driven circulation on longshore currents and transport is thought to be important (Nutz *et al.*, 2018), but is not quantified. When the low-energy beaches have a flood safety function, information on volume losses or gains due to longshore transport is of vital importance for developing an efficient maintenance strategy.

The goal of this research is to explore the nature of the large-scale circulation currents and assess how they affect nearshore longshore currents, relative to the importance of wave-driven currents. Moreover, we want to find out how these longshore currents affect longshore transport and what this implicates for the design of low-energy, non-tidal beaches.

The next section describes the study sites at which nearshore and offshore waves and currents were monitored, together with bathymetrical changes. It further describes the methods, among which the numerical model that was used. Section 3.4 shows the relation between the currents and morphological develop-

ment at the first study site and a validation via an application of the model to the second study site. In section 3.5 the results are discussed and the chapter ends with conclusions in section 3.6.

3.3. Study sites and methods

3.3.1. Study sites

Lake Markermeer is a shallow (~4 m deep) inland fresh-water lake with regulated water levels between approximately NAP -0.3 m and -0.1 m in summer and around NAP -0.25 m in winter (Rijkswaterstaat, 2018). NAP is the vertical reference datum in the Netherlands, close to mean sea level.

Lake Markermeer is separated from lake IJsselmeer by a dam, the Houtribdijk (fig. 3.1). Half of the Houtribdijk was reinforced by artificial sandy foreshores, constructed between 2018 and 2020 (Rijkswaterstaat, 2019). These sandy beaches provide a smooth transition between dike and lake, benefiting biodiversity and water quality in the lake. The first location, near monitoring station FL67, is located at the Houtribdijk on the side of the Markermeer (fig. 3.1). This beach is approximately 800 m long and situated between two groynes.

The second site is situated at the north side of the Marker Wadden. This artificial archipelago consists of shallow marsh islands, protected by two stretches of sandy beaches and dunes on the north and southwest side and a rubble mound revetment on the west side. The Marker Wadden are meant to improve water quality and ecological habitats in this area. They were constructed between 2016 and 2020 and extensions are still being built (Van Leeuwen *et al.*, 2021). The second site, FL66, is situated at the northwest side of the Marker Wadden archipelago, constructed since 2016. This beach is approximately 2100 m long in total, and 1400 m in between the dam on the southwesterly side and the "soft edge", the sandy protrusion on the northeasterly side. The 95-percentile H_{m0} at locations FL67 and FL66 is respectively 0.54 and 0.53 m (Ton *et al.*, 2021).

Generally the profiles of low-energy beaches have a steep foreshore with seaward a low-gradient, subaqueous platform (Jackson *et al.*, 2002). The Markermeer beaches show a similar profile shape, where the platform connects to the deeper lake bed with a steep slope (Ton *et al.*, 2021) (fig. 3.2).

3.3.2. Monitoring

At locations FL65, FL66, FL67 and FL68, approximately 400 m from the shoreline, ADCPs (Acoustic Doppler Current Profilers) were installed at the bed, looking up (fig. 3.1 and 3.2). These ADCPs measured current velocity and direction in layers over the water column. The bed levels at the four locations were NAP-4.50 m, NAP-4.29 m, NAP-2.87 m and NAP-3.52 m respectively, while the year-average water level is around NAP-0.3 m. All ADCPs had a blanking distance of 25 cm, layer sizes of 25 cm and measured with 500 pings per ensemble of 10 minutes.

At the Houtribdijk site, hydrodynamics were monitored by two ADVs (Acoustic Doppler Velocimeter) positioned in the cross-shore (fig. 3.2). The bed levels and

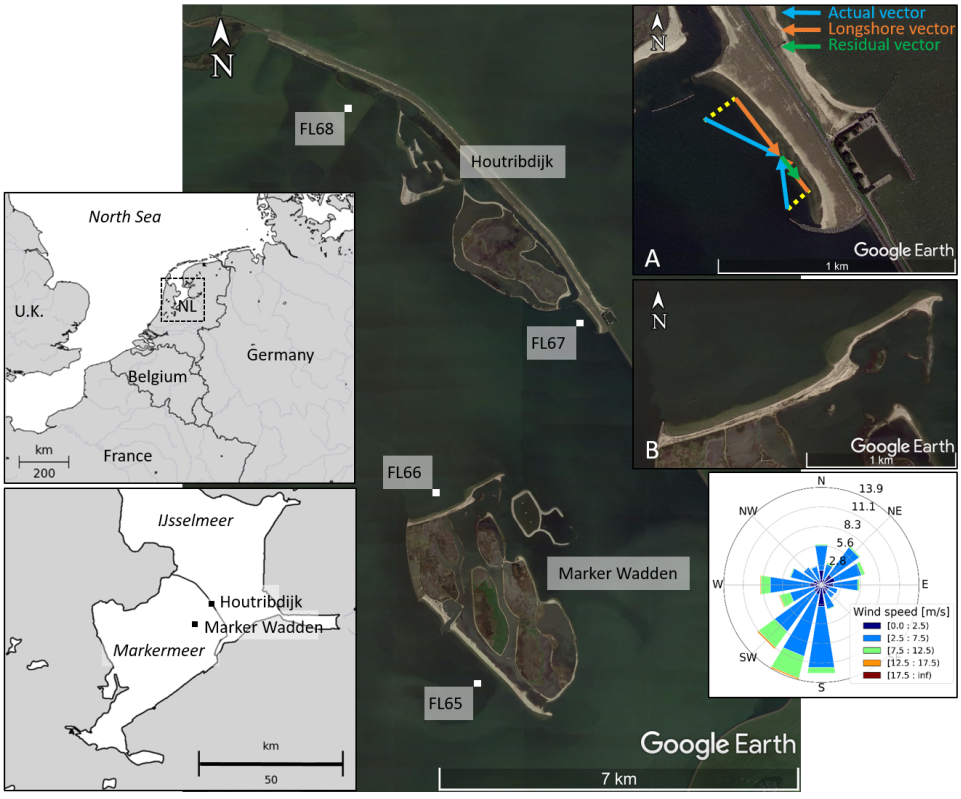

Figure 3.1: Overview of measurement locations, where locations FL65 and FL66 mark the measurement locations near respectively the Zuidstrand and Noordstrand of the Marker Wadden and FL67 and FL68 the measurement location on the Markermeer side of the Houtribdijk. The right top corner shows a top view of study site FL67, with a description of calculation residual vector. Wind rose of measurement period, 1-2-2019 to 10-2-2021 at KNMI station Lelystad

heights of the instruments are given in table 3.1. The measurement frequency was 8 Hz for both instruments.

	FL67C	FL67A
Bed level [NAP+m]	-2,51	-1,21
ADV height [NAP+m]	-1,74	-0,83
ADV height above bed [m]	0,77	0,38

Table 3.1: Bed levels and ADV heights averaged over measurement period.

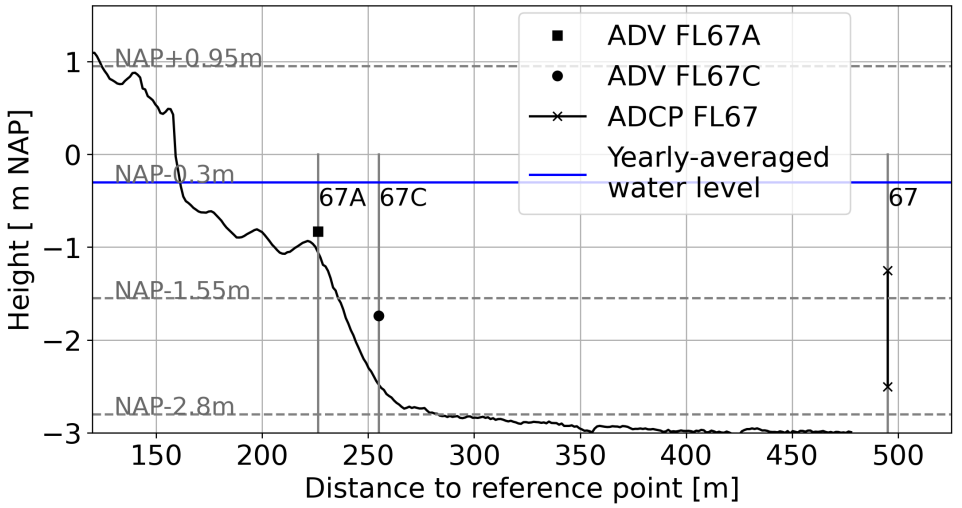

Figure 3.2: Overview of measurement locations, where ADV is Acoustic Doppler Velocimeter and ADCP is Acoustic Doppler Current Velocimeter shown on the Houtribdijk cross-shore profile, profile was measured in January 2021.

At the Houtribdijk, bathymetric data was collected monthly by the contractor between completion in May 2019 and October 2019, after which monitoring was conducted by a survey company between November 2019 and April 2021. At the Marker Wadden, every three months, the bathymetry was monitored. Different equipment was used for bathymetry, shallow bathymetry and topography (table 3.2). At the Houtribdijk (HRD), 35 transects were monitored with a spacing of 25 m. At the Marker Wadden (MW), the deep bathymetry and topography was monitored with a high density and the shallow bathymetry in transects. Transects covering the southwesterly 1400 m of the beach with a spacing of 50 m were measured almost every 3 months from October 2019 onwards.

	Houtribdijk (FL67)		Marker Wadden (FL66)
	May 2019 - October 2019	*November 2019 - April 2021*	*July 2018 - present*
Bathymetry	Singlebeam (±0.1m)	PingDSP (±0.1m)	Multibeam (±0.2m)
Shallow bathymetry	RTK-GNSS carrier* (±0.03m)	RTK-GNSS carrier*	RTK-GNSS carrier*
Topography	RTK-GNSS carrier*	LiDAR drone (±0.05m)	Structure-from-motion with drone (±0.05m)

Table 3.2: Measurement equipment used for bathymetry, shallow bathymetry and topography at different locations with vertical accuracy between brackets. *Accuracy of all RTK-GNSS carriers is equal.

3.3.3. Characterisation hydrodynamics

The wind climate in the Netherlands is dominated by south-westerly storms (fig. 3.1). For our study sites, this dominant wind direction coincides with the largest fetch. Waves are fully determined by local wind and they are depth-limited for the dominant wind direction and fetch-limited for other directions (northwest to southeast) (fig. 3.1). The significant wave height (H_{m0}) generally does not exceed 1.5 m and the peak period is typically between 2.5 and 3.5 s during storms. Since the Markermeer is a largely closed off basin, water level fluctuations are mainly caused by wind set-up. For southwesterly wind, location HRD (near FL67) is subjected to a rise in water level and wave height, while for northeasterly wind, a water level set-down and relatively small waves are observed (fig. 3.3a). The impact of simultaneous high water levels and wave heights on the shape of the cross-shore profile was described by Ton *et al.*, 2021.

The ADV at FL67 shows that currents at this location are bi-directional towards the northwest and southeast, i.e. the longshore direction (fig. 3.3b). A similar pattern is observed for more nearshore locations FL67C and FL67A. At location FL67C, currents predominantly come from the northwest (63.4%), while at the more nearshore location FL67A, currents are almost equally distributed over the northwest and southeast direction, with a slight predominance for currents coming from the southeast direction (53.2%). From literature we would suspect the current direction to be dependent on the wind direction (Jackson *et al.*, 2002; Nutz *et al.*, 2018), which is confirmed by the measurements (fig. 3.3b). For wind directions ranging from approximately 40 to 200 degrees, the flow direction at FL67 is towards the northwest, while for wind directions from 200 to 360 and 0 to 40 the flow directions is towards the southeast. The highest current velocities are found for winds ranging from 150 to 280 degrees for all three locations. These are also the directions with the strongest winds.

For more insight into the circulation patterns that are driven by the described water level set-up and down, the ADCP measurements are analysed. The ADCP measurements at locations FL65, FL66, FL67 and FL68 show no significant differences between the velocities and directions of the current in the top half of

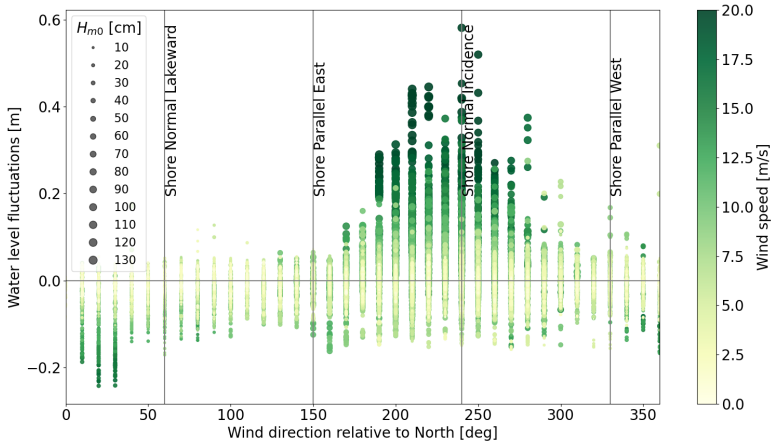

(a) Relation wind, water level fluctuation and wave height based on wave gauge data FL67

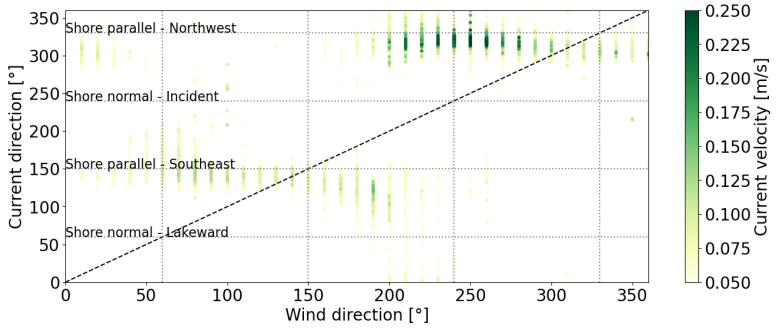

(b) Relation wind to flow direction (coming from), FL67

Figure 3.3: Wave, water level and flow characteristics, FL67, March 2019 - March 2021

the water column and the bottom half (fig. 3.4). Concluding, the large-scale circulations in lake Markermeer are mostly horizontal.

3.3.4. Modelling

Model setup

To extend our knowledge of the hydrodynamics around our study sites, we used a numerical model, Delft3D (Deltares, 2018). By using a model that includes the complete Markermeer, we can obtain insight into large-scale circulation currents. Moreover, the individual forcing of waves and currents can be researched.

Our model is based on the suspended sediment model of the Markermeer, as developed by Van Kessel *et al.*, 2008. Only the WAVE and FLOW module were adopted from this model. We use the model depth-averaged, since currents in

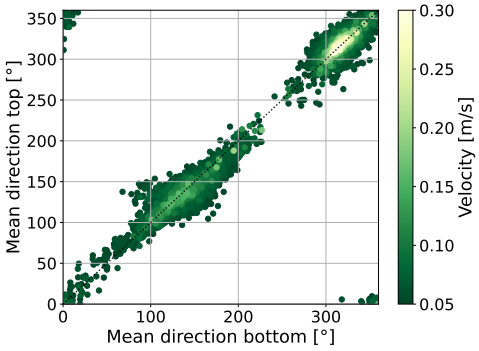

Figure 3.4: Relation bottom and top current direction, measured by the ADCP at location FL67

our area of interest are uniform over depth (fig. 3.4) and included Coriolis forcing. The original model has a grid cell size of approximately 150 m in our area of interest, which is not detailed enough for our application. Therefore, the northeastern corner of the model was nested in the original model (fig. 3.5). This nested grid is refined by a factor 9 in both directions and refined more along the southwestern beach of the Marker Wadden (FL65) and at the Houtribdijk (FL67). This nest has two new, open boundaries.

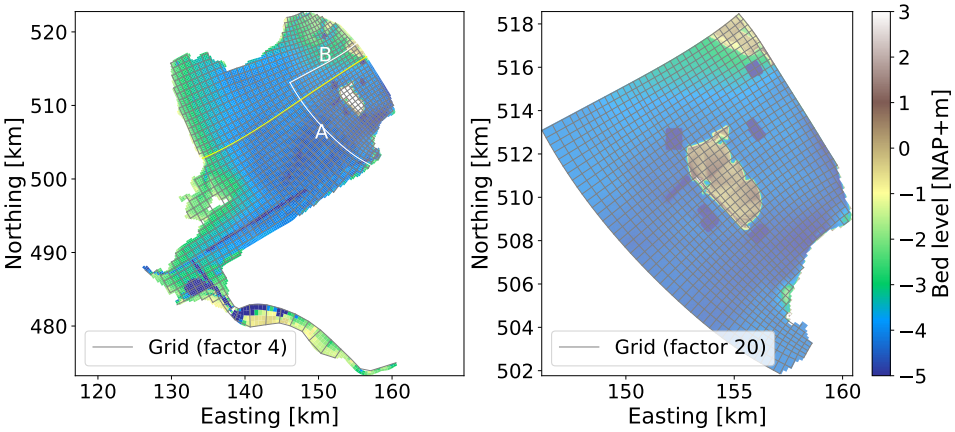

Figure 3.5: Left: The total Markermeer grid with bathymetry and the boundaries for the nested model. Boundary A is a water level boundary and boundary B is a flow boundary. Wave spectra are imposed on both boundaries. Right: The nested grid and bathymetry, in which six sand mining pits are visible (±40 m deep). The yellow line indicates a later described cross-section through FL67.

Model validation

Waves, water levels and flows are validated with measurements from locations FL65, FL66, FL67, FL67C, FL67A and FL68 for two periods (fig. 3.1). The first period is from February 7 to February 13, 2020, during which storm Ciara passed. During storm Ciara, the peak wind speed was around 23 m/s at lake Markermeer, and the wind direction was south to southwest. The second period lasts from June 1 to June 9, 2020, which is a calm period. During this period the maximum wind speed was around 15 m/s and directions varied from north to southwest.

Wave heights are somewhat overestimated by the model, especially at locations FL67, FL67C and FL67A, and modelled peaks have a slightly longer duration than measured peaks (fig. 3.6 and 3.7). Measured and modelled wave directions correspond very well during all periods. Water levels are well-simulated by the model, peaking at the right moment and the right level for location FL68, Fl66 and FL65, with just a slight underestimation at locations FL67, FL67C and FL67A. Flow velocities are reproduced well by the model at locations FL65, FL66, FL67 and FL68. At the nearshore locations FL67A and FL67C, where one or more (horizontal) circulation cells are present under certain conditions, the model results deviate slightly more. Since we are looking at just one point measurement, the exact location(s) of these cell(s) can make a big difference. However, at all locations flow directions match the measurements, apart from slight deviations around the tipping points. When incoming wind varies around the shore normal, longshore flow can switch 180°, which we call a flow reversal point. The flow reversal points and comparison between measurements and model are also visible in figure 3.14.

Above descriptions are reflected in the root mean squared errors (RMSE) (table 3.3). Although in general peaks and absolute values are close, the RMSE can be somewhat inflated, especially for the flow direction. The RMSE indicator specifically tends to exaggerate the larger deviations that occur at small flow velocities. Meanwhile, during moments of higher flow velocities when current are well-developed, deviations are smaller.

	FL67	FL67C	FL67A
H_{m0}	0.229	0.178	0.321
h	0.042	0.070	0.070
u_{vel}	0.032	0.083	0.073
u_{dir}	54.1	60.7	57.5

Table 3.3: RMSE of model versus ADV measurements significant wave height (H_{m0} [m]), water level (h [m]), flow velocity (u_{vel} [m/s]) and flow direction (u_{dir} [°]).

3.3.5. Calculation longshore current and transport

With the flow measurements and bathymetrical surveys at location HRD, current characteristics per morphological period are defined. The morphological period

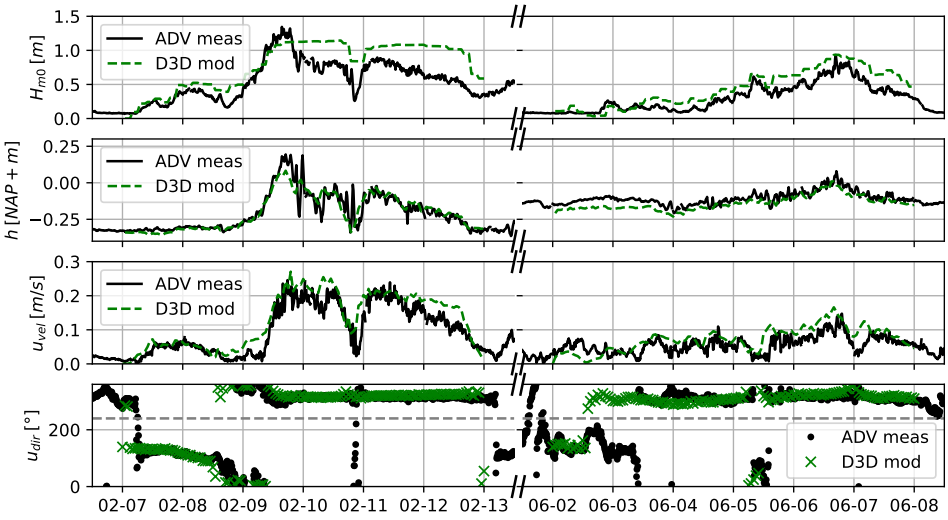

Figure 3.6: Validation of model results to ADV measurements of significant wave height (H_{m0} [m]), water level (h [m]), flow velocity (u_{vel} [m/s]) and flow direction (u_{dir} [°]) for location FL67

is the period between two surveys, which is approximately 1 month in winter and 2 months in summer. The continuously measured current vector is reduced to a 10-minute rolling mean and then translated to a number proportional to sediment transport with equation 3.1 (Bosboom *et al.*, 2021):

$$\langle S_b \rangle \propto \langle u|u|^2 \rangle, \tag{3.1}$$

where S_b is bed load transport and u is flow. Both bed load transport and suspended load transport are considered for the transport vector. This vector is projected on the coastline, as a longshore vector (fig. 3.1). The residual transport capacity based on current measurements for the morphological period is then calculated with the mean of the longshore transport vector, averaged over all 10-minute periods in the morphological period (hereafter referred to as $S_{b\ or\ s,long,net}$).

Based on the bathymetrical surveys, the actual volume flux can be estimated. We do this by calculating the volumes of different vertical sections separated by four vertical levels:

- above the beach face (NAP +0.95 m),
- the annual mean lake level (NAP-0.3 m),
- the submerged slope, just below the platform (NAP-1.55 m),
- just below the lake bottom (HRD: NAP-2.8 m, MW: NAP-4.2 m).

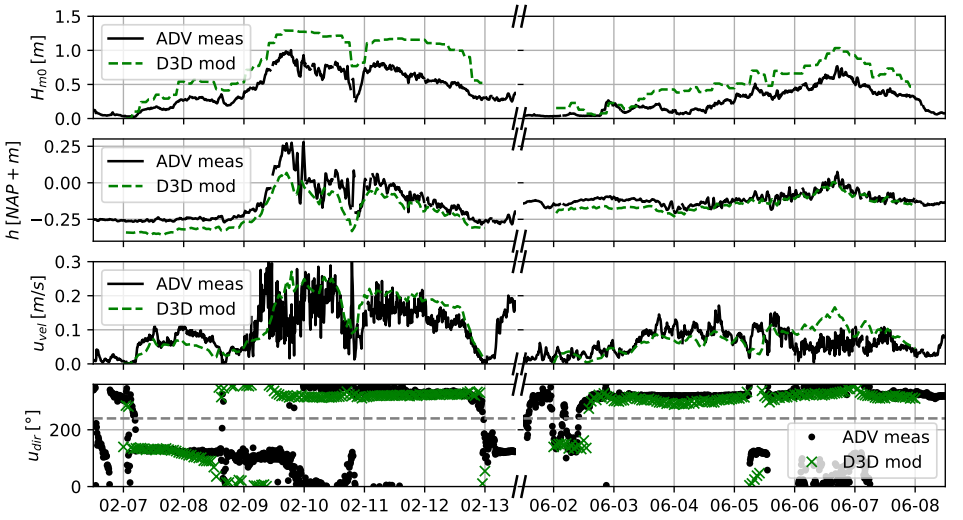

Figure 3.7: Validation of model results to ADV measurements of significant wave height (H_{m0} [m]), water level (h [m]), flow velocity (u_{vel} [m/s]) and flow direction (u_{dir} [°]) for location FL67A

	Name section	**Upper boundary**	**Lower boundary**
I	Beach face section	NAP+0.95 m	NAP-0.3 m
II	Platform section	NAP-0.3 m	NAP-1.55 m
III	Offshore section	NAP-1.55 m	NAP-2.8 m/NAP-4.2 m*

Table 3.4: Vertical morphological sections. *Respectively FL67 and FL66.

In between these levels, three sections are defined: the beach face section, the platform section and the offshore section (table 3.4).

The first and second vertical zones (I, II) are equal in height, as is the third vertical zone for location HRD (table 3.4). Because the offshore Markermeer bed level is deeper at location MW, the bottom level is lower over there. To analyse longshore sediment transport, the beach is divided into two horizontal sections. For location HRD this is the northwestern section, between transect 60.55 and 60.925, and the southeastern section, between transect 60.925 and 61.3 (fig. 3.11). Both sections are 350 m wide. Per morphological period, the change in volume over time for each vertical section and horizontal section is calculated with $Q_{sed} = \Delta V/\Delta t$ in m^3/day.

3.4. Results

3.4.1. Lake circulations

Large-scale

The large-scale lake circulations are thought to be related to differences in water level set-up due to bathymetrical variability (Van Ledden *et al.*, 2006; Vijverberg, 2008). The ADCP measurements showed that these currents are uniform over depth, and thus they are classified as horizontal.

The numerical model is fit to test the relation between set-up and currents. For southwesterly wind, indeed a higher water level set-up is found in the shallow areas in the north of the lake (fig. 3.8a). The set-up difference at the leeward shore, the Houtribdijk, induces a flow from shallow to deep. Therefore, a large-scale clockwise circulation occurs for these conditions (fig. 3.8a and 3.9). From southerly and westerly wind, a similar pattern occurs. For wind from the east, one large cell circulates counter-clockwise (fig. 3.8b). This can be explained following the same principle. Model runs without these shallow areas, but with a uniform depth, show very little large-scale circulation. This affirms our hypothesis. For both winds from the southwest and east, flow converges between the area northeast of the Marker Wadden, causing an acceleration in this area. For wind from the north, multiple circulation cells form, showing less distinct patterns, especially in the area around the Marker Wadden and FL67.

Nearshore

The large-scale currents are expected to influence the nearshore currents at the study sites. At the Houtribdijk beach two characteristic flow patterns can be distinguished. In the first situation, for wind from the west, we have uniform flow in the nearshore between the groynes (fig. 3.9c). In the second and most common situation, for wind from the south to southwest, a counterclockwise circulation cell occurs between the groynes, where flow at location FL67C and further offshore is towards the southeast, while at location FL67A and further nearshore it is towards the northwest (fig. 3.9a and 3.9b). The presence of a circulation cell at the Houtribdijk beach explains difference in the occurrence of flow directions that were measured at FL67A (nearshore) and FL67C (more offshore) (section 3.3.3). Especially for winds from the southwest to west, the offshore flows (around FL67) reach the nearshore. These offshore flows are part of the large-scale circulation, as they coincide with flows in the northwest region of the lake (fig. 3.8a). Moreover, since waves do not break around FL67, we can assume that the offshore flows are directly related to the large-scale lake circulations. Lastly, we would not expect significant wave-driven longshore currents, since waves are nearly normally incidence for southwesterly wind.

Bathymetry-induced differences in water level set-up cause large-scale, horizontal circulations. These circulations reach and influence the nearshore currents, as do local geometric features.

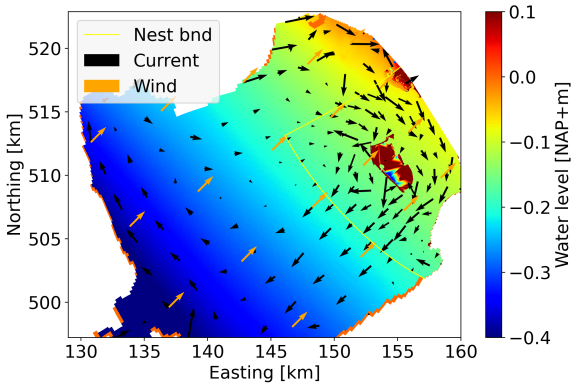

(a) Water level for schematic model with 15 m/s wind from 225°(orange vectors), with flow (black vectors)

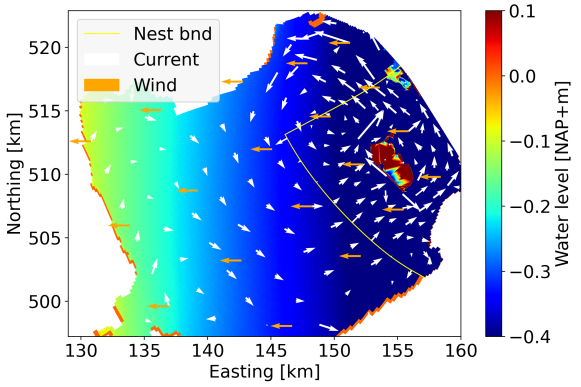

(b) Water level for schematic model with 15 m/s wind from 90°(orange vectors), with flow (white vectors)

Figure 3.8: Top view water levels and currents from Delft3D model.

3.4.2. Influence large-scale circulation and wave-driven flow

We hypothesized that the influence of the large-scale, wind-driven circulations on the longshore transport is significant. To quantify the influence of wave-driven currents, the numerical model with and without waves included is compared for a range of wind conditions. At location FL67A, the currents with and without waves point mostly toward the same direction for all wind conditions (fig. 3.10a), but differ in magnitude. At the more offshore location FL67C, currents with and without waves differ in direction for winds coming from 157.5°to 202.5°(fig. 3.10b). This difference is caused by the waves “pressing" the circulation cell against the beach for these wind directions, thus changing the current direction specifically at location FL67C. Blue colors indicate that the modelled current with waves in-

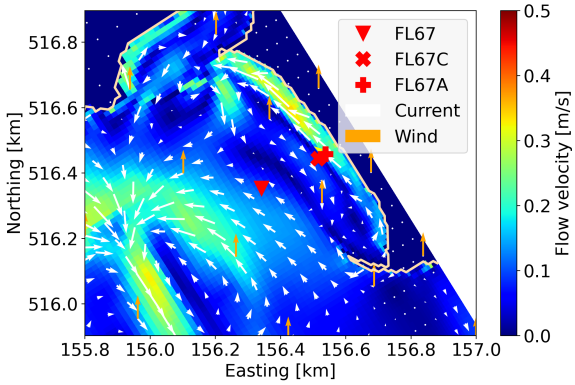

(a) Flows for schematic model with 15 m/s wind from 180°.

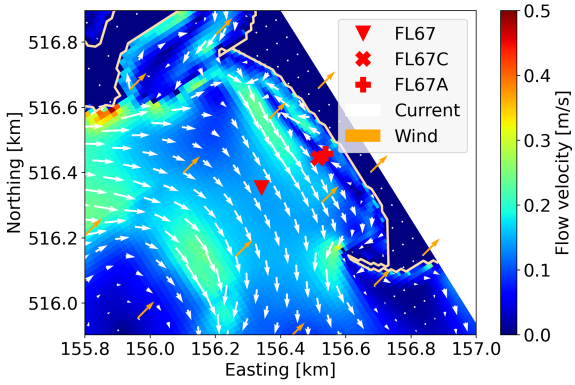

(b) Flows for schematic model with 15 m/s wind from 225°.

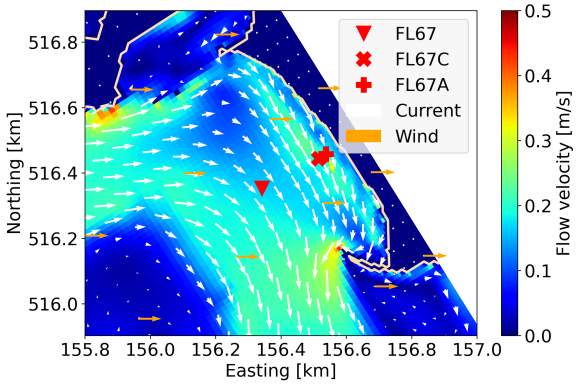

(c) Flows for schematic model with 15 m/s wind from 270°.

Figure 3.9: Top view of flows from schematic Delft3D model, with wind in orange vectors and flow in white vectors.

cluded is larger and red colors the opposite. The average difference in magnitude between including or excluding waves are 0.01 m/s for both locations, but the differences vary per wind condition (fig. 3.10). For most wind conditions and at both locations, nearshore flow velocity is decreased when waves are included in the model. The decrease can vary up to 0.1 m/s. For southwesterly wind, flow velocity is increased by waves at both locations. This is caused by the water level set-up in the northwest of the lake during these conditions. This set-up is enhanced by the waves, increasing also the offshore current in front of the beach, toward the southwest (fig. 3.9b). This "offshore" flow counteracts the nearshore flow toward the northeast, decreasing the flow with waves more than without waves. This velocity increase by waves is therefore not related to obliquely incident waves, but the effect of waves on the large-scale lake circulations. To conclude, large-scale circulation flow is a major component of the nearshore current, compared to the wave-driven current. Both components can enhance each other and oppose each other, depending on the wind direction.

3.4.3. Morphology

The morphology of the Houtribdijk beach is analysed, to be able to link currents to volume fluxes. A clear erosion and accretion pattern is visible at the Houtribdijk beach, (fig. 3.11). Most erosion takes place around the beach face and the platform over a period of 21 months. Sedimentation takes place in the offshore section, for the most part toward the groyne on the northwest side (between -850 m to -600 m in fig. 3.11). Although we see a strong net pattern over this long period, sedimentation and erosion do vary over time (fig. 3.12). The northwestern (NW) beach face and the southeastern (SE) beach face erode at a similar pace, apart from two periods. After construction in May 2019 and around March 2020, the NW beach face eroded greatly, while the SE beach face only eroded slightly. Apart from a few moments, the platform also shows a decreasing trend. Right after construction, a quick decrease of the platform volume is also visible, suggesting an adjustment effect for both the beach face and platform toward the natural profile shape (Ton *et al.*, 2021). The offshore volumes grow more steadily over time, showing a greater increase on the NW, as described above. Most volume fluctuations take place during the storm season, from October to April.

Morphological development shows clear signs of cross-shore transport at the beach face and longshore transport in the platform and offshore section.

3.4.4. Relation hydrodynamics and morphology

We hypothesized that $S_{b\,or\,s,long,net}$, based on (measured) longshore currents, is related to the longshore volume flux, based on difference in volumes of the NW-section and SE-section. To test the hypothesis, $S_{b,long,net}$ calculated from FL67A (nearshore) and FL67C (more offshore) are plotted against the volume changes (Q_{sed}) of the beach face section, platform section and offshore section (fig. 3.13). These results are compared to the results for $S_{s,long,net}$ later, based on R^2. In this figure, positive values for both the transport capacity and volume flux indicate

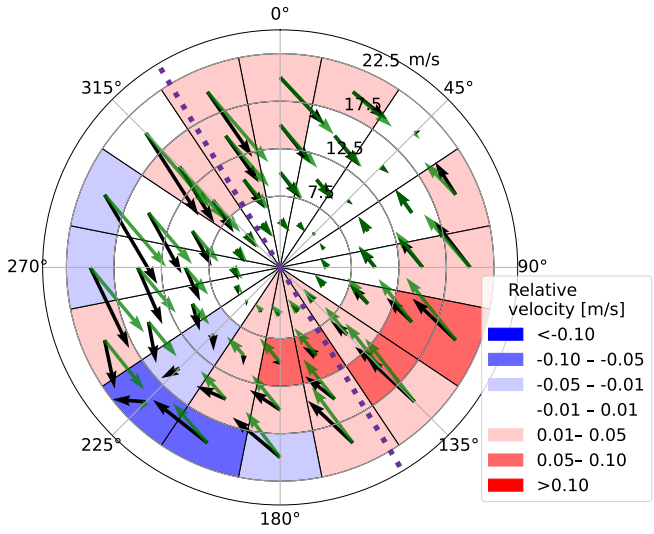

(a) Location FL67A

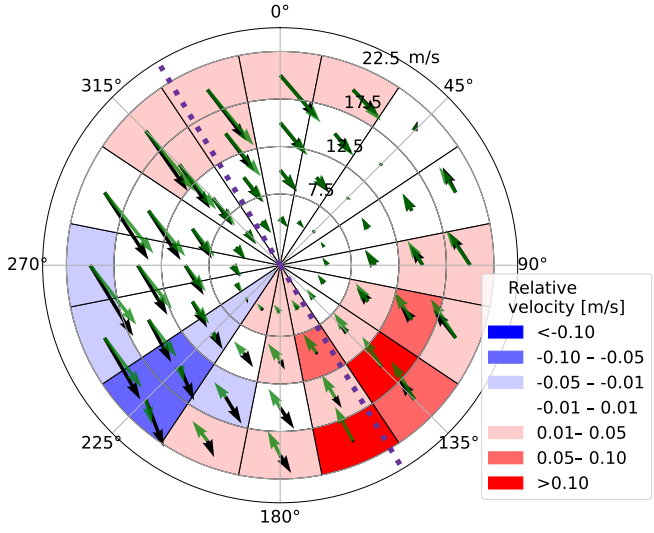

(b) Location FL67C

Figure 3.10: Equilibrium current direction from numerical model runs with waves (black vectors) and without waves (green vectors) for corresponding wind direction and velocity and difference in velocity (no waves-waves, colored). Shoreline orientation (purple dashed line).

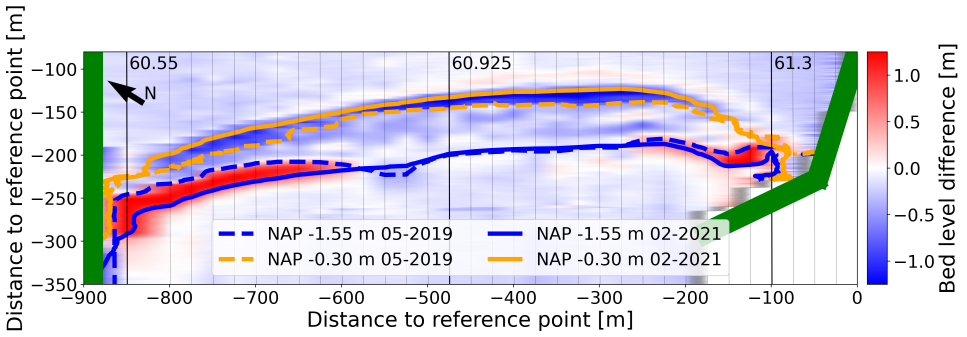

Figure 3.11: Morphological development location FL67 between as built, May 2019, and February 2021 . Groynes in green.

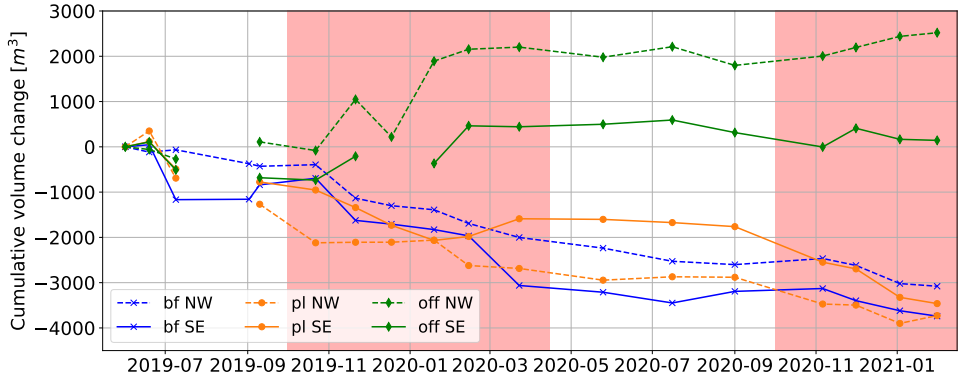

Figure 3.12: Volumes north-west (dashed) and south-east (solid) of transect 69.925 in beach face (bf), platform (pl) and offshore (off). Storm seasons are colored red.

transport towards the northwest, while negative values indicate transport toward the southeast.

For FL67A the fitted lines nearly cross (0,0), indicating that a positive $S_{b,long,net}$, toward the northwest, coincides with a positive Q_{sed}, toward the northwest (fig. 3.13). All $S_{b,long,net}$ values for FL67C are negative, which means toward the southeast and it is impossible for the fitted lines to cross (0,0). For this location we see a negative Q_{sed} (toward the southeast) for more negative values of $S_{b,long,net}$ and positive Q_{sed} (toward the northwest) for less negative values of $S_{b,long,net}$.

Both locations differ in range of $S_{b,long,net}$. Since FL67A is more nearshore and at a more shallow location (table 3.1), flow velocities are higher and more varied at this location. $S_{b,long,net}$ for the total period is small compared to the shorter periods. This indicates little net transport from NW to SE and vice versa. However, measurements show that not all gross transport comes back when deposited (fig.

3.11).

For the beach face, there is no significant relation between $S_{b,long,net}$ and Q_{sed} for both locations (table 3.5, fig. 3.13a and 3.13b). This implies that (solely) current-driven transports cannot explain the volume changes of the beach face. For the platform and offshore, the relation is more pronounced (fig. 3.13c, 3.13d, 3.13e and 3.13f). Despite the location of FL67A closer to the platform than FL67C, the relation for FL67A and the platform section is less significant. And although the location of FL67C is closer to the offshore section than FL67A, the relation for FL67C and the offshore section is less distinct.

Both the relations between $S_{b,long,net}$ and Q_{sed} and between $S_{s,long,net}$ and Q_{sed} are significant for the platform and offshore section (table 3.5). However, the relation for $S_{b,long,net}$ is stronger, especially for location FL67A. This indicates that morphological development at the platform and offshore section is driven by longshore currents in the nearshore and that bed load transport is likely to be more prevalent than suspended load transport at the platform.

	Beach face	Platform	Offshore
FL67A - S_b	0.35	0.76	0.86
FL67A - S_s	0.24	0.44	0.81
FL67C - S_b	-0.08	0.85	0.54
FL67C - S_s	-0.07	0.88	0.55

Table 3.5: R^2 relation $S_{b,long,net}$ or $S_{s,long,net}$ and Q_{sed}.

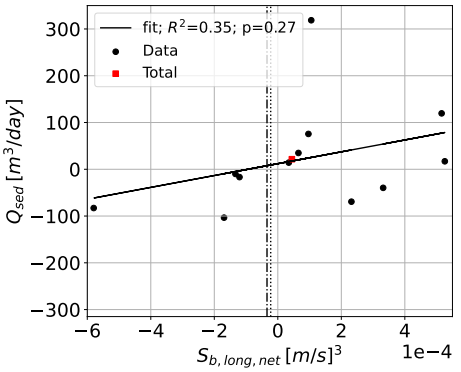

(a) Location FL67A, beach face section.

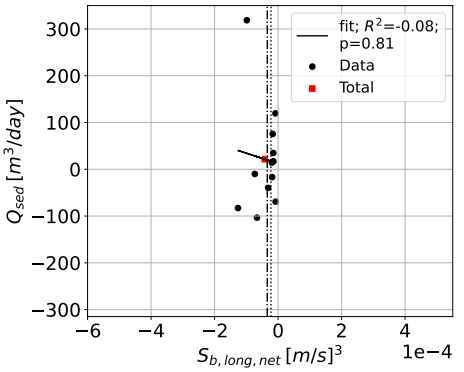

(b) Location FL67C, beach face section.

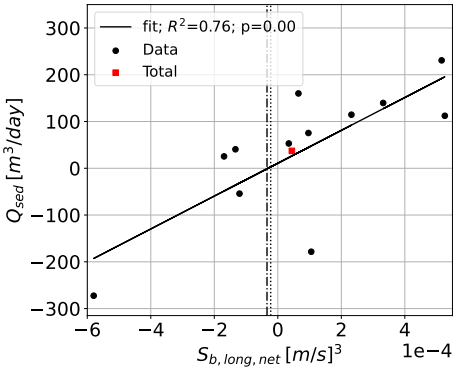

(c) Location FL67A, platform section.

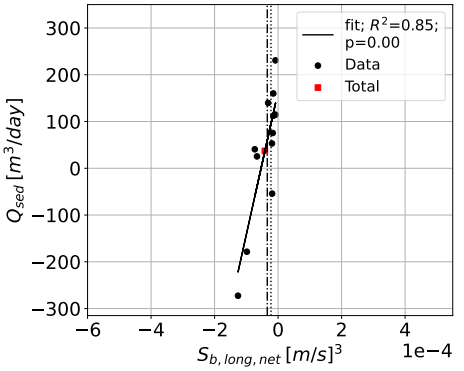

(d) Location FL67C, platform section.

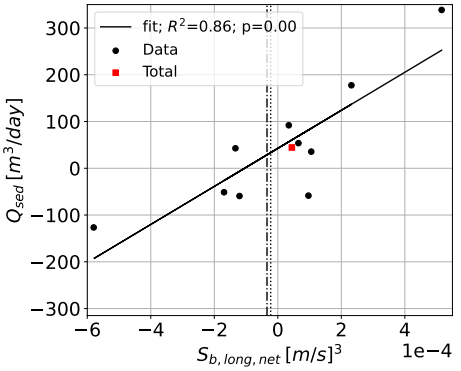

(e) Location FL67A, offshore section.

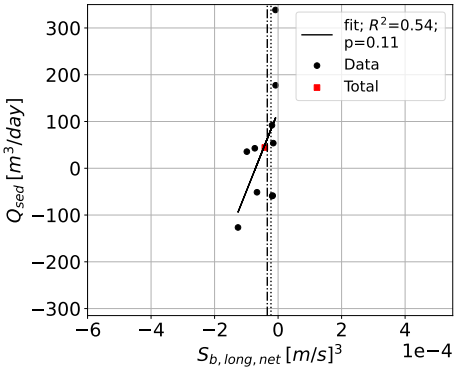

(f) Location FL67C, offshore section.

Figure 3.13: Relation residual transport capacity based on current measurements with actual volume flux from named measurement location and vertical volume section. Dotted line indicates residual transport capacity for the whole measurement period (June 2019-February 2021) for FL67A and dash-dotted line for FL67C.

3.4.5. Prediction longshore transport

Since $S_{b,long,net}$ and Q_{sed} are related for the platform and offshore section, the numerical hydrodynamic model can be used to predict direction and magnitude of the volume flux. To do so, we follow these steps:

1. Choose a range of wind conditions, i.e. combinations of wind direction and wind velocity.
2. Predict the flow direction and magnitude per wind condition with a numerical model with waves and flow.
3. Convert the predicted flow into $S_{b,long,net}$.
4. Calculate the occurrence of every wind condition.
5. Combine the predicted potential transports and wind statistics, to find the total net transport capacity, $S_{b,long,net,tot}$.

From this we can learn the net volume flux direction for a certain period or a long-term mean value, if the wind statistics are based on a long enough period.

The directions and magnitudes of the predicted nearshore flow correspond well with the measurements for both locations (fig. 3.14). Most inaccuracies are found for the wind conditions near the flow reversal point for which the currents change direction. For FL67A this is around 202.5°and for FL67C around 180°. The predicted velocities for these scenarios are smaller than the measured velocities and the direction is less distinctly towards the northwest for southerly wind directions.

$S_{b,long,net}$ is calculated for all wind conditions by combining the flows to the third power (eq. 3.1) with the occurrence of these scenarios over the measurement period (June 2019 - February 2021). For location FL67A the measured flows toward the northwest and southeast almost cancel each other out, resulting in a southwesterly directed transport capacity (i.e. offshore). The predicted flows for this location result in a southerly directed transport capacity. The measured and predicted residual transport capacities for FL67C are both toward the southeast, although differing somewhat in magnitude. The longshore component of the modelled residual transport capacity are visualized with the relation between transport and actual flux (fig. 3.13, dotted and dash-dotted lines). The total transport capacity is small compared to the values per morphological period (fig. 3.13).

3.4.6. Implications to design - Marker Wadden

The study site at the Marker Wadden is used to test whether a prediction based on flow vectors can help to predict volume flux direction at a location with no nearshore measurement. This study site lies under an angle relative to the most common southwesterly winds, so a distinct signal is expected compared to the study site at the Houtribdijk.

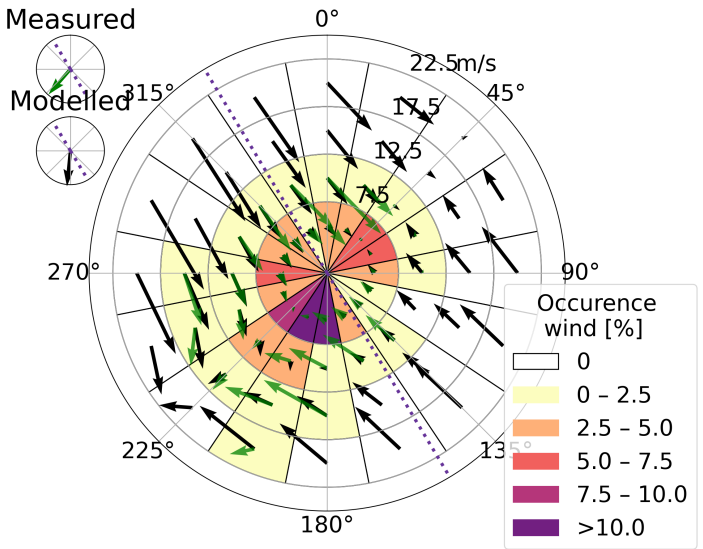

(a) Location FL67A

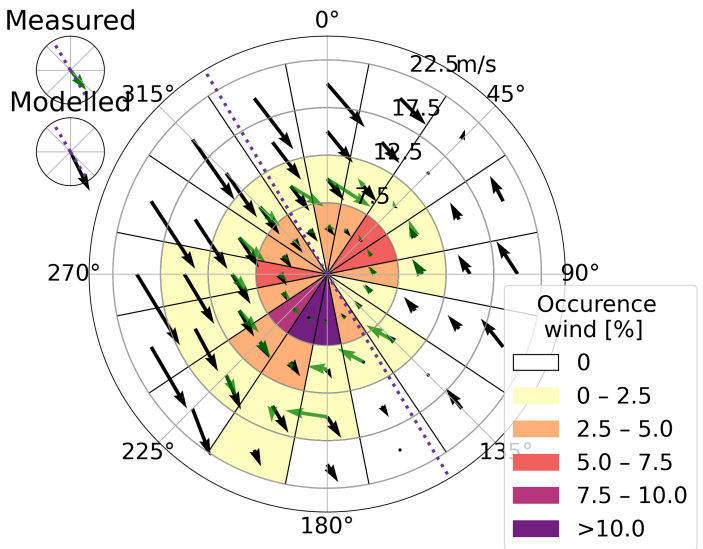

(b) Location FL67C

Figure 3.14: Center: Flows measured at measurement location (green vectors) and equilibrium current direction from numerical model runs at same location (black vectors) for corresponding wind direction and velocity and wind statistics (colored). Shoreline orientation (purple dashed line). Top left: $S_{b,long,net}$ for 10-year period, taking only measured wind conditions into account.

Longshore current

At the Marker Wadden, a circulation cell is present for southwesterly wind, similar to the one at the Houtribdijk site (fig. 3.15a). More offshore, the flow is directed toward the southwest, while it is directed toward the northeast in the nearshore.

We analysed the nearshore data for multiple wind conditions at a similar water depth as FL67A, approximately 1 m, and named it FL66A (fig. 3.15a). At this location, also two flow reversal points for flow direction were visible but at different wind angles, around 157.5°and 337.5°(fig. 3.15b). From winds from the south to northwest, nearly alongshore flows toward the northeast are predicted and for opposite winds opposite flows. The average difference in current magnitude when including and excluding waves from the model is 0.01 m/s, the same number as for location FL67A and FL67C. The waves affect the currents in two manners. The first is visible for winds between the southwest and west, for which flows from the model without waves are stronger. This is caused by the water level set-up in the northwest of the lake during these conditions. This set-up is enhanced by the waves, increasing also the return current in front of the beach, toward the southwest (fig. 3.9 and 3.15a). This “offshore" flow counteracts the nearshore flow toward the northeast, decreasing the flow with waves more than without waves. This velocity decrease by waves is not related to obliquely incident waves, but the effect of waves on the large-scale lake circulations. For winds between the northwest and northeast, especially for higher wind velocities, the second process is visible and we see that waves do reach the nearshore and amplify the longshore current. Moreover, we see more offshore directed flows for shore normal winds in the model with waves. Concluding, the effect of waves on longshore currents depends on the wind direction and is low on average.

Model prediction

For the prediction of longshore transport, we studied a short period from April 2019 to July 2019. Since winds from the southwest are dominant during this period, the $S_{b,long,net,tot}$ is towards the east with a magnitude of $2.1 * 10^{-}2\ (m/s)^3$ (fig. 3.15b). Over this period, the southwestern part of the study site loses sediment at the beach face and the platform, while the northeastern part loses less or even gains sediment (table 3.6, fig. 3.16). This shows sediment transport from southwest to northeast, which is the same direction as $S_{b,long,net}$. The morphological development of the Marker Wadden beach is only coherent when taking the circulation cell and thus the impact of the large-scale currents into account. Without these, the erosion seen in the lee of the dam was not expected.

To conclude, knowledge of large-scale currents are important for understanding morphological development of the Marker Wadden beach, and have significant impact on the design and maintenance.

	Beach face	Platform	Offshore
Southwest	-888	-1.385	46
Northeast	-138	42	280
Net	-750	-1,427	234

Table 3.6: Volume changes between April and July 2019, for the southwestern and northeastern part of the beach and the vertical sections in m^3, over the 500 m wide sections.

3.5. Discussion

As was stated in the introduction, different studies expect for this type of water body to have three-dimensional flows, with a return current flowing opposite to the dominant fetch (Nutz *et al.*, 2018; Van Ledden *et al.*, 2006; Vijverberg, 2008). Our measurements do not show this type of flow, but indicate a two-dimensional pattern with horizontal return current. The ADCP's monitor approximately 78% to 93% of the water column, taking into account the blanking distance (0.25 m) and varying upper wave region. Since flows are exceptionally uniform in this part of the water column, we have no reason to assume 3D flow patterns in our region of interest. The water bodies analysed by Nutz *et al.*, 2018 range from a depth of 6 and 30 km fetch to hundreds of meters deep and hundreds of kilometers wide. Lakes as shallow and wide as lake Markermeer were not taken into account. The shallow lake researched by Liu *et al.*, 2018 also shows three-dimensional currents, but dedicates that to a complex bathymetry. The relatively uniform but shallow bed level of lake Markermeer, could explain the lack of observations of vertical return currents.

The model validation shows good agreement between the model results and the ADV measurements. However, the significant wave height is somewhat overestimated by the model. For conclusions on the relative impact of large-scale currents and wave-driven currents on the total longshore currents, this would be a conservative choice in favor of the wave-driven current. Yet, the influence of large-scale currents is high and thus might be even higher in practice.

For the calculation of $S_{b,long,net}$, we assumed bed load transport, since ripples were observed in the nearshore at all locations and throughout all seasons. A sensitivity analysis showed that with this assumption, the best relation between $S_{b,long,net}$ and Q_{sed} was found. This might be specific for the lake Markermeer beaches.

Relations between $S_{b,long,net}$ and Q_{sed} for the platform and offshore section were found to be significant, but the development of the beach face section cannot be related to this flow-based parameter. Ton *et al.*, 2021 describe that the sediment transport at the beach face is primarily in the cross-shore direction, and that eroded sediment only travels in the cross-shore and longshore direction once it reaches the platform. These results imply that wave action is dominant over current-driven transports for development of the beach face.

The orientation of the Houtribdijk beach, almost perpendicular to the most com-

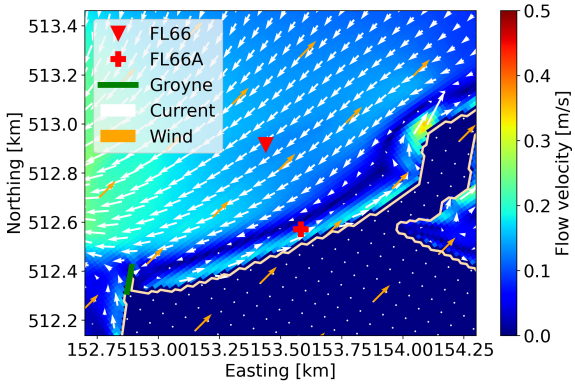

(a) Flows for schematic model with 15 m/s wind from 225°.

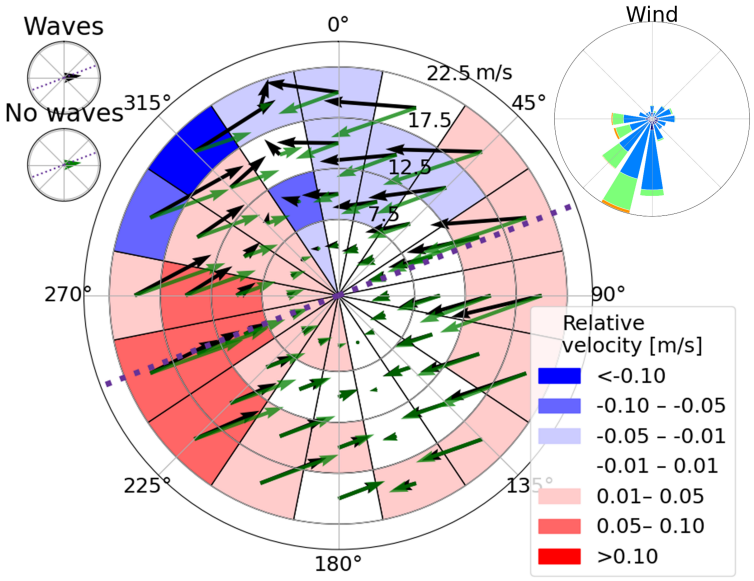

(b) Center: Equilibrium current direction from numerical model runs at nearshore Marker Wadden beach with waves (black vectors) and without waves (green vectors) for corresponding wind direction and velocity and difference in velocity (no waves-waves, colored). Shoreline orientation (purple dashed line). Top left: weighted net transport capacity for period from October 2019 to April 2020.

Figure 3.15: Flows from Delft3D at Noordstrand, Marker Wadden.

mon southwesterly storms, makes it difficult to predict to which direction the net longshore transport will be. Firstly, because $S_{b,long,net}$ calculated per period is not as strong compared to a beach under an angle such as the Marker Wad-

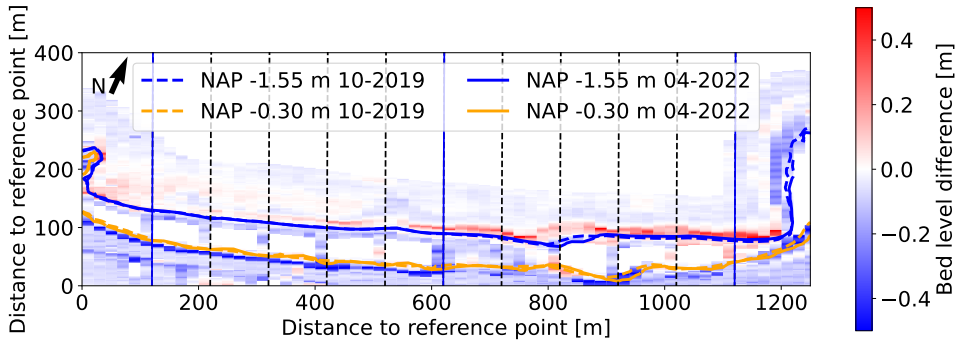

Figure 3.16: Morphological development Marker Wadden beach between October 2019 and April 2020. Southwestern section on the left, between the blue transects and northeastern section on the right.

den beach. And secondly, because $S_{b,long,net,tot}$ and $Q_{sed,tot}$ are close to zero (fig. 3.13). $S_{b,long,net}$, based on flow measurements at the Houtribdijk beach, is slightly positive, indicating net transport towards the northwest, while $S_{b,long,net}$ from the model is slightly negative, indicating the opposite. Since both values are very close to zero, this confirms the sensitivity to minor changes in forcing of a beach under this angle once more. It is favorable for the beach to approach a net zero longshore volume flux on the long term in terms of maintenance. However, we do see longshore transport reflected in the sedimentation spots near the dams (fig. 3.11). We observe that sediment that has settled near the dams, does not come back towards the middle of the beach. This is because most of the sediment settles below the depth of closure (Ton *et al.*, 2021). So even though net sediment transport is close to zero, the middle of the beach is net eroding. The Marker Wadden beach has a different orientation, which makes the prediction more distinctly to one direction and an $S_{b,long,net}$ of $O\ 10^{-2}$ instead of $O\ 10^{-4}$ at the Houtribdijk. Since the dominant southwesterly storms coincide with a transport capacity direction towards the northeast, a flux towards the northeast is no surprise.

The Marker Wadden beach is a great example where taking into account the large-scale circulations, gives insight into morphodynamic processes. Based on just wave-driven longshore currents, some transport towards the northeast was expected given the dominance of southwesterly winds. The groyne in the southwest was expected to create a lee and retain sediment (fig. 3.15a). However, this groyne turns out to reverse the offshore flow, making the “lee-side" of the groyne especially vulnerable for erosion (fig. 3.16). This affirms that insight into large-scale circulations is crucial for understanding longshore flow in this case.

The development of the Delft3D model, in addition to the field measurements, was crucial in gathering information on circulating flows. This model was essential in understanding the system. With the new knowledge on the importance of large- and small-scale circulations for morphodynamics of lake beaches, adapted

field measurements could be done, to make the model less essential. With opposite reasoning, a complex numerical model could replace the need for measurements in similar systems. However, the combination of measurements and model has many added benefits compared to using either one.

3.6. Conclusion

The goal of this research was to find what causes the described large-scale lake circulations and how these influence nearshore, longshore currents compared to wave-driven currents. Furthermore, to determine how these longshore currents affect longshore transport and its implication on the design of low-energy, non-tidal beaches. Lake Markermeer is characterised as a shallow, wind-driven water body. ADCP and ADV measurements show flows that are nearly uniform over depth, and that flow directions are closely related to wind directions.

To gain more spatial insight into large-scale circulations, a depth-averaged Delft3D model was set up and validated to the measured waves, water levels and currents. This model showed that bathymetry induced differences in water level set-up cause large-scale, horizontal circulations. These circulations affect the nearshore currents greatly, and are dominant over wave-driven longshore currents for most wind conditions regarding nearshore sediment transport. Local geometric features, such as groynes, also influence the flow, inducing smaller scale nearshore circulation cells under distinct conditions.

Longshore volume and coastline changes were measured through monthly bathymetric surveys. Based on flow measurements, sediment transport capacity ($S_{b,long,net}$) was calculated and linked to volume flux (Q_{sed}). A significant relation was found between $S_{b,long,net}$ and Q_{sed} for the full cross-shore profile, except the steep beach face. Through this relation longshore sediment flux can be predicted with model derived flow parameters for a variety of wind conditions, accounting for the complexity of flow circulation patterns discussed above. This is evaluated for a second study site, where we confirmed that the predicted $S_{b,long,net}$ can be a good indicator for longshore volume flux. Moreover, this study site shows that insight into large-scale currents is essential for understanding morphological development, and are a key element to take into account for design an maintenance of sandy beaches in low-energy environments.

Concluding, large-scale circulations are of vital importance for morphological development of low-energy, non-tidal beaches in shallow, wind-driven water bodies.

Acknowledgements

This research is part of the LakeSIDE project, which is funded by Rijkswaterstaat, The Netherlands. We want to thank Rijkswaterstaat Centrale Informatievoorziening for guiding and executing the (hydrodynamic) monitoring campaign. Shore Monitoring and Combinatie Houtribdijk are acknowledged for carrying out the morphological surveys at the Houtribdijk. We thank Boskalis Nederland for shar-

ing their bathymetric and topographic data of the Marker Wadden. Finally, we like to thank graduate student Fleur Wellen for her work at the Noordstrand, Marker Wadden.

4

Prediction of sediment transport for lake beaches and implications for their design and maintenance

Highlights:

- The effect of wave-driven longshore flow is overestimated compared to ambient flow, in the traditional longshore sediment transport bulk equations.
- Longshore sediment transport can be predicted in low-energy, non-tidal environments with an adjusted version of the Van Rijn (2014) equation.
- The uncertainty due to calibration of the bulk equation is larger than the uncertainty due to the yearly wind variability on yearly longshore transport.
- Yearly beach face erosion volumes can be linked to the 95^{th} percentile significant wave height.

This chapter is submitted as: **Ton, A.M.**, Vuik, V., & Aarninkhof, S.G.J. (submitted). Prediction of sediment transport for lake beaches and implications for their design and maintenance.

4.1. Abstract

Knowledge on low-energy, non-tidal beaches has been growing over the last years, but mostly on understanding the hydrodynamic processes steering morphological development. These interactions are different from morphodynamics in high-energy, tidal environments. As sediment transport prediction methods are mostly based on high-energy environments, it is uncertain whether they capture the key driving processes of low-energy environments. The lack of simple methods for predicting longshore and cross-shore sediment transport complicates the design and maintenance of low-energy beaches. In this research, we established bulk prediction methods for longshore and cross-shore sediment transport at low-energy, non-tidal, sandy beaches, based on simultaneous hydrodynamic and morphological monitoring, and quantified their uncertainties. A longshore bulk sediment transport formula is proposed, based on the Van Rijn (2014) formula. In the Van Rijn (2014) formula, longshore flow is derived from incoming wave direction and ambient flow. As the flow derived from the incoming wave direction is overestimated compared to the ambient flow, it is replaced by total measured of modelled longshore flow. Through this method, large-scale lake circulations are taken into account, resulting in more reliable predictions. The yearly cross-shore transport at the beach face is related to the 95th percentile significant wave height, which can thus be used as a predictor. Cross-shore and longshore morphological effects are in the same order of magnitude, which means that they both need to be accounted for in designing and maintaining beaches. With knowledge of the total lake system, predictions on longshore and cross-shore sediment transport can be made with more certainty, and more knowledge of their uncertainties. The proposed prediction methods will contribute to better design and maintenance of low-energy, non-tidal beaches.

4.2. Introduction

Knowledge on low-energy or sheltered beaches has been growing over the last years. Studies have focussed on wave signatures (Rahbani *et al.*, 2022), the interaction between hydrodynamics and morphology (Eelsalu *et al.*, 2022; Fellowes *et al.*, 2021; Gallop *et al.*, 2020; Mujal-Colilles *et al.*, 2019; Ton *et al.*, 2023, 2021), modelling (Tran *et al.*, 2021) and providing a review (Vila-Concejo *et al.*, 2020). However, commonly applied methods for quantifying sediment transport are not reliable for these types of beaches, as they are mostly validated for high-energy beaches. As hydrodynamic processes for basin, bay and estuary beaches (BBEBs) differ from high-energy beaches (Ton *et al.*, 2023), traditional (bulk) sediment transport formulas may not take into account the key driving processes.

Several methods for predicting longshore sediment transport have been developed in the past decades. Table 4.1 gives an overview of several common bulk formulas and the influencing factors they take into account. The most widely used bulk formula is the CERC equation (CERC, 1984), based on the assumption that longshore transport rate is proportional to longshore wave power (table 4.1). This formula was refined by Kamphuis (1991), adding the effects of particle di-

ameter and bed slope. Mil-Homens *et al.* (2013) re-evaluated this equation with a new dataset. Besides these approaches, bulk formulas based on the Bagnold (1963) energetics concept are used. Originally, Inman *et al.* (1963) derived a bulk formula based on this fundamental approach. They assume that a proportion of the wave power is transferred to bottom friction and with that bed load transport.

A more recent bulk equation has been developed by Van Rijn (2014). This equation differs from the others, as ambient currents can be accounted for (table 4.1). It is based on the process-based model CROSMOR, of which the results have been parametrized and based on Van Rijn (2002). Van Rijn (2014) compares bulk methods based on a new, expanded dataset and finds that the CERC and Kamphuis (1991) equation overestimate longshore transport for low wave conditions, while Mil-Homens *et al.* (2013) and Van Rijn (2014) reach much better results. Van Rijn (2014) concluded this his equation gives better results for coarse grains than the aforementioned methods.

Low-energy lake beaches are generally out of the range of sediment transport formulas. Although the bulk formula by Van Rijn (2014) included cases with low wave energy in the validation datasets, most of them had relatively long wave periods and some included swell. At some lake beaches, currents in the nearshore are generated both by waves and large-scale lake circulations (Ton *et al.*, 2023). Ideally, the lack of swell and the presence of these ambient currents is taken into account when quantifying the longshore sediment transport. More complex (numerical) models may be able to take all these processes into account, but are expensive and not always available for design and maintenance. Calibrated and simple methods for predicting longshore and cross-shore sediment transport would be ideal for design and maintenance, but are not available for low-energy lake beaches.

	H_s	∂_{wave}	D_{50}	T_p	∂_{slope}	$u_{ambient}$	K_{swell}
CERC (1984)	x	x					
Inman *et al.* (1963)	x	x	x	o*			
Kamphuis (1991)	x	x	x	x	x		
Van Rijn (2002)	x	x	x		x	x	
Mil-Homens *et al.* (2013)	x	x	x	x			
Van Rijn (2014)	x	x	x		x	x	x

Table 4.1: Overview of bulk transport formulas and its components, in which H_s is wave height, ∂_wave is wave directions, D_{50} is grain size, T_p is wave period, ∂_{slope} is the beach slope, $u_{ambient}$ is non-wave driven currents and K_{swell} is a swell correction factor. o* is wave phase velocity

No bulk formulas exist for cross-shore transport. Cross-shore volume changes are affected by wave energy and the actual profile shape relative to the equilibrium shape (Ludka *et al.*, 2015). As morphological changes are not only dependent on hydrodynamic processes, but also on the morphological state, it is difficult to predict long-term cross-shore transports based on hydrodynamic pa-

rameters only. Most prediction methods are based on equilibrium shoreface profiles (Davidson *et al.*, 2013; Yates *et al.*, 2009). The cross-shore morphology of low-energy, non-tidal beaches differs from typical high-energy profiles. Therefore equilibrium profile shapes also differ and the mentioned cross-shore transport methods are difficult to apply to lake beaches.

In the past years, multiple sandy beaches were constructed around lake Markermeer and lake IJsselmeer, the Netherlands (Figure 1). For the design of these beaches, local pilots were used (Steetzel *et al.*, 2017), combined with known prediction methods. Although some sheltered beaches may be exposed to swell (Fellowes *et al.*, 2019; Rahbani *et al.*, 2022), the lake beaches in the Netherlands are typically exposed to wind-driven, short waves (~4 s during storms). For some beaches, surprising morphological evolution was observed. This confirms that the "traditional" prediction methods may not always suffice.

The goal of this research is to establish bulk prediction methods for longshore and cross-shore transport at low-energy, non-tidal, sandy beaches based on two years of bathymetrical surveys and hydrodynamic monitoring and to quantify the uncertainties in these methods. We will use the found prediction methods to create guidance for design and maintenance for beaches in these environments.

The next section describes the study sites at which waves, currents and bathymetry were monitored. It further describes methods, among which the instruments used for the monitoring and the numerical model that was used. Section 4.4 shows the calibration of a bulk sediment transport formula to our monitoring data, a relation between wave height and cross-shore transport and outcomes on how to optimize beach design. In section 4.5 the results are discussed. Section 4.6 gives implications of this work on engineering practice and section 4.7 presents the conclusions.

4.3. Study sites and methods

4.3.1. Study sites

Lake Markermeer and lake IJsselmeer are non-tidal, inland fresh-water lakes in the centre of the Netherlands (fig. 4.1). Lake IJsselmeer is separated from the Wadden Sea by a dam called the Afsluitdijk and both lakes are separated by the Houtribdijk. Both lakes have regulated water levels, between approximately NAP -0.3 m and -0.1 m in summer for lake Markermeer and lake IJsselmeer. In winter, the lake Markermeer water level is between NAP -0.4 m and -0.2 m and that of lake IJsselmeer between NAP -0.4 m and -0.05 m (Rijkswaterstaat *et al.*, 2018). NAP is the vertical reference datum in the Netherlands, close to mean sea level.

The constructed sandy beaches in these lakes are (amongst others) located at the Houtribdijk (HRD) and the Marker Wadden islands (fig. 4.1). The Houtribdijk beaches were constructed on both sides of the dam between 2018 and 2020 (Rijkswaterstaat, 2019). These sandy foreshores provide a smooth transition between dike and lake, benefitting biodiversity and water quality in the lake. The Marker Wadden (MW) archipelago consists of shallow marsh islands, protected by two stretches of sandy beaches and dunes on the northwest and southwest side

and a rubble mound breakwater in the west. These islands are meant to improve biodiversity and water quality in lake Markermeer. They were constructed between 2016 and 2018 and expansion works are still ongoing (Van Leeuwen *et al.*, 2021).

At six locations near the beaches, monitoring took place; FL65 to FL70 (fig. 4.1). Measurements were most extensive and long-lasting at location FL67 at the Markermeer-side of the Houtribdijk. The beach near this location is approximately 800 m long, has a D50 of 270 m and is situated between two groynes (fig. 4.1A). The beach near location FI68 is protected by a shore-parallel breakwater. The D50 of the Houtribdijk beaches at the Markermeer side is around 250 m and on the IJsselmeer side around 320 m.

The Marker Wadden beaches, called Noordstrand (NS) on the northwest side and Zuidstrand (ZS) on the southwest side, are both enclosed by a dam on the west side and have an open end (spit) on the east side. The Noordstrand and Zuidstrand are approximately 2000 m and 2500 m long respectively. They were constructed of 350 m D50 sand.

Low-energy beach profiles generally have a steep foreshore and a seaward low-gradient, subaqueous platform (Jackson *et al.*, 2002). The Houtribdijk and Marker Wadden beaches show a similar shape, where the platform connects to the offshore lake bed with a steep slope (Ton *et al.*, 2021). A representative cross-shore profile is shown in fig. 4.2.

4.3.2. Monitoring

At locations FL65 to FL70, approximately 400 m from the shoreline, step gauges were used to monitor water level and thus wave characteristics. The step gauges, or water level gauges, have electrodes with a spacing of 5 cm which measure at a frequency of 4 Hz. In the nearshore, currents are measured with ADVs (Acoustic Doppler Velocimeter) at 8 Hz at location FL67A and FL67C (fig. 4.2).

Bathymetric surveys were conducted monthly in winter and bimonthly in summer between November 2019 and April 2021 at the Houtribdijk. Different equipment was used for offshore bathymetry, shallow bathymetry and topography. Bathymetry was measured with a PingDSP (accuracy of ±0.1 m). Shallow bathymetry was measured using an RTK-GNSS carrier (±0.03 m). For topography, a LiDAR drone (±0.05 m) was used. Transects have a spacing of 25 m near the monitoring locations. The beach near FL67 consists of 35 transects.

4.3.3. Calculation transports from methods

To distinguish different morphological zones, the beach profiles are divided into three vertical sections, separated by four vertical levels (fig. 4.2):

- above the beach face (NAP +0.95 m),
- the annual mean lake water level (NAP -0.3m),
- the submerged slope, just below the platform (NAP -1.55 m),

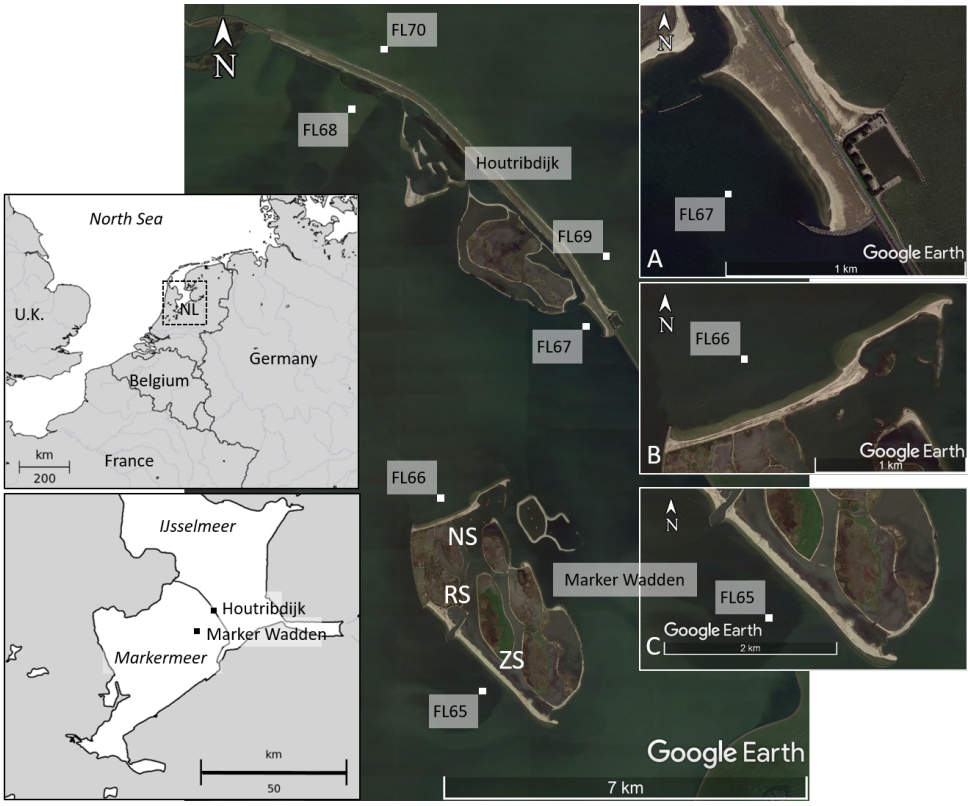

Figure 4.1: Overview of measurement locations, where locations FL65 and FL66 mark the measurement locations near respectively the Zuidstrand (ZS) and Noordstrand (NS) of the Marker Wadden and FL67, FL68, FL69 and FL70 the measurement locations around the Houtribdijk. Subfigure A shows a top view of the study site near FL67. Subfigure B and C show a top view of the study sites Noordstrand and Zuidstrand.

- just below the lake bed (HRD: NAP -2.8 m, MW: NAP -4.2 m).

The sections, from top to bottom, are called: the beach face section, the platform section, and the offshore section. All sections are equal in height for the HRD beaches, while the offshore section is twice as high for the MW beaches as the lake is deeper there.

To analyse longshore sediment transport at the FL67 beach, the beach is divided into two horizontal sections: the northwest section and the southeast section ((Ton *et al.*, 2023), figure 10). Both section are 350 m wide. Per morphological period, the change in volume over time for each vertical and horizontal section is calculated with $Q_{sed} = \Delta V / \Delta t$ in m^3/day.

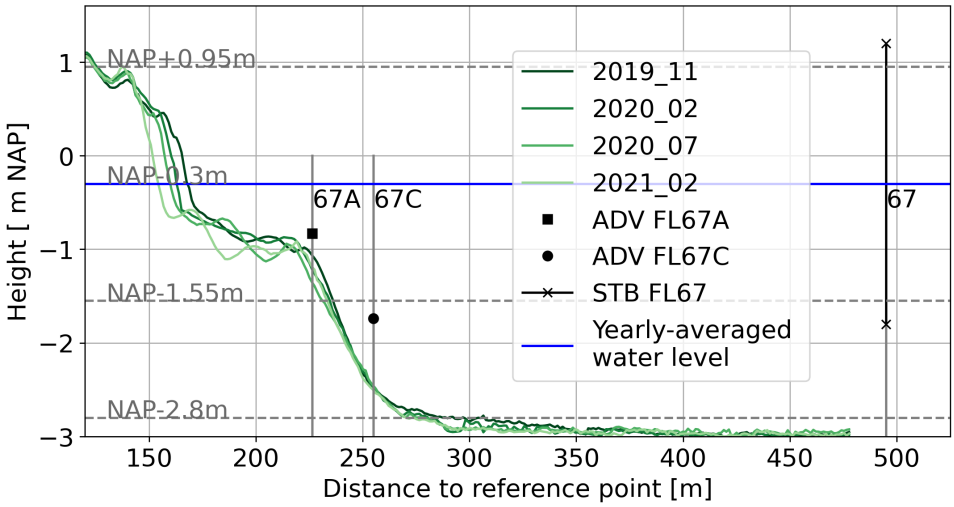

Figure 4.2: Overview of measurement locations, where ADV is Acoustic Doppler Velocimeter and STB is water level step gauge shown on the Houtribdijk cross-shore profiles measured in November 2019, February 2020, July 2020 and February 2021

4.3.4. Model set-up

A Delft3D model is used to quantify the hydrodynamics of lake Markermeer (Deltares, 2018). Our model is based on the suspended sediment model of lake Markermeer, as developed by Van Kessel *et al.* (2008). We adopted the WAVE and FLOW module of this model and use it depth-averaged and including Coriolis forcing. The model was validated with measurement data from our monitoring campaign for waves, water levels and flows for a stormy period with wind speeds up to 23 m/s and a calm period with wind up to 15 m/s (Ton *et al.*, 2023). Measured and modelled wave directions correspond very well, while wave heights are slightly overestimated by the model. Water levels and flow velocity and direction are predicted well by the model.

In the northeast corner of the lake, we nested a detailed domain in the model. The nested grid is refined with a factor 9 in both directions, as the grid cell size of the original model in our area of interest is approximately 150 m. An extra refinement was applied along the Zuidstrand of the Marker Wadden and at the Houtribdijk. The nest has two open boundaries in the southwest and northwest, which are forced with water levels and flow respectively.

4.3.5. Prediction of longshore transport

As discussed in the introduction, the bulk formula for longshore sediment transport at our lake beaches should cater for the absence of swell and the presence

of ambient currents. The Van Rijn (2014) formula meets both criteria:

$$Q_{t,mass} = K_{cal} K_{swell} \rho_s d_{50} tan\beta^{-0.6} H_{s,br}^{2.6} * V_{eff,L}, \tag{4.1}$$

Where $Q_{t,mass}$ is total longshore sediment transport (kg/s), K_{cal} is a calibration coefficient $(-)$, K_{swell} is a factor to account for the presence of swell waves, that is 0.99 for absent swell $(-)$, ρ_s is the sediment density in kg/m^3, d_{50} is the median grain size (m), tanβ is the slope of the beach/surf zone $(-)$, $H_{s,br}^{2.6}$ is the significant wave height (m) at the breaker line and $V_{eff,L}$ is effective longshore velocity (m/s) at mid surf zone. $V_{eff,L}$ represents the effect of both wave-induced and ambient flows, calculated as:

$$V_{eff,L} = 0.3(gH_{s,br}^{0.5} sin(2\partial_{br}) + V_{flow}, \tag{4.2}$$

Where is g is the acceleration of gravity (m^2/s), ∂_{br} is the wave angle at the breaker line with respect to shore-normal and V_{flow} is the ambient current velocity in the breaker zone (m/s) due to tide or wind.

To predict longshore transport on a yearly basis, the wind climate and its accompanying wave and flow conditions need to be taken into account. With the numerical model, wave and flow conditions are predicted for a number of wind conditions. With bins of 22.5 degrees and wind speeds of 5, 10, 15 and 20 m/s, 64 wind conditions were modelled. The Schiphol wind station has recordings of averaged wind speed and direction over the last 10 minutes per hour from 1951 to present, and therefore gives a good insight into wind statistics in the Netherlands. Hourly waves and flow were predicted from the hourly Schiphol wind time series, by classifying the wind conditions in the mentioned modelled bins. This leads to an hourly Qt,mass time series, from which the distribution of yearly Qt,mass for any location in the model can be determined.

4.4. Results

4.4.1. Calibrate longshore transport formula to measurement data

We analysed whether conventional prediction methods for longshore transport work for low-energy, lake beaches. Longshore transport is monitored through consecutive bathymetric surveys at location FL67. At this location, waves and currents were measured during the same period as the bathymetric surveys, making it ideal for comparing predicted and measured longshore transport (LST). Qt,mass is predicted with the Van Rijn (2014) equation (Equation 1) from locally measured waves and flow. Measured and predicted Qt,mass only match relatively well for negative values, for transport towards the southeast (fig. 4.3, in black). The values for January/February 2020 and February/March 2020 stand out, as they were high-energetic and their prediction does not match the measurements. For these periods the mean incoming wave directions were -10.1° and -10.7° relative to shore normal, towards the northwest, while mean flow directions were 0.023 and 0 m/s, around 0 or towards the southeast. As flow and wave directions were opposite, the deviation was likely caused by the large-scale

lake circulation. This is taken into account already through possibility to add an ambient current in the prediction (Equation 2, V_{flow}). However, even when taking this flow into account, predicted Qt,mass directions do not match the measurements. To make the prediction method more suitable for this system, measurements of nearshore longshore flow from FL67A are used for the entire effective longshore current term $V_{eff,L}$ (Equation 1):

$$V_{eff,L} = V_{tot,L} = V_{wave} + V_{flow}, \tag{4.3}$$

Location FL67A is chosen, as for this location the best relation between LST and total flow is found in earlier work (Ton *et al.*, 2023). This adjustment improves the direction of the predicted Qt,mass (fig. 4.3, in red). However, the magnitude of Qt,mass is underestimated. To further improve the prediction method, the equation is calibrated to the measurements with calibration coefficient K_{cal}. A curve fitting method is applied, from which the slope (K_{cal}) and root mean squared error (RMSE) are calculated. The calibration coefficient K_{cal} is determined at 0.0019 and the RMSE of the predicted daily sediment transport is 13.3 m^3/day. The standard error, the standard deviation of the model errors, is calculated with $s = \sqrt{\Sigma(y_i - \hat{y}_i)^2}/(n-2)$ and has a value of 14.8 m^3/day, which is 5420 $m^3/year$. The value of 0.0019 indeed gives good results for the predicted LST (fig. 4.3, in blue markers). Concluding, the altered and calibrated formula develops into:

$$Q_{t,mass} = 0.0019 * K_{swell}\rho_s d_{50} tan\beta^{-0.6} H_{s,br}^{2.6} * V_{tot,L}, \tag{4.4}$$

With the new method, predictions are a factor 5 smaller and in the opposite direction over a calibration period of 1.5 year, but also a factor 2 higher and in the opposite direction for a storm month (fig. 4.3).

4.4.2. Yearly longshore transport

With the calibrated equation of Qt,mass, yearly LST predictions can be done. For yearly LST values, the uncertainties in environmental conditions, such as wind climate, need to be considered. In this system, the most important environmental conditions driving LST;, waves and currents, are strongly correlated to the wind climate. Therefore, yearly LST can vary because the wind climate varies year by year. To explore this variation, wave and flow conditions are derived from the model, based on 71 years of wind data (for method, see section 2.5). With this, yearly LST is predicted for 71 years with the altered and calibrated equation for instantaneous LST for the FL67 beach (eq. 4.4, fig. 4.4). In the hourly LST transport towards both the northwest and southeast are determined. This results in net transport towards the northwest on a yearly basis, which decreased over time.

The dataset of annual LST estimates can be approximated by a normal distribution with a mean of -4600 m^3/year and a standard deviation of 2000 m^3/year (fig. 4.5). When only considering data since the year 2000, the LST reduces to 3500 m^3/year mean with a standard deviation of 1200 m^3/year, confirming the decrease of the yearly LST over time. Thus, yearly LST and its uncertainty can

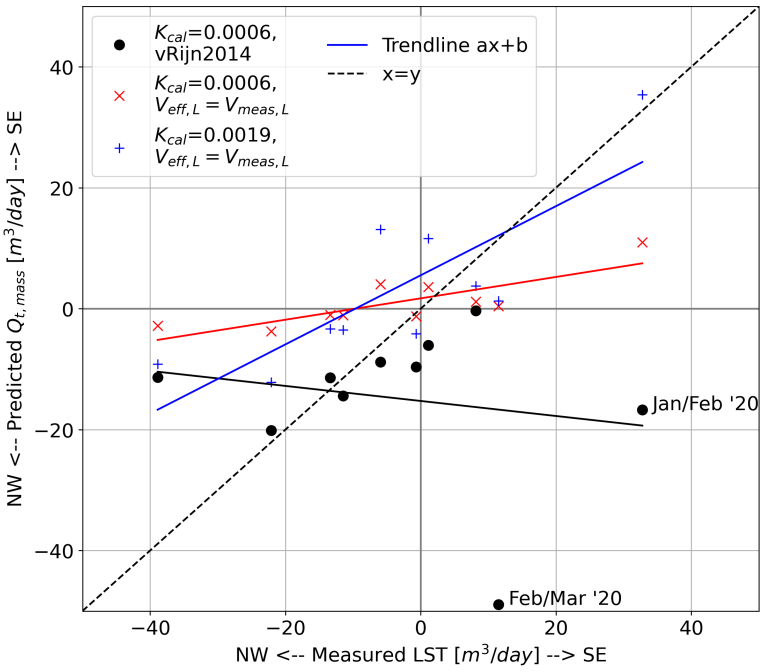

Figure 4.3: Measured LST compared to predicted LST at location FL67, from Van Rijn (2014) (black), Van Rijn (2014) with $V_{eff,L} = V_{tot}$ (red) and with Kcal 0.0019 and $V_{eff,L} = V_{tot}$ (blue). Positive values represent transport towards the southeast, negative towards the northwest. Ideally, markers are on 1:1 line (dashed, black).

be calculated with long-term information on environmental conditions. A numerical model can be used to estimate these environmental conditions at various locations of interest.

4.4.3. Cross-shore transport

In earlier work, cross-shore directed processes were considered dominant in beach face development (Ton et al., 2021). Previous results suggested that the erosion of the beach face originates primarily from storm-driven cross-shore transport, caused by higher wave energy and elevated water levels. In the present study, we compare the influence of cross-shore transport (CST) and longshore transport (LST), based on the morphological development per study site. We assume that CST is equal to the morphological change of the beach face section (Figure 2).

For an overview of the spread of the CST for different locations, distributions for yearly CST are calculated per study site using all measured profiles (table 4.2). Mean yearly CST is highest for location ZS, the FL65 beach (table 4.2, Figure 1). This beach is oriented perpendicular to the most common and energetic wind

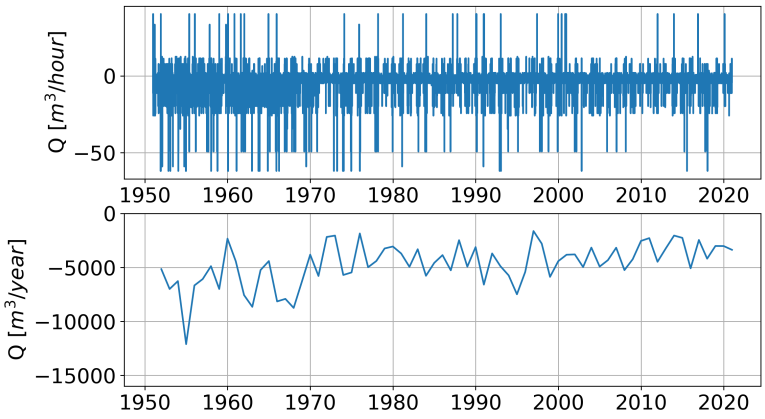

Figure 4.4: LST over time summed per hour and per year at location FL67. Negative: transport towards the northwest, positive: transport towards the southeast.

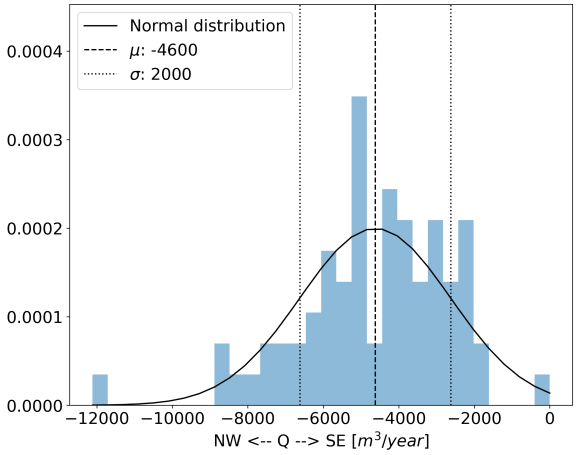

Figure 4.5: Distribution of yearly LST for uncertainty wind climate at the FL67 beach

direction, southwest. Other locations with high CST are RS and FL67, which have the same orientation. The standard deviation of the CST at the FL67 (total) beach is very high compared to the other sites, indicating great differences per transect. The FL70 beach also has a high CST, while at the less energetic IJsselmeer-side of the Houtribdijk. The NS beach (FL66) and the FL68 beach show little beach face erosion, while the FL69 beach even shows mean growth. Although the FL68 beach shows mean erosion, some transects show sedimentation of the beach face, considering the standard deviation. The growth of the FL69 beach is not

constant over time. The first monitoring period, between 11-2019 and 4-2020, some sedimentation is observed around the beach face. However, between 4-2020 and 3-2021, erosion takes place, indicating a trend break (table 4.2, “FL69 (later)”).

The standard deviation of the CST is most likely related to the local positioning of the site. Site FL67 is enclosed by two groynes, so transects near the groynes are sheltered from waves under certain conditions. This leads to an unequally divided amount of wave energy per transect and a high standard deviation for FL67 (table 4.2). The CST for the middle transects is the highest of all locations (table 4.2, “FL67 (centre)”).

To test the hypothesis of CST being storm- or wave-driven, mean beach face development per site is compared to the 95^{th} percentile of the significant wave height at the offshore measurement location, as these provided the longest time series (fig. 4.6). The FL67 beach has the highest wave height, and the most erosion when considering the transects in the centre of the beach. The sedimentation on the FL69 beach does not fit the expected trend. However, when considering the erosion at this location after the trend break (FL69 (later)), this data point would fit the hypothesis better. The lower wave height at the FL66 beach can be explained by its location, as it is situated in the lee of the Marker Wadden islands for southwesterly wind. Nearshore wave height at this beach is expected to be even lower. For the FL68 beach, offshore wave height is not representative for wave conditions at the beach, because of the breakwater in between the offshore measurement station and the beach. For March 2021, wave measurements are available both offshore and shoreward of the breakwater. The offshore 95^{th} percentile H_s is 0.48 m. Waves on the shoreward side were measured at a water depth of 1.9 m by a pressure sensor. For this month, the ratio between the offshore 95^{th} percentile Hs and shoreward waves is 0.011. The 95^{th} percentile H_s on the shoreward side is 0.006 m. Concluding, a trend between increasing wave height and beach face erosion is found. The trend line predicts beach face accretion for 95^{th} percentile H_s lower than 0.22 m in this relation. Although accretion

Beach	Period	Beach face erosion	
		$\mu[m^3/yr/m]$	$\sigma[m^3/yr/m]$
FL67 (total)	11-2019 to 2-2021	-5.5	10.0
FL67 (centre)	11-2019 to 2-2021	-12.3	4.1
FL68	10-2019 to 3-2021	-0.6	2.5
FL69	11-2019 to 4-2021	0.8	1.3
FL69 (later)	4-2020 to 4-2021	-2.4	2.0
FL70	11-2019 to 3-2021	-8.4	3.9
NS (FL66)	7-2018 to 9-2019	-2.9	1.0
RS (FL65)	7-2018 to 9-2019	-7.0	3.5
ZS (FL65)	7-2018 to 9-2019	-9.4	3.2

Table 4.2: Beach face erosion per monitoring period

is measured for the early measurement period of the FL69 beach, and in some profiles of the FL68 beach, this part of the relation is based on little information. This will be further addressed in the discussion.

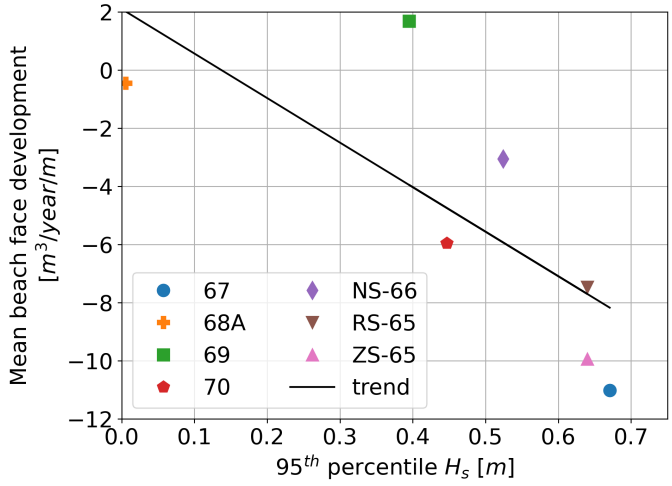

Figure 4.6: Relation measured mean beach face development and 95^{th} percentile H_s.

4.4.4. Transport sensitivity to profile shape development

In this study, we have developed a bulk LST formula for lake beaches and found a relation between 95^{th} percentile H_s and cross-shore beach face development. Now, we want to gain insight in the role of profile shape evolution in both LST and CST predictions. In our prediction, LST and CST are dependent on wave height and LST also on longshore flow, which are dependent on the width of the breaker zone and the geometry of the beaches. The wave height for predicting LST is taken at the breaker line, which is assumed at the offshore end of the platform, where waves start breaking. The FL67A measurement station is located here (Figure 2). For calculating LST, the wave breaking over the nearshore is therefore not relevant. The relation between the 95^{th} percentile of the significant wave height and CST is based on incoming wave conditions, before breaking. We recommend researching the breaking wave height as a parameter for CST processes, this is further elaborated on in the discussion.

In practice, platforms develop gradually, affecting waves and currents differently over time (Ton *et al.*, 2021). The development of profiles in low-energy environments is mostly horizontal, meaning that the platform widens through beach face erosion and sedimentation below the platform.

The first component that could vary with a widening platform is the significant wave height. We expect wave height to reduce over the platform. We

have observed that the transition from beach face slope to platform slope stays roughly at the same vertical position ((Ton *et al.*, 2021), fig. 4.7b). Therefore, the minimum water depth on the platform does not change in time. Consequently, depth-limited storm waves will not be significantly affected by the platform development. In our field measurement campaign, wave height was only measured on the offshore edge of the platform, making analyses of the wave height development over the platform impossible. As this data is lacking, the wave model is not calibrated for this process.

However, our model is capable of quantifying the second component, nearshore flow velocity. At our study sites, the platform widening has not surpassed the enclosing groynes, but no equilibrium has been reached either. Therefore the sensitivity of LST to profile development is tested in the model through comparing predicted yearly LST for the original profile shape and a platform that is twice as wide, extending to the end of the groyne. Hereby also more insight into possible equilibrium profiles can be created. We study the effect of profile development for both the FL67 and the FL66 beach. To address local deviations, flow velocity in multiple computational nodes is included. At the Houtribdijk beach, measurement location FL67A is considered, while at the Noordstrand of the Marker Wadden, we define an extra location FL66A, at a similar place in the cross-shore profile as FL67A. The grid cell size is approximately 15 m at FL67A and 20 m at FL66A. Both beaches indicate that velocities increase somewhat for beaches with a wider platform, in all analysed nodes, as factors are over 1 for (Table 3). At one node offshore of location FL66A, velocities increase significantly. This location is situated just offshore of the platform, in the centre of the local circulation cell. As a consequence, the original flow velocity is relatively small, which explains the large increase after widening. As grid cells are slightly smaller around location FL67A and situated more nearshore, the change in velocity is less pronounced.

4.4.5. Design optimization

Design parameters

Finding the best way to optimize the design of sandy beaches in low-energy, closed basins, starts with design parameters. Both longshore and cross-shore transport are taken into account as design parameters. However, for comparing and combining LST and CST some assumptions have to be made on LST gradients.

	FL67A	FL67A: 15 m shoreward	FL67A: 15 m offshore	FL66A FL66A FL66A	FL66A: 20 m shoreward	FL66A: 20 m offshore
μ [m/s]	1.19	1.08	1.2	1.17	1.13	2.49
σ [m/s]	0.74	0.59	0.69	0.74	0.76	3.12

Table 4.3: Ratio of longshore flow velocity between widened and original beach profile

Optimal beach location based on average waves and flow

With our knowledge of the average wind climate and model predicted flows for all wind conditions, a spatial view of annual mean flow conditions and wave height is calculated (fig. 4.7). The Marker Wadden islands are left out of this calculation. The flow pattern is similar to that for south-westerly wind, since winds from the southwest are most common. These average flows indicate the net longshore transport direction and relative magnitude. Velocities are higher around the boundaries of the lake and in the shallow areas in the north and west of the lake. The residual wave height is highest in the centre of the lake, as would be expected from fetch lengths.

When looking at the location of the Marker Wadden islands relative to the average flows, a flow towards the southwest would be expected at the Noordstrand (fig. 4.6). For the Zuidstrand the pattern would be less clear, and therefore maybe more balanced. In practice the nett offshore flow at the Noordstrand is indeed towards the southwest and the flow at the Zuidstrand is also balanced.

Optimal island locations

Four locations are chosen to evaluate further, based on the average flow pattern and wave heights (fig. 4.7). This evaluation will show the complexity of the system and the sensitivity of the combined effect of longshore flows and wave height. We choose four locations for beach design based on varying these input parameters. The first scenario is the base scenario, where we look at the Noordstrand and Zuidstrand at the current position of the Marker Wadden islands (MW). For the second scenario, the islands are moved towards the north of lake Markermeer (N). We expect wave energy to be similar to MW, but total longshore flows to differ in direction and velocity, as the orientation relative to the large-scale lake currents changes and flows north and northeast of N are converged more due to the shallow bathymetry. For the third scenario, W, the islands are placed in the west of lake Markermeer. For this location little wave energy is expected, while longshore currents are still significant due to the shallow bathymetry and flow convergence to the west and northwest of the island. For the last scenario, flow convergence is avoided as much as possible, placing the islands in the centre of lake Markermeer (C).

Sand mining pits around the Marker Wadden affect the flows around the islands. As these are very deep compared to their surroundings, 40 m compared to 4 m, they alter the surrounding flows in all dimensions (fig. 4.8). The locations of the sand mining pits are not only designed for not affecting the nearby beaches negatively, but also with practical dredging logistics in mind. However, the sand mining pits are not included in this calculation, to avoid complexity. For all scenarios the (coarse) model for the entire Markermeer is used.

Using the wave height and total longshore flow velocity from the Delft3D model, based on 71 years of wind data (for method, see section 2.5), yearly LST for all four locations is predicted and summarized in table 4.4. The variety in predicted yearly net LST is great, ranging from 500 m^3/year for the Zuidstrand (ZS) of location W to 11100 m^3/year for ZS of the original MW location. The predicted LST for

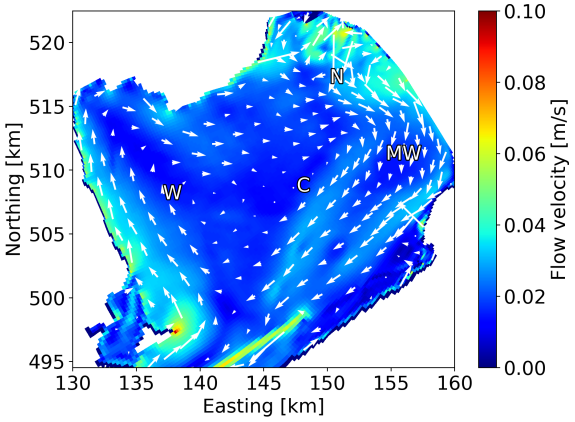

(a) Yearly average flow velocities.

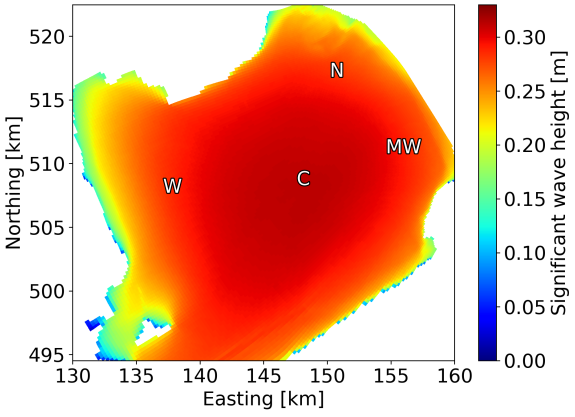

(b) Yearly average significant wave heights.

Figure 4.7: Yearly average parameters based on average yearly wind conditions with four island locations: MW – current location, N – North, C – Centre, W – West

the Noordstrand (NS) for all locations is smaller than that of ZS for most locations, except location W. Moreover, the standard deviation for NS locations is smaller.

Wave energy plays a large role in eq. 4.4. This comes back in the high LST predictions for locations that are prone to waves; ZS of MW, C and N (fig. 4.7b, fig. 4.10). The most LST is predicted for ZS of location MW. This location has the second highest average wave height, but limited average flow . For all locations, high average flow is predicted for the NS combined with limited wave energy. This leads to limited LST.

The total yearly LST can be understood better when looking at the (dis)balance

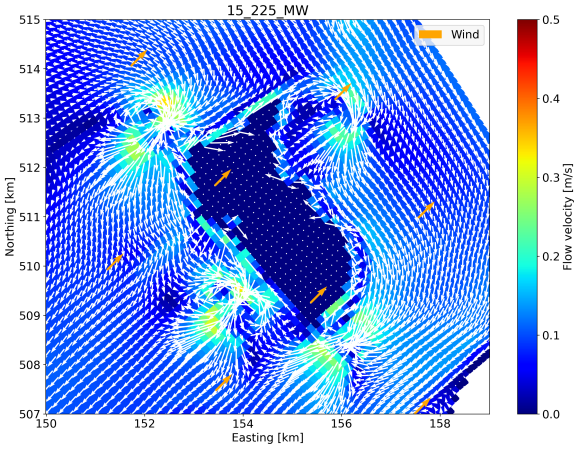

(a) Including sand mining pits

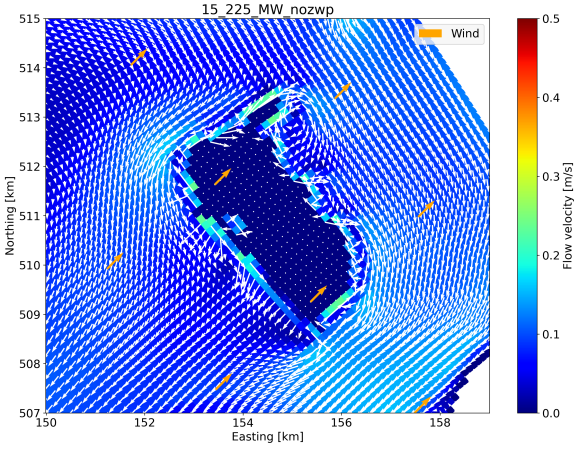

(b) Without sand mining pits

Figure 4.8: Modelled flow for 15 m/s wind from the southwest with and without sand mining pits

between the daily average gross LST in both alongshore directions (fig. 4.9). Daily transport to the southwest exceeds transport to the northeast greatly at ZS of MW. The flow towards the southwest occurs simultaneously with increased wave heights (fig. 4.9). This leads to a high nett yearly LST, even though sediment is transported in both directions. For ZS at the locations C and W, daily LST is much more balanced, leading to lower yearly LST. Net LST for NS of locations MW, C and N are similar, while gross daily transports are higher at location C, due to higher waves (fig. 4.10). This comparison shows once more the complexity of the system and that flow patterns are important in steering the sediment transport direction, but always combined with the stirring effect of waves.

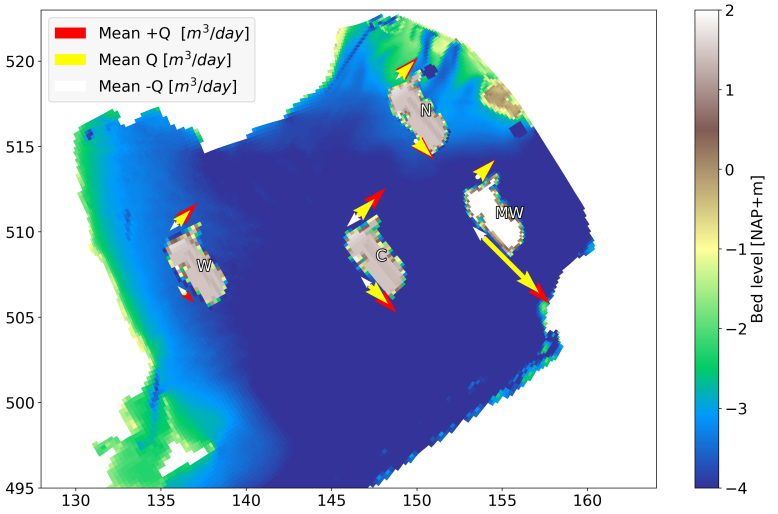

Figure 4.9: Overview of island locations with mean gross (red and white vectors) and net (yellow) daily transports. Subfigures show yearly LST distributions for the Zuidstrand (ZS) and Noordstrand (NS) of each location.

	Yearly average velocity	Yearly average H_s	H_s 95^{th} percentile	LST		Length beach	LST	CST
				μ	σ			
	(m/s)	(m)	(m)	(m^3/yr)	(m^3/yr)	(m)	(m^3/yr/m)	
W-ZS	-0.003	0.2	0.46	500	700	2500	-0.2	-5.0
W-NS	0.017	0.17	0.34	2500	1000	2000	-1.3	-1.5
N-NS	0.016	0.15	0.37	2600	900	2000	-1.3	-3.1
C-NS	0.019	0.19	0.38	2800	1300	2000	-1.4	-3.5
MW-NS	0.013	0.15	0.32	2900	1100	2000	-1.5	-2.9
N-ZS	0.004	0.23	0.6	3500	1300	2500	-1.4	-7.1
C-ZS	-0.002	0.25	0.63	3700	1800	2500	-1.5	-7.6
MW-ZS	0.003	0.24	0.65	11100	4900	2500	-4.4	-7.8

Table 4.4: Predicted longshore transport for possible island locations

Comparing cross-shore and longshore transport quantitatively gives more insight into the relative importance of both processes on low-energy, lake beaches. For this, LST is converted to a volume per linear meter. This conversion depends entirely on the setting of the beach. For all Noordstrand and Zuidstrand locations, sediment is transported away from an enclosing dam toward an open boundary with a spit. For this comparison, we assume that the sediment flux is uniform along the beach and no sediment is coming in from around the dam. With these assumptions, LST is converted to m^3/year/m (table 4.4). The CST is predicted using the relation found (fig. 4.6).

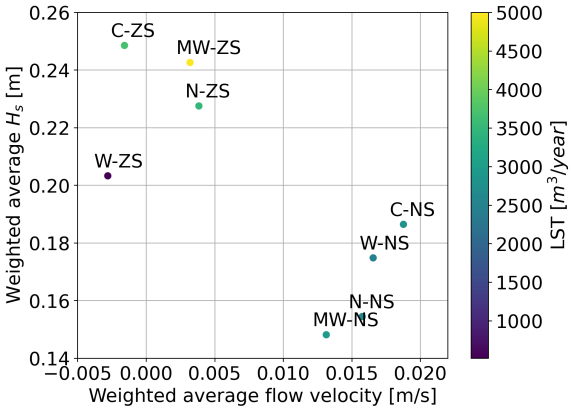

Figure 4.10: Relation yearly average flow velocity and wave height per location and corresponding LST

For all ZS beaches a high CST is predicted, due to higher wave heights than on the NS beaches. At the ZS beach of location W flows are balanced, but wave height is high, resulting in little LST compared to the CST. For the NS of this location, LST and CST are more balanced, due to more imbalanced flows and lower wave heights. Overall, LST and CST are in the same order of magnitude.

4.5. Discussion

4.5.1. Uncertainties LST prediction method

In the developed method for predicting longshore transport (LST) with the adjusted equation by Van Rijn (2014) in combination with measured or modelled longshore flow (eq. 4.4), three major components that give uncertainty were determined. The first was the calibration of the adjusted Van Rijn (2014) equation. The calibration is based on 9 data points describing volume changes between bathymetrical measurements. However, it would be better to have more data points for shorter periods of time.

The beach that was used for the calibration, near FL67, is enclosed by two groynes. We assumed no sediment transport across the groynes and thus a closed mass balance. In practice, sediment may cross and losses in the offshore direction may occur. The beach was split into two sections, assuming sediment transport from the northwest half towards the southwest half and vice versa. This simplification may not always represent reality, as sediment may be moving from the centre of the beach towards the groynes. This phenomenon is likely not fully captured through the assumptions made, but are regarded acceptable.

The second component is the wind climate. The wind measurements of Schiphol were used, as this wind station provided the longest time series. Measurements in this location, 40 kilometre from the centre of lake Markermeer, might not rep-

resent the local wind accurately. Moreover, the measured wind is then classified into one of the 64 wind scenarios, where more accuracy is lost. These uncertainties were considered of less significance than the yearly wind variability. The wind climate appears to change over time, as predicted LST becomes less negative (fig. 4.10). Researching the cause of this effect fell outside the scope of this research.

The standard error of the calibrated bulk sediment transport prediction is 5420 m^3/year. The standard deviation caused by the variability in wind climate at the calibration location is 2000 m^3/year. Both uncertainties may be correlated, as certain wind directions cause a bigger error between measured and modelled LST. However, their effect over time is different. The variability in LST caused by the wind climate is expected to decrease over longer time scales, due to averaging out of more extreme events. If the calibration is slightly off, the effects can add up over time (Kroon *et al.*, 2020), within physical boundaries. On a yearly scale, the uncertainty through the calibration is more than 2.5 times larger than that of the wind climate variability. This difference increases for periods longer than one year.

4.5.2. Cross-shore transport

The annual cross-shore transport is determined with time series that are in the order of one year. Although spatial variation is accounted for, differences over longer periods of time are not. Ideally, longer time series would be used, but these were not available.

To link CST to wave-energy, multiple beaches with different wave heights were considered. Ideally, development over time would be linked to wave energy over time. For our monitoring data this did not lead to a clear relation, because of the uncertainty in the morphologic signal. As we are looking at low-energy beaches, the signal of the beach face erosion is relatively small for all periods, due to small changes in bathymetry. Moreover, the system is more complex and wave energy is not the only process playing a role. Long-term water level changes, for instance due to changes in discharge of the river IJssel on the IJsselmeer-side of the Houtribdijk, affect the system. The complexity of the system has been proven once again in the data of the FL69 beach. For this location, the morphological development shows a trend break from beach face sedimentation to erosion. This might still be an effect of initial adjustment of the system after construction, or longshore sediment transport. As this location is not considered for longshore transport, further causes are not analysed. Besides, morphological changes of the beach face may be affected more by LST than CST under certain circumstances. However, over longer time periods, morphologic development averaged over the transects per beach can be linked to the 95^{th} percentile significant wave height.

The relation between the 95^{th} percentile significant wave height and beach face development is based on little data points and assumed linear. Since there are so few data points, assuming a non-linear relationship would come with more uncertainties. However, we would expect CST to be close to zero up to a wave

height for which enough sediment is stirred up to cause considerable morphological development. For higher wave heights, erosion would then increase.

Wave parameters were now derived from offshore measurements stations, as these provided the longest time series. Using incoming conditions to differentiate between different beaches is a reasonable assumption. However, for locations FL66 and FL68, it might not have been ideal. The measurement location FL66 is in the lee of the island, but not as much as the beach itself. Therefore incoming wave heights are probably overestimated somewhat. For FL68 there was also a discrepancy between measured wave at the offshore location and incoming waves at the beach, as a breakwater is present in between. By comparing the month-long measurements shoreward of the breakwater to the offshore measurements an estimate of the 95^{th} percentile H_s is made. The shoreward value is very low, as waves only transmit across the breakwater for high wave heights and water levels. Therefore, the 95^{th} percentile H_s might not be the optimal parameter for assessing CST for this specific location. If more data becomes available, we recommend to reconsider the relation.

Consolidation of the beach was not taken into account for the calculated beach face erosion. For our Houtribdijk study sites, consolidation is in the order of 10 to 20% of the mean and takes place primarily at the beach face and higher in the profile (Lenstra *et al.*, 2022). Consolidation was not measured at the Marker Wadden sites. As the known consolidation is significantly smaller than the standard deviation, we have chosen to neglect it in this study.

4.5.3. Sensitivity of parameter location in prediction

For predicting sediment transport, the location of the measured or modelled wave height (LST and CST) and flow velocity (LST) are important, as the values of the parameters vary spatially. As indicated in the results, the platform width influences the location of possible nearshore circulation flows. The location of extracting the flow used for predicting LST can therefore be important for the outcome and needs to be considered carefully.

The wave height at the breaker line is used for calculating LST. As the platform elevation will remain relatively constant over time, the wave height at the breaker line will not differ much over time. However, the location of the breaker line is hard to pinpoint exactly. Table 1 shows the sensitivity of relative LST changes for little changes in wave height. 10 cm change in wave height can lead to 44 or even 61% of change in LST (table 4.5).

$H_{s,br}$ (m)	0.5	0.45	0.4	0.55	0.6
LST (order of magnitude)	0.16	0.13	0.09	0.21	0.26
Decrease (%)		-24	-44	28	61

Table 4.5: Sensitivity analysis of LST to changes in wave height

The CST prediction is based on incoming wave height, because of better availability of that data compared to wave data on the platform. However, the break-

ing wave height near the beach face may prove to be a better parameter, as it is physically more linked to beach face processes. We recommend to analyse this in future research.

4.5.4. Comparison cross-shore and longshore transport

Cross-shore and longshore transport were compared for the optimal island locations (section 3.5.3 Optimal island locations). They can also be compared for the calibration location, FL67, taking the predicted LST and the measured mean CST (table 4.6). As this beach is enclosed between two dams, all longshore transport may not lead to a total volume loss. However, if we do make this assumption, we find LST to be approximately half of CST.

	LST		Length beach	LST	CST
	$\mu(m^3/year)$	$\sigma(m^3/year)$	(m)	$(m^3/year/m)$	$(m^3/year/m)$
FL67	4600	2000	800	-5.75	-12.3

Table 4.6: Longshore and cross-shore transport for location FL67

LST is smaller than CST for all locations, both measured and modelled. However, it is in the same order of magnitude. We have to take into consideration that yearly transports are a simplification of reality, as it consists of gross alternating transports that do not always lead to erosion over the whole length of the beach.

4.6. Conclusions

Traditional ways of calculating longshore and cross-shore transport are not suitable for sandy beaches in closed basins, such as lakes, with a low-energy wave climate. The Van Rijn (2014) formula for longshore transport calculates longshore transport direction based on the wave angle of incidence, which does not necessarily match the direction of total longshore flow in these environments. Shallow, closed basins such as lake Markermeer can be subject to large-scale lake circulations, affecting the nearshore flow. In this study, we proposed a new method, in which total longshore flow replaces the summed longshore flow derived from incoming wave direction and ambient flow in the Van Rijn (2014) formula. With two years of bathymetrical and hydrodynamic measurements at the Houtribdijk monitoring site (FL67), this adjusted formula is calibrated. When obtaining yearly longshore transports with this new method, two uncertainties have to be taken into account. The first is the uncertainty of the calibration (5400 m^3/year) and the second the variability in the annual wind climate (2000 m^3/year). Both give a relatively high uncertainty.

Long-term beach face erosion can be predicted by the 95^{th} percentile significant wave height. Although this relation is based on little data points, a relation is found, which is assumed to be linear. Cross-shore and longshore morphological effects were in the same order of magnitude. This means that both cross-shore

and longshore transport need to be accounted for in designing and maintaining beaches.

With the adjusted and calibrated bulk formula, a prediction of yearly longshore transport is possible for beaches in lake Markermeer and possibly other beaches in similar systems. In the past, longshore sediment transport was underestimated because of the omission of large-scale circulation currents, especially compared to cross-shore transport. With knowledge of the total lake system, predictions on longshore and cross-shore sediment transport can be made with more certainty, and more knowledge of their uncertainties.

Acknowledgements

This research is part of the LakeSIDE project, which is funded by Rijkswaterstaat, The Netherlands. We want to thank Rijkswaterstaat Centrale Informatievoorziening for guiding and executing the (hydrodynamic) monitoring campaign. Shore Monitoring and Combinatie Houtribdijk are acknowledged for carrying out the morphological surveys at the Houtribdijk.

5

Conclusions, reflection and outlook

5.1. Conclusions

The aim of this dissertation was to understand and quantify how hydrodynamic processes drive the morphological evolution of low-energy, non-tidal sandy beaches and to develop methods to predict these morphodynamics. The beaches of the IJsselmeer region, the Netherlands, were used to reach this aim, with a focus on the Houtribdijk and Marker Wadden beaches.

RQ1. What are the general features of low-energy, non-tidal, sandy beaches?

The morphology of sandy beaches in low-energy, non-tidal environments, like lake Markermeer, can vary per location, but often shows common features. The beaches generally have a narrow, steep foreshore or beach face, connecting to a low gradient, subaqueous platform. When considering the commonly used beach state descriptions by Wright *et al.* (1984), low-energy beaches would be regarded as reflective (Hegge *et al.*, 1996). However, the single reflective beach state cannot adequately describe the wide range of profiles and concavities observed. Several morphotype models for low-energy beaches were developed (Hegge *et al.*, 1996; Makaske *et al.*, 1998; Travers, 2007), all ranging the types from lower to higher energetic conditions. In summary, the least exposed sites generally have the steepest and narrowest beach face and the most distinct transition between the swash zone and the terrace or platform.

The sites studied during this research, beaches at the Houtribdijk and Marker Wadden, the Netherlands, all show the typical low-energy beach profiles. These beaches were constructed over the past years, in contrast to most of the natural beaches that served as a basis for the morphotypes. As they were constructed with an initial plane slope, they showed a rapid initial profile adjustment during the first years after construction towards the more natural profile shape. All beaches, independent of their location, eventually developed a steep beach face

and a platform at approximately NAP -1 m, which is 0.6 to 0.8 m below mean water level.

RQ2. How do hydrodynamic processes influence the morphology of the low-energy, non-tidal, sandy beaches in the cross-shore direction?

As all monitored beaches showed a low-gradient platform at a similar elevation, we hypothesized that the driving mechanism of this platform is the same for all locations. In lake Markermeer, there is a strong positive correlation between water level set-up and wave height, as both processes are strongly correlated to wind. Because of this correlation, waves during storms happen to break at approximately fixed locations. During the most common southwesterly storms, wave heights are depth-limited, and therefore also have a fixed height. These characteristics are very similar to early days laboratory experiments, from which Hallermeier (1979) concluded that under controlled wave conditions, commonly an equilibrium profile is reached with a platform. According to Hallermeier (1979), the equilibrium depth of this platform is at the depth at which the surface waves reach the limit of their erosive action. This depth was referred to as the depth of closure. Based on measurements of waves and water levels at our study sites, the depth of closure was calculated with the theoretical formulation by Hallermeier (1980) and compared to the measured elevation of the platform. We conclude that the elevation of the platform is indeed located near this depth of closure, and that after reaching this depth, the platform elevation stays relatively stable.

For further analysis of the cross-shore morphological development, three vertical zones were determined in the cross-shore profile: the beach face section, the platform section, and the offshore section. Results suggest that erosion of the beach face is caused primarily by wave-driven cross-shore transport, after which the sediment is most likely diffused in both cross-shore and longshore direction over the platform and offshore sections. Although the depth of the platform is stable, the platform width did not reach an equilibrium for any study sites and the widening is still in full development.

RQ3. How do (large-scale) hydrodynamic processes influence the morphology of the low-energy, non-tidal, sandy beaches in the longshore direction?

Based on flow measurements and bathymetric surveys, a relationship was determined between sediment transport capacity, based on hydrodynamics, and sediment volume flux in the longshore direction. A significant relation was found between the two for the full cross-shore profile, except the steep beach face. Flows measured at the offshore boundary of the platform corresponded best to measured volume fluxes.

The measured longshore flow direction did not always coincide with wind and wave directions. Therefore, we hypothesized a greater influence of large-scale lake circulation on the total longshore flow than originally expected. Bathymetry-induced differences in water level set-up cause large-scale, horizontal circulations. ADCP measurements showed that flow was uniform over the water depth of 3 to 5 m. The large-scale circulations affect the nearshore currents greatly, and are dominant over wave-driven longshore currents for most wind conditions. Local geometric features, such as groynes, also influence the flow, inducing smaller scale nearshore circulation cells under distinct conditions. Insight into large-scale currents is essential for understanding morphological development in shallow, wind-driven water bodies.

RQ4. How can morphological development be predicted for low-energy, non-tidal, sandy beaches?

The measured longshore volume flux could be explained by the sediment transport capacity, derived from nearshore flow. Therefore, prediction of longshore sediment transport based on hydrodynamic conditions should be possible. However, traditional ways of calculating longshore and cross-shore transport are not suitable for sandy beaches in closed basins, such as lakes, with a low-energy wave climate. The Van Rijn (2014) formula for longshore transport calculates longshore transport direction based on the wave angle of incidence, which does not always match the direction of total longshore flow in these environments since it does not take into account the large-scale lake circulations. We propose a new method, in which total measured or modelled longshore flow replaces the combination of flow derived from incoming wave direction and ambient flow in the Van Rijn (2014) formula. This adjusted formula is recalibrated with measurements from one of the Houtribdijk monitoring sites. With the new method, predictions are a factor 5 smaller and in the opposite direction over a calibration period of 1.5 year, but are also a factor 2 higher and in the opposite direction for a storm month.

When obtaining yearly longshore transports with this new method, two uncertainties have to be taken into account. The first is the uncertainty of the calibration and the second the uncertainty of the yearly wind climate. Both give a relatively high uncertainty, but the uncertainty from the calibration is more than 2.5 times larger than the wind climate variability. However, it is better to be aware of the uncertainty of the methods and account for them than to use the uncalibrated known bulk equations.

Yearly beach face erosion volumes in lake Markermeer and lake IJsselmeer system can be linked to the 95^{th} percentile significant wave height when averaging spatially. Cross-shore and longshore morphological effects are in the same order of magnitude, when compared with some simple assumptions, such as zero transport across groynes. This means that both cross-shore and longshore transport need to be accounted for in designing and maintaining beaches.

With the adjusted and calibrated bulk formula, a prediction of yearly longshore transport is possible for beaches in lake Markermeer and possibly other beaches in similar environments. In the past, longshore sediment transport was underestimated, especially compared to cross-shore transport, because of the omission of large-scale circulation currents. With knowledge of the total lake system, predictions on longshore and cross-shore sediment transport can be made with more certainty, and better knowledge of their uncertainties.

With the answers to the four research questions, the main question can be answered:

How can the robustness and required maintenance of low-energy, non-tidal, sandy beaches be assessed?

In this thesis, the hydrodynamic processes steering the morphology of low-energy, non-tidal, sandy beaches in the IJsselmeer region are determined. The beach face is mostly affected by cross-shore erosion, which is strongly linked to wave height in relatively energetic events (95% value) (fig. 5.1). Below the beach face, the platform and offshore section of the profile evolve through a combination of cross-shore and longshore processes. Combined wave heights and water levels steer the platform depth, while gradients in longshore transport, driven by waves and large-scale circulations, determine whether the platform extends offshore. The shape and development of the profile and the beach affect sediment supply for heightening of the platform and build out of the platform (fig. 5.1).

Cross-shore beach face erosion is linked to the yearly 95^{th} percentile wave height, implying the importance of higher energy conditions. However, the morphodynamics of individual events is difficult to ascertain, due to the design of the monitoring campaign, but also due to the similarity in morphodynamics caused by mid energy and higher energy conditions. Longshore sediment transport can be quantified through the adjusted and recalibrated Van Rijn (2014) bulk equation. By combining cross-shore beach face erosion, platform height and longshore sediment distribution at the platform and offshore, beach development can be predicted (fig. 5.1). Given the nature of the prediction method, beach face erosion due to high-energy waves can only be assessed on a yearly basis. However, the sedimentation lower in the profile can be predicted per event. With this a reliable first assessment of the robustness of low-energy, non-tidal, sandy beaches is feasible.

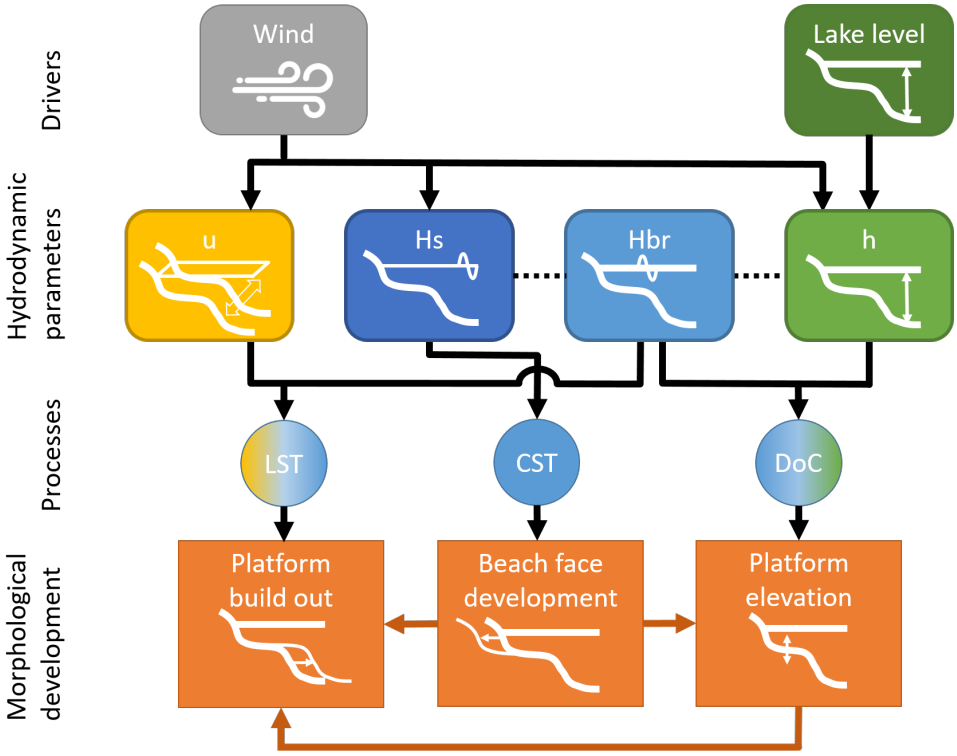

Figure 5.1: Conceptual model, in which CST is cross-shore transport, DoC is depth of closure and LST is longshore transport.

5.2. Reflection and outlook

5.2.1. IJsselmeer region vs. Elsewhere

The morphodynamic processes described in this thesis apply to the IJsselmeer region and we have discussed the possibility to generalise them to lakes or basins worldwide, or even bay and estuary beaches in earlier chapters. The profile shapes from our monitoring campaign are similar to other beaches in low-energy environments, particularly with low tidal amplitudes. The depth of closure depends on wave height and water level. In tidal systems, the breaker zone location is dynamic, preventing a platform to develop. For non-tidal environments the relation between platform elevation and the depth of closure is scalable.

The continuous erosion of the beach face, as observed at our study sites, is presumably more location dependent. Low-energy beaches, or bay and estuary beaches (BEBs), are described to have slow or limited post-storm recovery (Gallop *et al.*, 2020). However, the existence of low-energy beaches in natural settings would not be possible without sufficient restorative wave energy (Nordstrom *et al.*, 2012) or sediment supply from other sources. Low-energy beaches affected by swell appear to recover from erosion at higher rates than more pro-

tected beaches (Costas *et al.*, 2005). Counteraction of erosion is also possible through the supply of sediment by for instance rivers (Lorang, Stanford, *et al.*, 1993). In general, lake beaches are described to have vegetation (Lorang & Stanford, 1993; Nordstrom *et al.*, 2012). At the constructed lake IJsselmeer and lake Markermeer beaches, downward of 1 m above the water level, no vegetation grows, or persists through stormy conditions (Penning *et al.*, 2016). Vegetation can however play a significant role in preventing beach erosion (Möller *et al.*, 2011; Vuik *et al.*, 2016). Vegetation and supply of sediment are not taken into account in the prediction method of cross-shore erosion discussed in this thesis.

The prediction of longshore sediment transport with the Van Rijn (2014) equation is valid for beaches from mid to high energy, while wave direction is the strongest driver for longshore flow. As nearshore flow in our closed system is a combination of wave-driven flow and large-scale circulation flow, the mentioned equation is unreliable for these conditions. When using total measured or modelled flow and the recalibrated formula, it is applicable to low-energy basins. We recommend further validation and possibly recalibration of this adjusted formula when more flow data combined with longshore sediment transport data is available.

Our prediction methods for cross-shore and longshore erosion do not include prevention or counteraction of erosion. We recommend careful mapping of the relevant processes in new locations before using our prediction methods.

5.2.2. Equilibrium vs. Storm-driven

Literature suggests that capturing low-energy beaches in a beach state is possible, but that the states as described for high-energy systems do not apply (Hegge *et al.*, 1996). In this thesis, we found that a dynamic equilibrium is possible, but the definition must be determined carefully. As hydrodynamic conditions in lake Markermeer are very stable, with little to no energy during calm conditions and focused energy during more windy periods, profile shapes at all considered beaches are relatively constant over time, once the characteristic shape is reached. By profile shape we mean the steep beach face and low gradient platform. While this shape remains relatively constant, in terms of slope and platform height, erosion of the beach face continues as long as waves are breaking in the nearshore, and does not slow down over the course of several years after construction. From this characteristic, we may consider the system “storm-driven”. As morphological development happens during relatively windy conditions, here named mid and higher energy, but not necessarily storms, the term storm-driven is not completely suitable. In the high-energy beach vocabulary, the term storm-driven may imply a restorative force during calm conditions. For our study sites, negligible restoration occurred. Thus, the studied beaches may be in a dynamic equilibrium regarding the beach state and shape, while "energy-driven" morphological development continues.

The fact that the beaches studied in this research are constructed and not natural may influence the lack of an actual equilibrium state in both the cross-shore and the longshore direction. Around lake Markermeer and IJsselmeer, some nat-

ural beaches can be found. These are mostly located in lee areas where sand remains from the period when this area was still an inland sea, called “Zuiderzee”. This was before the Houtribdijk and Afsluitdijk were constructed (chapter 1). These pocket beaches rotate depending on incoming waves, but the beach face erosion is not comparable to the LakeSIDE study sites. These natural beaches are either rotated such that their orientation is perpendicular to incoming waves, or found at locations with very limited wave heights. At some locations with limited wave height, the beaches are surrounded by vegetation. This implies that waves and currents at these locations are of such low energy, that vegetation is able to settle and persists. From this we learn that constructed beaches without these enabling environmental conditions, will not reach an equilibrium state and will eventually disappear without maintenance. The Noordstrand at the Marker Wadden is a beach that is not oriented perpendicular to the incoming wave direction, and has no possibility to rotate adequately. Erosion at this beach is substantial and it does not reach a dynamic equilibrium. Thus, knowledge of natural beaches in a system can give guidance for constructing beaches in the same system.

5.2.3. Monitoring vs. Modeling

In the LakeSIDE project we were in the privileged position that we had an extensive field campaign with monitoring at six sites, in the offshore and nearshore, with measurements of both hydrodynamics and bathymetry. On top of that, a detailed Delft3D model could be developed for currents and waves, covering the entire lake Markermeer. Such a wealth in data and models is not common, therefore we would like to reflect on the need of both monitoring and model results and their priorities.

For understanding the robustness of a constructed beach in a less explored environment, monitoring was required. As known numerical models are based on high-energy environments, a model study alone would have had great uncertainties. As the knowledge on modelling low-energy, non-tidal systems has now advanced, less monitoring might be required for a numerical model study.

However, both in system understanding and modelling capacities, knowledge gaps persist. A gap in both elements is wave propagation in the nearshore. Wave measurements (long-term) in very shallow parts of the nearshore prove to be difficult. Reproducing the wave transformation over the characteristic profile under varying conditions required strongly varying breaker-parameters. Based on the (short-term) wave measurements, reproducing the wave transformation over the characteristic profile under varying conditions required strongly varying breaker-parameters (SWAN (module in Delft3D), XBeach) (M. van der Lugt, personal communication). This makes predictions related to cross-shore development and possible equilibrium states difficult, as wave propagation with widening platforms remains uncertain. Future work from the EURECCA project at the Prins Hendrik Zanddijk, Texel, the Netherlands is expected to gain further insight into this problem.

Knowledge on the amount of wave energy reaching the shoreline is essential for future erosion predictions. Other optimizations in monitoring, such as

more flow measurements in a longshore transect for a better understanding of nearshore circulation, may be less crucial. Modelling of wind-driven flow patterns in shallow lakes can be modelled well with limited effort. Flow measurements may add to the local system knowledge, but might not add as much to designing and maintaining beaches in low-energy, non-tidal environments. To this end, limited but regular bathymetrical monitoring and the modelling of geometrical variations or distinguishing between physical processes will improve our insights.

When designing or studying a beach in a low-energy, non-tidal environment, incoming wave conditions and nearshore flow velocities and direction are the most important parameters. If the system can be categorized as a wind-driven water body (Nutz *et al.*, 2015), and a bathymetrical map is available, a hydrodynamic model might be preferred, as it gives more insight into large-scale currents. If local geometrical features may play a role, the model should have a high enough resolution to take these into account. If no information at all is present, measuring waves and currents, at least at one nearshore location is advisable. Moreover, studying existing and/or natural beaches in the same system, through for example remote sensing, will add to the system knowledge and guide where to start with monitoring or modeling.

5.3. Implications for Engineering

When combining all results, implications for designing and maintaining beaches in low-energy, closed basins can be given, formulated like a guideline for engineers. For sandy beaches in low-energy, non-tidal environments, both cross-shore and longshore transport are important. Cross-shore transport is mostly found higher in the profile, from the yearly-averaged water level upward. Longshore transport is predominantly found in the region of the platform and downward. Although cross-shore transport is linked to wave height, quantitatively predicting erosion volumes is complex. Longshore transport can be predicted with an adjusted and recalibrated version of the Van Rijn (2014) method. In this method, longshore transport direction is not determined by incoming wave direction and ambient flow, but by total longshore flow. For all morphological development, stirring up of sediment by waves is essential. The guidelines to take into account are:

1. Knowledge of the total system is required before human interference.
2. Take into account large-scale lake circulations for nearshore longshore flow.
3. Large-scale circulations generally have more velocity near the edges of the basin than in the centre.
4. Sand mining pits alter currents in their vicinity, take this into account when deciding on their location and shape.
5. Longshore sediment transport can contribute equally to or more than cross-shore transport to total sediment transport.
6. There is no indication of decreasing sediment transport over time induced by profile development, maintenance will always be needed.
7. To reduce longshore sediment transport, cross-shore and longshore structures can be effective, but can also affect longshore flow direction. The total system must be taken into account when designing these structures.
8. To reduce cross-shore transport, wave energy reducing shore-parallel structures can be effective. However, for the location and shape of these structures, the total system must be taken into account.

In this thesis, the existing knowledge on processes steering the morphological development of low-energy, non-tidal, sandy beaches was expanded and quantified. Quantification of these relations has led to prediction methods, crucial for design and maintenance of these beaches.

Bibliography

Ashton, A. D., Murray, A. B., Littlewood, R., Lewis, D. A., & Hong, P. (2009). Fetch-limited self-organization of elongate water bodies. *Geology*, *37*(2), 187–190. https://doi.org/10.1130/G25299A.1

Bagnold, R. (1963). Mechanics of marine sedimentation. In M. Hill (Ed.), *The sea* (pp. 507–528). Interscience.

Bosboom, J., & Stive, M. J. (2021). *Coastal Dynamics* (Revision n). TU Delft Open. https://doi.org/https://doi.org/10.5074/T.2021.001

CERC. (1984). Shore Protection Manual. *Waterways Experiment Station, Vicksburg, USA*.

Costas, S., Alejo, I., Vila-Concejo, A., & Nombela, M. A. (2005). Persistence of storm-induced morphology on a modal low-energy beach: A case study from NW-Iberian Peninsula. *Marine Geology*, *224*(1-4), 43–56. https://doi.org/10.1016/j.margeo.2005.08.003

Davidson, M. A., Splinter, K. D., & Turner, I. L. (2013). A simple equilibrium model for predicting shoreline change. *Coastal Engineering*, *73*, 191–202. https://doi.org/10.1016/j.coastaleng.2012.11.002

Deltares. (2018). *Delft3D-Flow User Manual* (tech. rep.).

de Vriend, H. J., van Koningsveld, M., Aarninkhof, S. G., de Vries, M. B., & Baptist, M. J. (2015). Sustainable hydraulic engineering through building with nature. *Journal of Hydro-Environment Research*, *9*(2), 159–171. https://doi.org/10.1016/j.jher.2014.06.004

Eelsalu, M., Parnell, K. E., & Soomere, T. (2022). Geomorphology Sandy beach evolution in the low-energy microtidal Baltic Sea : Attribution of changes to hydrometerological forcing. *Geomorphology*, *414*(July), 108383. https://doi.org/10.1016/j.geomorph.2022.108383

Eliot, M. J., Travers, A., & Eliot, I. (2006). Morphology of a Low-Energy Beach, Como Beach, Western Australia. *Journal of Coastal Research*, *221*, 63–77. https://doi.org/10.2112/05A-0006.1

Fellowes, T. E., Vila-concejo, A., & Gallop, S. L. (2019). Morphometric classification of swell-dominated embayed beaches. *Marine Geology*, *411*(November 2018), 78–87. https://doi.org/10.1016/j.margeo.2019.02.004

Fellowes, T. E., Vila-Concejo, A., Gallop, S. L., Schosberg, R., de Staercke, V., & Largier, J. L. (2021). Decadal shoreline erosion and recovery of beaches in modified and natural estuaries. *Geomorphology*, *390*, 107884. https://doi.org/10.1016/j.geomorph.2021.107884

Gallop, S. L., Vila-Concejo, A., Fellowes, T. E., Harley, M. D., Rahbani, M., & Largier, J. L. (2020). Wave direction shift triggered severe erosion of beaches in estuaries and bays with limited post-storm recovery. *Earth Surface Pro-*

cesses and Landforms, *45*(15), 3854–3868. https://doi.org/10.1002/esp.5005

Goodfellow, B. W., & Stephenson, W. J. (2005). Beach morphodynamics in a strong-wind bay: A low-energy environment? *Marine Geology*, *214*(1-3), 101–116. https://doi.org/10.1016/j.margeo.2004.10.022

Hallermeier, R. J. (1979). Uses for a Calculated Limit Depth To Beach Erosion. *Proceedings of the Coastal Engineering Conference*, *2*(1977), 1493–1512. https://doi.org/10.9753/icce.v16.88

Hallermeier, R. J. (1980). A profile zonation for seasonal sand beaches from wave climate. *Coastal Engineering*, *4*(100), 253–277. https://doi.org/10.1016/0378-3839(80)90022-8

Hegge, B., Eliot, I., & Hsu, J. (1996). Sheltered sandy beaches of southwestern Australia. *Journal of Coastal Research*, *12*(3), 748–760. https://doi.org/10.1144/SP346.3

Hinton, C., & Nicholls, R. J. (1998). Spatial and temporal behaviour of depth of closure along the Holland coast. *Proceedings of the Coastal Engineering Conference*, *3*, 2913–2925. https://doi.org/10.1061/9780784404119.221

Inman, D., & Bagnold. (1963). Litoral Processes. In M. Hill (Ed.), *The sea* (pp. 529–553). Wiley-Interscience.

Jackson, N. L., & Nordstrom, K. F. (1992). Site Specific Controls on Wind and Wave Processes and Beach Mobility on Estuarine Beaches in New-Jersey, USA. *Journal of Coastal Research*, *8*(1), 88–98. https://doi.org/10.2307/4297955

Jackson, N. L., Nordstrom, K. F., Eliot, I., & Masselink, G. (2002). 'Low energy' sandy beaches in marine and estuarine environments a review. *Geomorphology*, *48*(1-3), 147–162. https://doi.org/10.1016/S0169-555X(02)00179-4

Kamphuis, J. W. (1991). Alongshore sediment transport rate. *Journal of Waterway, Port, Coastal, and Ocean Engineering*, *117*(6), 624–640.

Kroon, A., de Schipper, M. A., van Gelder, P., & Aarninkhof, S. G. (2020). Ranking uncertainty: wave climate variability versus model uncertainty in probabilistic assessment of coastline change. *Journal of Coastal Engineering*, *158*(April 2019), 1–11.

Lenstra, K., Vuik, V., Van der Heijden, S., Steetzel, H. J., & Lambregts, P. (2022). *Onderzoek suppletievolumes Houtribdijk* (tech. rep. november).

Liu, S., Ye, Q., Wu, S., & Stive, M. J. (2018). Horizontal circulation patterns in a large shallow lake: Taihu Lake, China. *Water (Switzerland)*, *10*(6). https://doi.org/10.3390/w10060792

Lorang, M. S., Komar, P. D., Stanford, J. A., & Stanfordt, J. A. (1993). Lake Level Regulation and Shoreline Erosion on Flathead Lake, Montana: A Response to the Redistribution of Annual Wave Energy. *Journal of Coastal Research*, *9*(9), 494–508. http://www.jstor.org/stable/4298105%5Cnhttp://www.jstor.org/page/

Lorang, M. S., & Stanford, J. A. (1993). Variability of shoreline erosion and accretion within a beach compartment of Flathead Lake, Montana. *Limnology*

and Oceanography, *38*(8), 1783–1795. https://doi.org/10.4319/lo.1993.38.8.1783

Lorang, M. S., Stanford, J. A., Hauer, F. R., & Jourdonnais, J. H. (1993). Dissipative and reflective beaches in a large lake and the physical effects of lake level regulation. *Ocean and Coastal Management*, *19*(3), 263–287. https://doi.org/10.1016/0964-5691(93)90045-Z

Lowe, M. K., & Kennedy, D. M. (2016). Stability of artificial beaches in port Phillip Bay, Victoria, Australia. *Journal of Coastal Research*, *1*(75), 253–257. https://doi.org/10.2112/SI75-51.1

Ludka, B., Guza, R., O'Reilly, C., & Yates, M. (2015). Field evidence of beach profile evolution toward equilibrium. *Journal of Geophysical Research: Oceans*, 7574–7597. https://doi.org/10.1002/2014JC010320.Received

Makaske, B., & Augustinus, P. G. E. F. (1998). Morphologic Changes of a Micro-Tidal, Low Wave Energy Beach Face during a Spring-Neap Tide Cycle, Rhône-Delta, France. *Journal of Coastal Research*, *14*(2), 632–645. https://doi.org/10.2112/JCOASTRES-D-12-00

Mil-Homens, J., Ranasinghe, R., Vries, J. S. M. V. T. D., & Stive, M. J. F. (2013). Re-evaluation and improvement of three commonly used bulk longshore sediment transport formulas. *Coastal Engineering*, *75*, 29–39. https://doi.org/10.1016/j.coastaleng.2013.01.004

Möller, I., Mantilla-contreras, J., Spencer, T., & Hayes, A. (2011). Estuarine , Coastal and Shelf Science Micro-tidal coastal reed beds : Hydro-morphological insights and observations on wave transformation from the southern Baltic Sea. *Estuarine, Coastal and Shelf Science*, *92*(3), 424–436. https://doi.org/10.1016/j.ecss.2011.01.016

Mujal-Colilles, A., Grifoll, M., & Falqués, A. (2019). Rhythmic morphology in a microtidal low-energy beach. *Geomorphology*, *334*, 151–164. https://doi.org/10.1016/j.geomorph.2019.02.037

Natuurmonumenten. (2019). Project Marker Wadden | Natuurmonumenten. https://www.natuurmonumenten.nl/projecten/marker-wadden

Neumann, B., Vafeidis, A. T., Zimmermann, J., & Nicholls, R. J. (2015). Future coastal population growth and exposure to sea-level rise and coastal flooding - A global assessment. *PLoS ONE*, *10*(3). https://doi.org/10.1371/journal.pone.0118571

Nicholls, R. J., Birkemeier, W. A., & Lee, G.-h. (1998). Evaluation of depth of closure using data from Duck , NC , USA. *Marine Geology*, *148*, 179–201.

Nordstrom, K. F., & Jackson, N. L. (2012). Physical processes and landforms on beaches in short fetch environments in estuaries, small lakes and reservoirs: A review. *Earth-Science Reviews*, *111*(1-2), 232–247. https://doi.org/10.1016/j.earscirev.2011.12.004

Nordstrom, K. F., Jackson, N. L., Sherman, D. J., & Allen, J. R. (1996). Hydrodynamics and beach change on a micro-tidal lagoon shoreline. In K. F. Nordstrom & C. T. Roman (Eds.), *Estuarine shores: Evolution, environments and human alterations* (pp. 213–232). Wiley.

Nutz, A., Schuster, M., Ghienne, J. F., Roquin, C., & Bouchette, F. (2018). Wind-driven waterbodies: a new category of lake within an alternative sedimentologically-based lake classification. *Journal of Paleolimnology*, *59*(2), 189–199. https://doi.org/10.1007/s10933-016-9894-2

Nutz, A., Schuster, M., Ghienne, J. F., Roquin, C., Hay, M. B., Rétif, F., Certain, R., Robin, N., Raynal, O., Cousineau, P. A., Team, S., & Bouchette, F. (2015). Wind-driven bottom currents and related sedimentary bodies in lake saint-jean (Québec, Canada). *Bulletin of the Geological Society of America*, *127*(9-10), 1194–1208. https://doi.org/10.1130/B31145.1

Penning, W., Steetzel, H. J., van Santen, R., Fiselier, J., de Lange, H. J., Vuik, V., Ouwerkerk, S., & van Thiel de Vries, J. S. M. (2015). Natural Foreshores as an Alternative to Traditional Dike Re-enforcements: a Field Pilot in the Large Shallow Lake Markermeer, the Netherlands. *E-proceedings of the 36th IAHR World Congress 28 June - 3 July, 20145, The Hague, The Netherlands*, 1–4.

Penning, W., Steetzel, H. J., van Santen, R., de Lange, M., Ouwerkerk, S., Vuik, V., Fiselier, J., & de Vries, J. v. T. (2016). Establishing vegetated foreshores to increase dike safety along lake shores. *E3S Web of Conferences*, *7*, 12008. https://doi.org/10.1051/e3sconf/20160712008

Rahbani, M., Vila-concejo, A., Fellowes, T. E., Gallop, S. L., Winkler-prins, L., & Largier, J. L. (2022). Spatial patterns in wave signatures on beaches in estuaries and bays. *Geomorphology*, *398*, 108070. https://doi.org/10.1016/j.geomorph.2021.108070

Rijkswaterstaat. (2018). *Peilbesluit IJsselmeergebied* (tech. rep.). https://www.helpdeskwater.nl/@185393/peilbesluiten/

Rijkswaterstaat. (2019). Houtribdijk reinforcement. https://www.rijkswaterstaat.nl/en/about-us/gems-of-rijkswaterstaat/houtribdijk-reinforcement

Rijkswaterstaat & Stichting EcoShape. (2018). *Pilot zandige vooroever Houtribdijk - Hoofdrapportage* (tech. rep.).

Schindler, D. E., & Scheuerell, M. D. (2002). Habitat coupling in lake ecosystems. *Oikos*, *98*(2), 177–189. https://doi.org/10.1034/j.1600-0706.2002.980201.x

Schuster, M., Roquin, C., Duringer, P., Brunet, M., Caugy, M., Fontugne, M., Mackaye, H. T., Vignaud, P., & Ghienne, J. F. (2005). Holocene Lake Mega-Chad palaeoshorelines from space. *Quaternary Science Reviews*, *24*(16-17), 1821–1827. https://doi.org/10.1016/j.quascirev.2005.02.001

Steetzel, H. J., van der Goot, F., Fiselier, J., de Lange, M., Penning, W., van Santen, R., & Vuik, V. (2017). Building with Nature Pilot Sandy Foreshore Houtribdijk: Design and Behaviour of a Sandy Dike Defence in a Lake System. *Coastal Dynamics*, (063).

Ton, A. M., Vuik, V., & Aarninkhof, S. G. J. (2023). Longshore sediment transport by large-scale lake circulations at low-energy , non-tidal beaches : A field and model study. *Coastal Engineering*, *180*. https://doi.org/10.1016/j.coastaleng.2022.104268

Ton, A. M., Vuik, V., & Aarninkhof, S. G. (2021). Sandy beaches in low-energy, non-tidal environments: Linking morphological development to hydrodynamic forcing. *Geomorphology*, *374*, 107522. https://doi.org/10.1016/j.geomorph.2020.107522

Tran, Y. H., Marchesiello, P., Almar, R., Ho, D. T., & Nguyen, T. (2021). Combined Longshore and Cross-Shore Modeling for Low-Energy Embayed Sandy Beaches.

Travers, A. (2007). Low-Energy Beach Morphology with Respect to Physical Setting: A Case Study from Cockburn Sound, Southwestern Australia. *Journal of Coastal Research*, *232*(232), 429–444. https://doi.org/10.2112/04-0275.1

Travers, A., Eliot, M. J., Eliot, I., & Jendrzejczak, M. (2010). Sheltered beaches of southwestern Australia. In *Australian landscapes* (pp. 23–42). Geological Society of London. https://doi.org/10.16309/j.cnki.issn.1007-1776.2003.03.004

Van Kessel, T., Gerben, D. B., & Boderie, P. (2008). *Calibration suspended sediment model Markermeer* (tech. rep.). Deltares.

Van Ledden, M. (H., Gerrits, G. (H., Van Kessel, T. (D. H., & Mosselman, E. (D. H. (2006). *Verdiepingsslag en maatregelen slibproblematiek Markermeer: Analyse kennisleemten en inventarisatie maatregelen* (tech. rep.).

Van Leeuwen, C. H., Temmink, R. J., Jin, H., Kahlert, Y., Robroek, B. J., Berg, M. P., Lamers, L. P., Van den Akker, M., Posthoorn, R., Boosten, A., Olff, H., & Bakker, E. S. (2021). Enhancing ecological integrity while preserving ecosystem services: Constructing soft-sediment islands in a shallow lake. *Ecological Solutions and Evidence*, *2*(3), 1–10. https://doi.org/10.1002/2688-8319.12098

Van Rijn, L. C. (2002). LONGSHORE SAND TRANSPORT Leo C. van Rijn 1. *28th ICCE, Cardiff, UK*, 1–13.

Van Rijn, L. C. (2014). A simple general expression for longshore transport of sand, gravel and shingle. *Coastal Engineering*, *90*, 23–39. https://doi.org/10.1016/j.coastaleng.2014.04.008

Van Wesenbeeck, B. K., Mulder, J. P., Marchand, M., Reed, D. J., De Vries, M. B., De Vriend, H. J., & Herman, P. M. (2014). Damming deltas: A practice of the past? Towards nature-based flood defenses. *Estuarine, Coastal and Shelf Science*, *140*, 1–6. https://doi.org/10.1016/j.ecss.2013.12.031

Vijverberg, T. (2008). *Mud dynamics in the Markermeer. Silt traps as a mitigation measure for turbidity* (Doctoral dissertation).

Vila-Concejo, A., Gallop, S. L., & Largier, J. L. (2020). Sandy beaches in estuaries and bays. In D. Jackson & A. D. Short (Eds.), *Sandy beach morphodynamics* (pp. 343–362). Elsevier Ltd. https://doi.org/10.1016/B978-0-08-102927-5/00015-1

Vila-Concejo, A., Hughes, M. G., Short, A. D., & Ranasinghe, R. (2010). Estuarine shoreline processes in a dynamic low-energy system. *Ocean Dynamics*, *60*(2), 285–298. https://doi.org/10.1007/s10236-010-0273-7

Vuik, V., Jonkman, S. N., Borsje, B. W., & Suzuki, T. (2016). Nature-based flood protection: The efficiency of vegetated foreshores for reducing wave loads on coastal dikes. *Coastal Engineering*, *116*, 42–56. https://doi.org/10.1016/j.coastaleng.2016.06.001

Wright, L. D., & Short, A. D. (1984). Morphodynamic variability of surf zones and beaches: A synthesis. *Marine Geology*, *56*(1-4), 93–118. https://doi.org/10.1016/0025-3227(84)90008-2

Wright, L. D., Short, A. D., & Green, M. O. (1985). Short-term changes in the morphodynamic states of beaches and surf zones: An empirical predictive model. *Marine Geology*, *62*(3-4), 339–364. https://doi.org/10.1016/0025-3227(85)90123-9

Yates, M. L., Guza, R. T., & Reilly, W. C. O. (2009). Equilibrium shoreline response: Observations and modeling. *114*(July), 1–16. https://doi.org/10.1029/2009JC005359

Biography

Anne Ton was born on the 27th of December 1991 in Middelburg, the Netherlands. After finishing secondary school in Middelburg, she started the Civil Engineering bachelor at Delft University of Technology. In 2014, she started the Civil Engineering master, specializing in Coastal Engineering. She finished her MSc with a thesis on process-based modelling of hydro- and morphodynamics around the Anmok submerged breakwater in South Korea at Deltares, Delft.

After graduation, she worked as a project engineer at Witteveen+Bos at the department of Hydrodynamics and Morphology. At this company, she worked on simulating waves, currents and morphology at coasts and rivers.

From 2018 to present, she returned to the Coastal Engineering section at the Delft University of Technology to pursue a PhD, where she studied sandy beaches in low-energy, non-tidal environments. From 2021 to present, she worked as a Postdoc on morphology of the Marker Wadden beaches in the same section.

List of Publications

Peer-reviewed journal papers

First author

3. **Ton, A.M.**, Vuik, V., Aarninkhof, S.G.J. (*submitted*). Prediction of sediment transport for lake beaches and implications for their design and maintenance. (Chapter 4)

2. **Ton, A.M.**, Vuik, V., Aarninkhof, S.G.J., (2023). Longshore sediment transport by large-scale lake circulations at low-energy , non-tidal beaches: A field and model study. *Coastal Engineering*, 180. (Chapter 3)

1. **Ton, A.M.**, Vuik, V., Aarninkhof, S.G.J. (2021). Sandy beaches in low-energy, non-tidal environments: Linking morphological development to hydrodynamic forcing. *Geomorphology*, 374, 107522. (Chapter 2)

Co-author

1. Van Kouwen, N.C., **Ton, A.M.**, Vos, S.E., Vijverberg, T., Reniers, A.J.H.M., Aarninkhof, S.G.J., (2023). Quantifying complex relations between spit growth and its hydrodynamic drivers, in non-tidal, wind-dominated lake environments. Application to the Marker Wadden (Lake Markermeer, The Netherlands). *Geomorphology*

Book chapters

1. **Ton, A.M.**, Lee, M., Vos, S.E., Gawehn, M., den Heijer, K., Aarninkhof, S.G.J. (2020). Beach and nearshore monitoring techniques. *Elsevier Ltd*.

Peer-reviewed conference papers

1. **Ton, A.M.**, Vuik, V., Aarninkhof, S.G.J. (2019). Formation of Sandy Foreshores in Low-Energy Microtidal Environments. *Coastal Sediments*, 754–764.

Conference abstracts, presentations and posters

7. **Ton, A.M.**, Vuik, V., Wilmink, R.J.A., Aarninkhof, S.G.J., Field observations and model simulations of longshore transport on low-energy, non-tidal beaches in lake Markermeer. *NCK Days 2022*.

6. **Ton, A.M.**, Vuik, V., Wilmink, R.J.A., Aarninkhof, S.G.J. Impact of longshore sediment transport on the design and maintenance of low-energy,non-tidal sandy beaches. *International Conference of Coastal Engineering 2022*.

5. **Ton, A.M.**, Vuik, V., Wilmink, R.J.A., Aarninkhof, S.G.J. Field observations and model simulations of longshore transport on low-energy, non-tidal beaches. *Coastal Dynamics 2021*.

4. **Ton, A.M.**, Vuik, V., Wilmink, R.J.A., Aarninkhof, S.G.J. Field observations of longshore transport on low-energy, non-tidal beaches. *NCK Days 2021*.

3. **Ton, A.M.**, Vuik, V., Wilmink, R.J.A., Aarninkhof, S.G.J. (2020). Morphodynamics of Sandy Beaches in Low Energy, Non-Tidal Environments. *Coastal Engineering Proceedings*, (36v), 47.

2. Molino, G., **Ton, A.M.**, Aarninkhof, S.G.J. Hydrodynamic factors influencing beach profiles in shallow, low-energy lakes: a case study in the Markermeer and IJsselmeer. *NCK Days 2019*.

1. **Ton, A.M.**, Vuik, V., Wilmink, R.J.A., Aarninkhof, S.G.J. Sandy Foreshores as Dike Reinforcement in Lake Systems: A nature-based solution at the Houtribdijk. *NCK Days 2018*.

Acknowledgements

First of all, I would like to thank my supervisors Stefan and Vincent. Thank you for introducing me into the wonderful world of the Dutch lakes, which unmistakably have coasts.

Vincent, you surprised me on my first day with the question: "What do you want to do?". This marked your role as an advisor and the freedom you gave me to make my own choices. Although I sometimes found this tough, it was incredibly valuable. Our journey ended in a spectacular trip to Australia, where I could finally see your love for birds up close. Thank you for all your advice, detailed feedback and always having time for more brainstorm sessions.

Stefan, I enjoyed our meetings, where we always talked about non-work related things first. Your ability to show me the bigger picture and zoom out has helped me tremendously. Your question: "Why not go with Delft3D then?" has definitely changed the direction of this thesis in an important way. Thank you for encouraging me and helping me in staying connected throughout the more difficult work-from-home situation we all found ourselves in.

Outside of the TU Delft, a lot of people were involved in our LakeSIDE project. Most importantly, Rijkswaterstaat, who were not only responsible for the funding, but helped us greatly by setting up and running the monitoring campaign. When joining the CIV crew aboard, it always felt more like an outing than work. Too many names to mention, but I should at least acknowledge Rinse Wilmink, Evelien Brand, Henk Meuldijk, Jan-Willem Mol and Arjen Ponger.

All this monitoring data was stored in a very well set up data management system, developed by HKV and Tauw, who were always available for questions and other requests. Thank you, Boskalis and Natuurmonumenten, for welcoming me to the Marker Wadden and sharing your data. After so many visits, I feel quite at home on the islands.

When out on fieldwork, I was never alone, but always in the company of graduate students or interns. Thank you for your enthusiasm and inspiration, Grace, Tom, Fleur, Niels, Bart, Meye, Casper and the students of fieldwork course.

We started with just four PhDs at the third floor: Anna, Matthijs, Christa and me. Anna, thank you for inviting me into 3.95, where we started the PhD room together. We clicked immediately, being typical Delft women. We always sat opposite each other, giving each other a "veelbetekenende blik" every now and then. Thank you for helping me start up in the very beginning and all the great conversations, either offline or online, since. In all these years we went sailing only

once, and although Florida waters are hard to beat, I hope we will try. Matthijs, if we sounded like more than just four, you might have had something to do with that. You were always incredibly creative in entertaining us with for instance self-made didgeridoos, but also making our office a home with lots of plants. Thanks for all the laughs. Christa, you completed this foursome with some non-Delft energy. Due to your incredible efficiency our schedules started lining up more and more. This resulted in us being each others paranimph for more than just the practical reasons. Thank you for always looking at my plots and enduring some sighing from my side, but also for many happy conversations. After sitting side by side for quite some years at our desks, and then even in our big and sturdy camper van for way more than 1000 km in Australia, I'm very happy that you will sit by my side through my defense.

The coastal section expanded over time, into a great group with many fun lunches, drinks and even a camper trip in Australia! Thanks Ana, Arjen, Bart, Bram, Caroline, Danny, Erik, Floris, Gijs, Jakob, Jill, José, Mario, Marion, Marlies, Matthieu, Mia, Nina, Paul B., Paul v. W., Sander, Shelby, Sierd, Silke, Stuart, Su, Tosca and many more.

Bedankt lieve vrienden, kiwi's, zeeuwse meisjes, lowlanders, flambo's, voor de nodige afleiding en ontspanning. In het bijzonder Hanna, voor de spontane belletjes, alle schrijfsessies thuis en op plekken met airco, borreltjes, en het zijn van mijn paranimf.

Pap en mam, bedankt voor alle steun tijdens mijn promotie, maar ook in alle jaren daarvoor. Wouter, ik kan me geen betere broer wensen. En ook geen leukere schoonzus, Nynke. Vermeertjes, dankjulliewel dat jullie me altijd welkom laten voelen, en voor jullie interesse in mijn soms toch wel gekke werk.

Lieve Chris, ik ben ontzettend blij dat we dit PhD avontuur konden delen. Jouw onverminderde vertrouwen in mij gaf me veel steun en jouw lieve reacties op mijn doorgestuurde figuren konden mijn dag maken. Gelukkig konden we samen het werk ook goed wegleggen en hebben we ook veel andere mooie avonturen beleefd. Of we nu op reis waren naar bijzondere plekken, of gewoon thuis klusjes deden. Ik hoop dat er nog heel veel avonturen gaan komen.